



## Cross-conjugation in expanded -systems

Nielsen, Mogens Brøndsted

*Publication date:*  
2018

*Document version*  
Publisher's PDF, also known as Version of record

*Citation for published version (APA):*  
Nielsen, M. B. (2018). *Cross-conjugation in expanded -systems*. Department of Chemistry, Faculty of Science, University of Copenhagen. [https://soeg.kb.dk/permalink/45KBDK\\_KGL/1pioq0f/alma99122121102805763](https://soeg.kb.dk/permalink/45KBDK_KGL/1pioq0f/alma99122121102805763)



---

# Cross-Conjugation in Expanded $\pi$ -Systems

*Thesis for the  
Doctor of Science  
degree*

**Mogens Brøndsted Nielsen**

Department of Chemistry, University of Copenhagen



# **Cross-Conjugation in Expanded $\pi$ -Systems**

Doktorafhandling

*af Mogens Brøndsted Nielsen*

Denne afhandling er af Det Natur- og Biovidenskabelige Fakultet ved Københavns Universitet antaget til offentligt at forsvares for den naturvidenskabelige doktorgrad, doctor scientiarum (dr.scient.).

København, den 24/1 2018 John Renner Hansen (Dekan).

Forsvaret finder sted den 16/3 2018, kl. 13.15

Auditorium 2, Kemisk Institut, Københavns Universitet,

Universitetsparken 5, 2100 København Ø





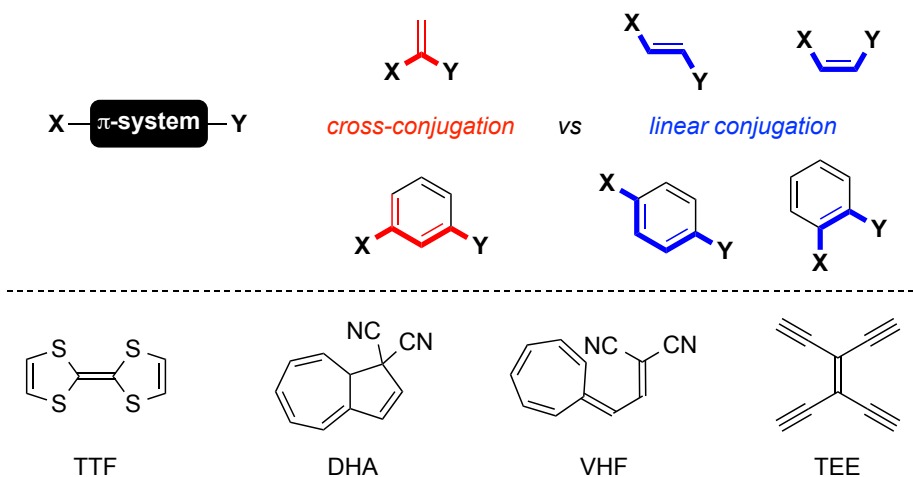
## PREFACE

There are a number of people I would like to thank for making this dissertation possible. First of all, I am sincerely grateful to all my former and current group members who have contributed to the results I am presenting. I have been extremely lucky to have had so many talented and enthusiastic students and post docs working in my group. I would also like to thank all colleagues with whom I have collaborated at the Department of Chemistry, University of Copenhagen. This involves a very long list, but a special thank goes to Profs Kristine Kilså, Ole Hammerich, Thomas Bjørnholm, Kurt V. Mikkelsen, and Henrik G. Kjærgaard, with all of whom I have made many joint papers. A special thank also goes to Prof. Michael Pittelkow for many fruitful and stimulating research discussions over the years and for his valuable input to this dissertation. Also I like to thank the department for providing me with excellent conditions for doing research. A special thank goes to Profs Steen Hammerum and Thomas Bjørnholm for welcoming me in 2004 to *Kemisk Lab. 2* (organic chemistry) and the *Nano-Science Center* and for helping me to establish my group in Copenhagen. Also I like to thank University of Copenhagen for providing me with funding to establish *Center for Exploitation of Solar Energy*, which has boosted my research in the last 4 years, and I am grateful to Head of Department, Prof. Mikael Bols, for providing this center with optimum research conditions at the department. A warm thank also goes to NMR Lab Manager Christian G. Tortzen and MS Lab Manager Theis Brock-Nannestad for helping my group with advanced NMR and MS experiments, and a thank goes to the entire technical staff at the department for creating an excellent infrastructure. I am grateful to Prof. Anders Kadziola for solving many of the X-ray crystal structures presented in this thesis. I am also grateful to the dept. of chemistry at Univ. of Southern Denmark in Odense for allowing me to start my independent career there before moving to Copenhagen, and some of the results presented in this dissertation are from my time in Odense. The research would not have been possible either without generous support over the years from the Danish Research Councils (FNU & FTP) and the Villum, Lundbeck, and Carlsberg Foundations. Finally, I like to thank my collaborators from all over the world; many of the results presented in this thesis have resulted from fruitful collaborative work. It is too extensive to list names, but they appear in the list of publications and are mentioned in several of the chapters. A special thank goes to Prof. Martina Cacciarini (Firenze) and to Prof. Steen Brøndsted Nielsen (Aarhus).

*Mogens Brøndsted Nielsen, Copenhagen, February 2017*

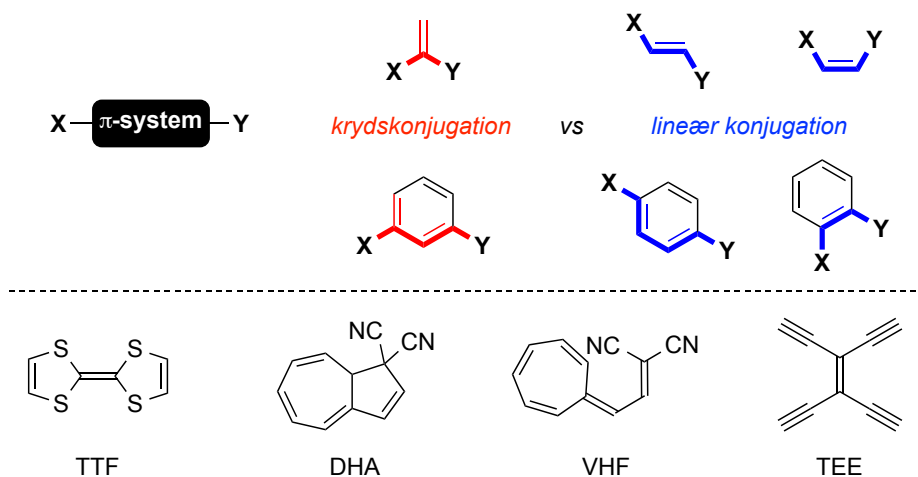
## ABSTRACT

The focus of this dissertation is on  $\pi$ -electron delocalization via cross-conjugation in expanded  $\pi$ -systems that have been synthesized in my research group during the past fourteen years. I will show how the optical properties of donor-acceptor chromophores derived from extended nitrophenolates strongly depend on the bridging unit between donor and acceptor units. In addition, the optical properties of chromophores such as extended tetrathiafulvalenes (TTFs) and functionalized dihydroazulenes (DHAs) will be covered. Cross-conjugated bridges alter the electronic communication between redox-active units in comparison to linearly conjugated bridges, and this will become apparent from a variety of redox-active systems derived from TTF. Alkyne-expanded quinoid structures will be presented that are interesting redox-active systems of the Wurster type, which gain aromaticity upon reduction. Dicyano-functionalized vinylheptafulvenes (VHFs) are cross-conjugated molecules that can be formed by photoisomerization of related DHAs. Not only do the optical properties of these molecules rely on whether functional groups are placed in cross- or linear conjugation to the cores, but also the DHA and VHF interconversions depend hereupon. In particular, I shall show how we have performed systematic studies on the kinetics of the thermal VHF to DHA ring-closure reaction as a function of the location and electronic character of the substituents. The degree of  $\pi$ -electron delocalization is also revealed from single-molecule conductance studies, which have been performed on both the DHA/VHF system and redox-active, cruciform-shaped molecular wires derived from TTF. My research is synthesis-driven, and synthetic protocols for achieving or functionalizing a large selection of cross-conjugated molecules shall be presented. Synthesis by acetylenic scaffolding plays a key role, and the planar tetraethynylethene (TEE) unit has been employed as a bridging unit between functional entities in several of the systems presented.



## ABSTRACT IN DANISH (Resumé på dansk)

I denne afhandling vil jeg beskrive  $\pi$ -elektrondelokalisering i store, udvidede  $\pi$ -systemer, som er blevet syntetiseret i min forskningsgruppe de sidste 14 år. Jeg vil vise, hvorledes de optiske egenskaber af donor-acceptor kromoforer afledt af nitrophenolater i høj grad afhænger af den bro-enhed, som adskiller donor- og acceptor-enhederne. Derudover vil de optiske egenskaber af udvidede tetrathiafulvalen (TTF) og funktionaliserede dihydroazulen (DHA) kromoforer blive dækket. Krydskonjugerede broer ændrer graden af elektronisk kommunikation mellem redox-aktive enheder ift. lineært konjugerede broer, og dette vil blive belyst ved studier på en samling redox-aktive systemer afledt af TTF. Alkyn-udvidede quinoid-strukturer er krydskonjugerede strukturer, som også vil blive behandlet; de er redox-aktive systemer hørende til Wurster-typen, hvilket betyder, at de opnår aromaticitet ved reduktion. Dicyano-funktionaliserede vinylheptafulvener (VHF'er) er krydskonjugerede molekyler, som kan dannes ved fotoisomerisering af relaterede DHA'er. Ikke blot afhænger de optiske egenskaber af disse molekyler af, hvorvidt funktionelle grupper er placeret i kryds- eller lineær konjugation til kernerne, men også DHA-VHF omdannelserne afhænger heraf. Jeg vil i særdeleshed vise systematiske kinetiskstudier af VHF's termiske ringlukningsreaktion til DHA som en funktion af placering og elektroniske karakter af substituentgrupper. Graden af  $\pi$ -elektrondelokalisering er også bestemmende for enkelt-molekyle-ledningsevnen, som er blevet studeret for både DHA/VHF systemet og redox-aktive, cruciform-lignende molekulære ledninger afledt af TTF. Min forskning er syntesedrevet, og synteseprotokoller til opnåelse eller funktionalisering af en stor samling krydskonjugerede molekyler vil blive gennemgået. Alkynkoblingsreaktioner spiller en stor rolle for mange af synteserne, og det plane tetraethynylethen (TEE) molekyle er blevet brugt som broenhed imellem funktionelle grupper i mange af systemerne.



## LIST OF ABBREVIATIONS

Ac	acetyl
Ar	aryl
Bu	butyl
cat.	catalyst
CC	coupled cluster
CT	charge transfer
CuAAC	Copper Catalyzed Azide-Alkyne Cycloaddition
<i>d</i>	deuterium
DCC	dicyclohexyl carbodiimide
DCE	1,2-dichloroethane
dba	dibenzylideneacetone
DDQ	4,5-dichloro-3,6-dioxo-1,4-cyclohexadiene-1,2-dicarbonitrile
DHA	dihydroazulene ( <i>usually referring to the 1,8a-dihydroazulene</i> )
DIBAL-H	diisobutylaluminium hydride
DMF	<i>N,N</i> -dimethylformamide
dpephos	bis[(2-diphenylphosphino)phenyl] ether
DTF	dithiafulvene ( <i>1,4-dithiafulvene</i> )
Ed.	editor
EDG	electron-donating group
Et	ethyl
EWG	electron-withdrawing group
ext	extended
Fc	ferrocene
GC	gas chromatography
Hex	hexyl
HOMO	highest occupied molecular orbital
IF	indeno[1,2- <i>bc</i> ]fluorene
LiHMDS	lithium hexamethyldisilazide
LN	lithium naphthalenide
LUMO	lowest unoccupied molecular orbital
Me	methyl
MS	mass spectrometry or molecular sieves
MW	microwave

## List of Abbreviations

NaHMDS	sodium hexamethyldisilazide
NBS	<i>N</i> -bromosuccinimide
NLO	non-linear optical
NMR	nuclear magnetic resonance
NOE	nuclear Overhauser effect
OPE	oligo(phenyleneethynylene)
OPV	oligo(phenylenevinylene)
PA	polyacetylene
PAH	polycyclic aromatic hydrocarbon
PDA	poly(diacetylene)
PDI	perylene diimide
Ph	phenyl
Pr	propyl
PTA	poly(triacetylene)
Ref.	reference
RuAAC	Ruthenium Catalyzed Azide-Alkyne Cycloaddition
RuPhos	2-dicyclohexylphosphino-2',6'-diisopropoxybiphenyl
S <sub>N</sub>	nucleophilic substitution
SubPc	subphthalocyanine
TBDMS	<i>tert</i> -butyldimethylsilyl
TCCA	trichloroisocyanuric acid
TCNQ	7,7,8,8-tetracyanoquinodimethane
TEE	tetraethynylethene ( <i>3,4-diethynylhexa-3-en-1,5-diyne</i> )
THF	tetrahydrofuran
TMEDA	<i>N,N,N',N'</i> -tetramethylethylenediamine
Tf	triflic
Ts	<i>p</i> -toluenesulfonyl (tosyl)
TTF	tetrathiafulvalene
UV	ultraviolet
VHF	vinylheptafulvene
Vis	visible

# PUBLICATIONS

**This thesis covers work from the publications listed below**

*Senior author(s) is/are indicated by a \* for each publication.*

*Original Research Papers (and references to chapters were selected parts are covered to a minor or large degree):*

- M. B. Nielsen, M. Schreiber, Y. G. Baek, P. Seiler, S. Lecomte, C. Boudon, R. R. Tykwinski, J.-P. Gisselbrecht, V. Gramlich, P. J. Skinner, C. Bosshard, P. Günter, M. Gross, F. Diederich\*, "Highly Functionalized Dimeric Tetraethynylethenes and Expanded Radialenes: Strong Evidence for Macrocyclic Cross-conjugation," *Chem. Eur. J.* **2001**, 7, 3263-3280. (*Post-doctoral work*)

CHAPTER

1
- M. B. Nielsen, N. F. Utesch, N. N. P. Moonen, C. Boudon, J.-P. Gisselbrecht, S. Concilio, S. P. Piotto, P. Seiler, P. Günter, M. Gross, F. Diederich\*, "Novel Extended Tetrathiafulvalenes Based on Acetylenic Spacers: Synthesis and Electronic Properties," *Chem. Eur. J.* **2002**, 8, 3601-3613. (*Post-doctoral work*)

CHAPTER

2
- E. Burri, F. Diederich\*, M. B. Nielsen\*, "Synthesis and Characterization of Multinanometer-Sized Expanded Dendralenes with an *iso*-Poly(triacetylene) Backbone," *Helv. Chim. Acta* **2002**, 85, 2169-2182. (*Post-doctoral work*)

CHAPTER

1
- C. Lepetit, M. B. Nielsen, F. Diederich, R. Chauvin\*, "Aromaticity and electron affinity of *carbo*<sup>k</sup>-[3]radialenes, *k* = 0, 1, 2," *Chem. Eur. J.* **2003**, 9, 5056-5066.

CHAPTER

1
- M. B. Nielsen\*, "Synthesis of New Tetrathiafulvalene Modules for Acetylenic Scaffolding," *Synlett* **2003**, 1423-1426.

CHAPTER

6
- M. B. Nielsen\*, J.-P. Gisselbrecht, N. Thorup, S. P. Piotto, C. Boudon, M. Gross, "Synthesis and characterisation of alkene-extended tetrathiafulvalenes with lateral alkyne appendages," *Tetrahedron Lett.* **2003**, 44, 6721-6723.

CHAPTER

3

CHAPTER

6
- K. Qvortrup, A. S. Andersson, J.-P. Mayer, A. S. Jepsen, M. B. Nielsen\*, "Cross-coupling Reactions with Acetylenic Dithiafulvenes," *Synlett* **2004**, 2818-2820.

CHAPTER

2

CHAPTER

3

CHAPTER

6
- K. Qvortrup, M. T. Jakobsen, J.-P. Gisselbrecht, C. Boudon, F. Jensen, S. B. Nielsen\*, M. B. Nielsen\*, "Donor strength of  $\pi$ -extended tetrathiafulvalenes: Ionisation energies vs. oxidation potentials. A joint theoretical and experimental study," *J. Mater. Chem.* **2004**, 14, 1768-1773.

CHAPTER

6

- A. S. Andersson, K. Qvortrup, E. R. Torbensen, J.-P. Mayer, J.-P. Gisselbrecht, C. Boudon, M. Gross, A. Kadziola, K. Kilså, M. B. Nielsen\*, "Synthesis and Characterization of Extended Tetrathiafulvalenes with Di-, Tri-, and Tetraethynylethene Cores," *Eur. J. Org. Chem.* **2005**, 3660-3671.
- M. B. Nielsen\*, J. C. Petersen, N. Thorup, M. Jessing, A. S. Andersson, A. S. Jepsen, J.-P. Gisselbrecht, C. Boudon, M. Gross, "Acetylenic dithiafulvene derived donor- $\pi$ -acceptor dyads: synthesis, electrochemistry and non-linear optical properties," *J. Mater. Chem.* **2005**, 15, 2599-2605.
- J. K. Sørensen, M. Vestergaard, A. Kadziola, K. Kilså, M. B. Nielsen\*, "Synthesis of Oligo(phenyleneethynylene) – Tetrathiafulvalene Cruciforms for Molecular Electronics," *Org. Lett.* **2006**, 8, 1173-1176.
- A. S. Andersson, K. Kilså, T. Hassenkam, J.-P. Gisselbrecht, C. Boudon, M. Gross, M. B. Nielsen\*, F. Diederich\*, "Synthesis and Characteristics of a Non-aggregating Tris(tetrathiafulvaleno)dodecadehydro[18]annulene," *Chem. Eur. J.* **2006**, 12, 8451-8459.
- M. Å. Petersen, L. Zhu, S. H. Jensen, A. S. Andersson, A. Kadziola, K. Kilså\*, M. B. Nielsen\*, "Photoswitches Containing the Dithiafulvene Electron Donor," *Adv. Funct. Mater.* **2007**, 17, 797-804.
- M. Å. Petersen, K. Kilså, A. Kadziola, M. B. Nielsen\*, "A Novel Route to a Bromo-Cyano-substituted Azulene and Exploitation hereof in the Construction of Conjugated Acetylenic Scaffolds," *Eur. J. Org. Chem.* **2007**, 1415-1418.
- M. B. Nielsen\*, S. P. A. Sauer, "On the aromaticity of tetrathiafulvalene cations," *Chem. Phys. Lett.* **2008**, 453, 136-139.
- M. Vestergaard, K. S. Jennum, J. K. Sørensen, K. Kilså, M. B. Nielsen\*, "Synthesis and Characterization of Cruciform-conjugated Oligomers Based on Tetrathiafulvalene," *J. Org. Chem.* **2008**, 73, 3175-3183.
- M.-B. S. Kirketerp, M. Å. Petersen, M. Wanko, L. A. E. Leal, H. Zettergren, F. M. Raymo, A. Rubio\*, M. B. Nielsen\*, S. B. Nielsen\*, "Absorption Spectra of 4-Nitrophenolate Ions measured *in Vacuo* and in Solution," *ChemPhysChem* **2009**, 10, 1207-1209.
- M. Å. Petersen, A. S. Andersson, K. Kilså\*, M. B. Nielsen\*, "Redox-Controlled Dihydroazulene-Vinylheptafulvene Photoswitch Incorporating Tetrathiafulvalene," *Eur. J. Org. Chem.* **2009**, 1855-1858.
- M. Å. Petersen, S. L. Broman, A. Kadziola, K. Kilså, M. B. Nielsen\*, "Dihydroazulene Photoswitches: The First Synthetic Protocol for Functionalizing the Seven-Membered Ring," *Eur. J. Org. Chem.* **2009**, 2733-2736. *Highlighted in SYNFACTS 2009*, 978.
- M. H. Vilhelmsen, A. S. Andersson, M. B. Nielsen\*, "Synthesis of 1-Chloroalkynes from Alkynylsilanes Using trichloroisocyanuric Acid as Chlorinating Agent," *Synthesis* **2009**, 1469-1472; *Synthesis* **2011**, 158.

CHAPTER 236

CHAPTER 2

CHAPTER 5

CHAPTER 2

CHAPTER 4

CHAPTER 6

CHAPTER 11

CHAPTER 5












CHAPTER 2

CHAPTER 4

CHAPTER 26













CHAPTER 6



- D. Shanks, S. Preus, K. Qvortrup, T. Hassenkam, M. B. Nielsen\*, K. Kilså\*, "Excitation Energy Transfer in Novel Acetylenic Perylene Diimide Scaffolds," *New J. Chem.* **2009**, 33, 507-516. 
- A. S. Andersson, L. Kerndrup, A. Ø. Madsen, K. Kilså, M. B. Nielsen\*, P. R. La Porta, I. Biaggio, "Synthesis and Characterization of Tetrathiafulvalene-Substituted Di- and Tetraethynylethenes with *p*-Nitrophenyl Acceptors," *J. Org. Chem.* **2009**, 74, 375-382. 
- S. L. Broman, M. Å. Petersen, C. Tortzen, A. Kadziola, K. Kilså, M. B. Nielsen\*, "Arylethynyl Derivatives of the Dihydroazulene / Vinylheptafulvene Photo/Thermoswitch – Tuning the Switching Event," *J. Am. Chem. Soc.* **2010**, 132, 9165-9174. 
- S. L. Broman, S. L. Brand, C. R. Parker, M. Å. Petersen, C. G. Tortzen, A. Kadziola, K. Kilså, M. B. Nielsen\*, "Optimized synthesis and detailed NMR spectroscopic characterization of the 1,8a-dihydroazulene-1,1-dicarbonitrile photoswitch," *Arkivoc* **2011**, ix, 51-67. 
- L. Skov, M. Å. Petersen, S. L. Broman, A. D. Bond, M. B. Nielsen\*, "New synthetic route to substituted dihydroazulene photoswitches," *Org. Biomol. Chem.* **2011**, 9, 6498-6501. 
- K. Jennum, M. Vestergaard, A. H. Pedersen, J. Fock, J. Jensen, M. Santella, J. J. Led, K. Kilså, T. Bjørnholm, M. B. Nielsen\*, "Synthesis of Oligo(phenyleneethynylene)s with Vertically Disposed Tetrathiafulvalene Units," *Synthesis* **2011**, 539-548. 
- T. H. Jepsen, M. Larsen, M. Jørgensen, M. B. Nielsen\*, "An efficient protocol for synthesizing dibenzodithiapentalenes," *Tetrahedron Lett.* **2011**, 52, 4045-4047. *Highlighted in SYNFACTS* **2011**, 950. 
- T. H. Jepsen, M. Larsen\*, M. Jørgensen, K. A. Solanko, A.D. Bond, A. Kadziola, M. B. Nielsen\*, "Synthesis of Functionalized Dibenzothiophenes – An Efficient Three-Step Approach Based on Pd-Catalyzed C-C and C-S Bond Formations," *Eur. J. Org. Chem.* **2011**, 53-57. 
- M. Å. Petersen\*, S. L. Broman, K. Kilså, A. Kadziola, M. B. Nielsen\*, "Gaining Control: Direct Suzuki Arylation of Dihydroazulenes and Tuning of Photo/Thermochromism," *Eur. J. Org. Chem.* **2011**, 1033-1039. 
- C. R. Parker, C. G. Tortzen, S. L. Broman, M. Schau-Magnussen, K. Kilså, M. B. Nielsen\*, "Lewis acid enhanced switching of the 1,1-dicyanodihydroazulene / vinylheptafulvene photo/thermoswitch," *Chem. Commun.* **2011**, 47, 6102-6104. 
- M.-B. S. Kirketerp, L. A. E. Leal, D. Varsano, A. Rubio\*, T. J. D. Jørgensen, K. Kilså, M. B. Nielsen\*, S. B. Nielsen\*, "On the Intrinsic Optical Absorptions by Tetrathiafulvalene Radical Cations and Isomers," *Chem. Commun.* **2011**, 47, 6900-6902. 

- M. Wanko, J. Houmøller, K. Støchkel, M.-B. S. Kirketerp, M. Å. Petersen, M. B. Nielsen, S. B. Nielsen\*, A. Rubio\*, "Substitution effects on the absorption spectra of nitrophenolate isomers," *Phys. Chem. Chem. Phys.* **2012**, *14*, 12905-12911. CHAPTER 2
- K. Lincke, A. F. Frellsen, C. R. Parker, A. D. Bond, O. Hammerich, M. B. Nielsen\*, "A Tetrathiafulvalene-Functionalized Radiaannulene with Multiple Redox States," *Angew. Chem. Int. Ed.* **2012**, *51*, 6099-6102. CHAPTER 1 CHAPTER 3
- S. L. Broman, A. U. Petersen, C. G. Tortzen, J. Vibenholt, A. D. Bond, M. B. Nielsen\*, "A Bis(heptafulvenyl)dicyanoethylene Thermoswitch with Two Sites for Ring-Closure," *Org. Lett.* **2012**, *14*, 318-321. CHAPTER 6
- J. Fock, M. Leijnse, K. Jennum, A. S. Zyazin, J. Paaske, P. Hedegård, M. B. Nielsen, H. S. J. van der Zant, "Manipulation of organic polyradicals in a single-molecule transistor," *Phys. Rev. B.* **2012**, *86*, 235403. CHAPTER 5
- V. Mazzanti, M. Cacciarini, S. L. Broman, C. R. Parker, M. Schau-Magnussen, A. D. Bond, M. B. Nielsen\*, "On the bromination of the dihydroazulene/vinylheptafulvene photo-/thermoswitch," *Beilstein J. Org. Chem.* **2012**, *8*, 958-966. CHAPTER 2 CHAPTER 4 CHAPTER 6
- S. L. Broman, S. Lara-Avila, C. L. Thisted, A. D. Bond, S. Kubatkin, A. Danilov\*, M. B. Nielsen\*, "Dihydroazulene Photoswitch operating in Sequential Tunneling Regime: Synthesis and Single-Molecule Junction Studies," *Adv. Funct. Mater.* **2012**, *22*, 4249-4258. CHAPTER 5 CHAPTER 6
- M. Santella, V. Mazzanti, M. Jevric, C. R. Parker, S. L. Broman, A. D. Bond, M. B. Nielsen\*, "Dihydroazulene – Buckminsterfullerene Conjugates," *J. Org. Chem.* **2012**, *77*, 8922-8932. CHAPTER 4
- M. Cacciarini\*, E. A. Della Pia, M. B. Nielsen, "Colorimetric Probe for the Detection of Thiols: the Dihydroazulene/Vinylheptafulvene System," *Eur. J. Org. Chem.* **2012**, 6064-6069. CHAPTER 6
- C. R. Parker, Z. Wei, C. A. Rodríguez, K. Jennum, T. Li, M. Santella, N. Bovet, G. Yhao, W. Hu, H. S. J. van der Zant, M. Vanin, G. C. Solomon, B. W. Laursen, K. Nørgaard, M. B. Nielsen\*, "A New Class of Extended Tetrathiafulvalene Cruciform Molecules for Molecular Electronics with Dithiafulvene-4,5-dithiolate Anchoring Groups," *Adv. Mater.* **2013**, *25*, 405-409. CHAPTER 5 CHAPTER 6
- T. Li, M. Jevric, J. R. Hauptmann, R. Hviid, Z. Wei, R. Wang, N. E. A. Reeler, E. Thyrhaug, S. V. Petersen, J. A. S. Meyer, N. E. Bovet, T. A. J. Vosch, J. Nygård, X. Qiu, W. Hu, Y. Liu, G. C. Solomon, H. G. Kjaergaard, T. Bjørnholm, M. B. Nielsen, B. W. Laursen\*, K. Nørgaard\*, "Ultrathin Reduced Graphene Oxide Films as Transparent Top-Contacts for Light Switchable Solid-State Molecular Junctions," *Adv. Mater.* **2013**, *25*, 4164-4170. CHAPTER 5
- M. Jevric, S. L. Broman, M. B. Nielsen\*, "Palladium-mediated Strategies for Functionalizing the Dihydroazulene Photoswitch: Paving the Way for its Exploitation in Molecular Electronics," *J. Org. Chem.* **2013**, *78*, 4348-4356. CHAPTER 5

- S. L. Broman, M. Jevric, M. B. Nielsen\*, "Linear Free-energy Correlations for the Vinylheptafulvene Ring Closure: a Probe for Hammett  $\sigma$  values," *Chem. Eur. J.* **2013**, *19*, 9542-9548. CHAPTER 14
- O. Schalk, S. L. Broman, M. Å. Petersen, D. V. Khakhulin, R. Y. Brogaard, M. B. Nielsen, A. E. Boguslavkiy, A. Stolow, T. I. Sølling\*, "On the Condensed Phase Ring-Closure of Vinylheptafulvalene and Ring-Opening of Gaseous Dihydroazulene," *J. Phys. Chem. A* **2013**, *117*, 3340-3347. CHAPTER 2
- M. H. Vilhelmsen\*, J. Jensen, C. G. Tortzen, M. B. Nielsen\*, "The Glaser-Hay Reaction: Optimization and Scope based on  $^{13}\text{C}$ -NMR Kinetics Experiments," *Eur. J. Org. Chem.* **2013**, 701-711. CHAPTER 6
- S. S. Schou, C. R. Parker, K. Lincke, K. Jennum, J. Vibenholt, A. Kadziola, M. B. Nielsen\*, "On the phosphite-mediated synthesis of dithiafulvenes and  $\pi$ -extended tetrathiafulvalenes," *Synlett* **2013**, *24*, 231-235. CHAPTER 2 CHAPTER 6
- M. A. Christensen, M. Rimmen, M. B. Nielsen\*, "Unsymmetrical coupling of 1-chloroalkynes and terminal alkynes under experimental Sonogashira conditions," *Synlett* **2013**, *24*, 2715-2719. CHAPTER 6
- M. A. Christensen, E. A. Della Pia, J. Houmøller, S. Thomsen, M. Wanko, A. D. Bond, A. Rubio, S. B. Nielsen, M. B. Nielsen\*, "Cross-Conjugation vs. Linear Conjugation in Donor-Bridge-Acceptor Nitrophenol Chromophores," *Eur. J. Org. Chem.* **2014**, 2044-2052. CHAPTER 2
- K. Fjelbye, T. N. Christensen, M. Jevric, S. L. Broman, A. U. Petersen, A. Kadziola, M. B. Nielsen\*, "Comparison of Linear and Cross-Conjugation from Rates of Vinylheptafulvene Ring-Closures," *Eur. J. Org. Chem.* **2014**, 7859-7864. CHAPTER 4
- H. Lissau, S. L. Broman, M. Jevric, A. Ø. Madsen, M. B. Nielsen\*, "CuAAC and RuAAC with Alkyne-functionalised Dihydroazulene Photoswitches and Determination of Hammett  $\sigma$ -Constants for Triazoles," *Aust. J. Chem.* **2014**, *67*, 531-534. CHAPTER 4
- S. L. Broman, M. Jevric, A. D. Bond, M. B. Nielsen\*, "Syntheses of Donor-Acceptor Functionalized Dihydroazulenes," *J. Org. Chem.* **2014**, *79*, 41-64. CHAPTER 4 CHAPTER 6
- C. R. Parker, E. Leary\*, R. Frisenda, Z. Wei\*, K. S. Jennum, E. Glibstrup, P. B. Abrahamsen, M. Santella, M. A. Christensen, E. A. Della Pia, T. Li, M. T. Gonzalez, B. W. Laursen, K. Nørgaard, H. van der Zant\*, N. Agraït, M. B. Nielsen\*, "A Comprehensive Study of Extended Tetrathiafulvalene Cruciform Molecules for Molecular Electronics: Synthesis and Electrical Transport Measurements," *J. Am. Chem. Soc.* **2014**, *136*, 16497-16507. CHAPTER 5 CHAPTER 6
- V. Mazzanti, J. Huixin, H. Gotfredsen, T. J. Morsing, C. R. Parker, M. B. Nielsen\*, "The Gilded Edge in Acetylenic Scaffolding: Pd-Catalyzed Cross-Coupling Reactions of Phosphine-Gold(I) Oligoynyl Complexes," *Org. Lett.* **2014**, *16*, 3736-3739. CHAPTER 6

- M. A. Christensen, C. R. Parker, T. J. Sørensen, S. de Graaf, T. J. Morsing, T. Brock-Nannestad, J. Bendix, M. M. Haley, P. Raptá, A. Danilov, S. Kubatkin, O. Hammerich\*, M. B. Nielsen\*, "Mixed Valence Radical Cations and Intermolecular Complexes Derived from Indenofluorene-Extended Tetrathiafulvalenes," *J. Mater. Chem. C* **2014**, 2, 10428-10438. 
- M. A. Christensen, G. E. Rudebusch, C. R. Parker, C. L. Andersen, A. Kadziola, M. M. Haley\*, O. Hammerich\*, M. B. Nielsen\*, "Diindenoethienoacene-tetrathiafulvalene redox systems," *RSC Adv.* **2015**, 5, 49748-49751. 
- H. Jiang, V. Mazzanti, C. R. Parker, S. L. Broman, J. H. Wallberg, K. Lušpai, A. Brincko, H. G. Kjaergaard, A. Kadziola, P. Raptá\*, O. Hammerich\*, M. B. Nielsen\*, "Interactions between Tetrathiafulvalene Units in Dimeric Structures – The Influence of Cyclic Cores," *Beilstein J. Org. Chem.* **2015**, 11, 930-948.  
- A. U. Petersen, S. L. Broman, S. T. Olsen, A. S. Hansen, L. Du, A. Kadziola, T. Hansen, H. G. Kjaergaard, K. V. Mikkelsen, M. B. Nielsen\*, "Controlling Two-Step Multimode Switching of Dihydroazulene Photoswitches," *Chem. Eur. J.* **2015**, 21, 3968-3977. 
- M. Cacciarini, A. B. Skov, M. Jevric, A. S. Hansen, J. Elm, H. G. Kjaergaard, K. V. Mikkelsen, M. B. Nielsen\*, "Towards Solar Energy Storage in the Photochromic Dihydroazulene-Vinylheptafulvene System," *Chem. Eur. J.* **2015**, 21, 7454-7461. 
- S. L. Broman\*, O. Kushnir, M. Rosenberg, A. Kadziola, J. Daub, M. B. Nielsen, "Dihydroazulene / Vinylheptafulvene Photoswitch: Ultrafast Back-reaction Induced by Dihydronaphthalene Annulation," *Eur. J. Org. Chem.* **2015**, 4119-4130. 
- M. H. Larsen\*, M. B. Nielsen, "The Gilded Edge in Acetylenic Scaffolding II: A Computational Study of the Transmetalation Processes Involved in Pd-Catalyzed Cross-Couplings of Gold(I) Acetylides," *Organometallics* **2015**, 34, 3678-3685. 
- J. F. Petersen, C. G. Tortzen, F. P. Jørgensen, C. R. Parker, M. B. Nielsen\*, "Phosphite-mediated conversion of benzaldehydes into stilbenes via umpolung through dioxaphospholane intermediate," *Tetrahedron Lett.* **2015**, 56, 1894-1897. 
- H. Lissau, R. Frisenda, S. T. Olsen\*, M. Jevric, C. R. Parker, A. Kadziola, T. Hansen, H. S. J. van der Zant\*, M. B. Nielsen\*, K. V. Mikkelsen, "Tracking Molecular Resonance Forms of Donor-Acceptor Push-Pull Molecules by Single-Molecule Conductance Experiments," *Nature Commun.* **2015**, 6:10233. 
- H. Gotfredsen, M. Jevric, A. Kadziola, M. B. Nielsen\*, "Acetylenic Scaffolding with Subphthalocyanines," *Eur. J. Org. Chem.* **2016**, 17-21. 
- H. Gotfredsen, M. Jevric, S. L. Broman, A. U. Petersen, M. B. Nielsen\*, "Aluminum Chloride Mediated Alkynylation of Boron Subphthalocyanine Chloride Using Trimethylsilyl-Capped Acetylenes," *J. Org. Chem.* **2016**, 81, 1-5. 

## Publications

- M. Mansø, M. Koole, M. Mulder, I. J. Olavarria-Contreras, C. L. Andersen, M. Jevric, S. L. Broman, A. Kadziola, O. Hammerich, H. S. J. van der Zant\*, M. B. Nielsen\*, "Synthesis and Single-Molecule Conductances of Neutral and Cationic Indenofluorene-Extended Tetrathiafulvalenes – Kondo Effect Molecules," *J. Org. Chem.* **2016**, *81*, 8406-8414. CHAPTER 5
- M. Cacciarini\*, M. Jevric, J. Elm, A. U. Petersen, K. V. Mikkelsen, M. B. Nielsen, "Fine-tuning the lifetimes and energy storage capacities of meta-stable vinylheptafulvenes *via* substitution at the vinyl position," *RSC Adv.* **2016**, *6*, 49003-49010. CHAPTER 6
- M. D. Kilde, S. L. Broman, A. Kadziola, M. B. Nielsen\*, "On the solvent dependent bromination of dihydroazulenes," *Synlett* **2016**, *27*, 450-454. CHAPTER 6
- A. U. Petersen, M. Jevric, J. Elm, S. T. Olsen, C. G. Tortzen, A. Kadziola, K. V. Mikkelsen, M.B. Nielsen\*, "Azulenium chemistry – towards new derivatives of photochromic dihydroazulenes," *Org. Biomol. Chem.* **2016**, *14*, 2403-2412. CHAPTER 6
- A. Vlasceanu, C. L. Andersen, C. R. Parker, O. Hammerich, T. J. Morsing, M. Jevric, S. L. Broman, A. Kadziola, M. B. Nielsen\*, "Multistate Switches: Ruthenium Alkynyl – Dihydroazulene / Vinylheptafulvene Conjugates," *Chem. Eur. J.* **2016**, *22*, 7514-7523. CHAPTER 4
- A. Vlasceanu, S. L. Broman, A. S. Hansen, A. B. Skov, M. Cacciarini, A. Kadziola, H. G. Kjaergaard, K. V. Mikkelsen, M. B. Nielsen\*, "Solar Thermal Energy Storage in a Photochromic Macrocycle," *Chem. Eur. J.* **2016**, *22*, 10796-101800. CHAPTER 4 CHAPTER 6
- A. B. Skov, S. L. Broman, A. S. Gertsen, J. Elm\*, M. Jevric, M. Cacciarini, A. Kadziola, K. V. Mikkelsen\*, M. B. Nielsen\*, "Aromaticity-Controlled Energy Storage Capacity of the Dihydroazulene-Vinylheptafulvene Photochromic System," *Chem. Eur. J.* **2016**, *22*, 14567-14575. CHAPTER 4 CHAPTER 6
- M. D. Kilde, M. H. Hansen, S. L. Broman, K. V. Mikkelsen\*, M. B. Nielsen\*, "Expanding the Hammett Correlations for the Vinylheptafulvene Ring-Closure Reaction," *Eur. J. Org. Chem.* **2017**, 1052-1062. CHAPTER 4 CHAPTER 6
- F. P. Jørgensen, J. F. Petersen, C. L. Andersen, A. B. Skov, M. Jevric, O. Hammerich, M. B. Nielsen\*, "Synthesis of Covalently Linked Oligo(phenyleneethynylene) Wires Incorporating Dithiafulvene Units – Redox-Active "H-Cruciforms," *Eur. J. Org. Chem.*, In press. DOI: 10.1002/ejoc.201601367 CHAPTER 6
- S. L. Broman, C. L. Andersen, T. Jouselin-Oba, M. Mansø, O. Hammerich, M. Frigoli\*, M. B. Nielsen\*, "Tetraceno[2,1,12,11-*opqra*]tetracene-extended tetrathiafulvalene – redox-controlled generation of a large PAH core," *Org. Biomol. Chem.* **2017**, *15*, 807-811. CHAPTER 3
- A. B. Skov, J. F. Petersen, J. Elm, B. N. Frandsen, M. Santella, M. D. Kilde, H. G. Kjaergaard, K. V. Mikkelsen, M. B. Nielsen\*, "Towards Storage of Solar Energy in Photochromic Molecules: Benzannulation of the CHAPTER 4 CHAPTER 6

Dihydroazulene/Vinylheptafulvene Couple," *ChemPhotoChem*, In press. DOI: 10.1002/cptc.201600046

- C. Huang, M. Jevric, A. Borges, S. T. Olsen, J. Hamill, A. Rudnev, M. Baghernejad, P. Broekman, T. Wandlowski, K. V. Mikkelsen\*, G. C. Solomon\*, M. B. Nielsen\*, W. Hong\*, "Single-molecule detection of dihydroazulene photo-thermal reaction using break junction technique," *Nat. Commun.*, In revision.

CHAPTER  
5

### Review Papers

- J.-P. Gisselbrecht, N. N. P. Moonen, C. Boudon, M. B. Nielsen\*, F. Diederich\*, M. Gross\*, "Redox Properties of Linear and Cyclic Scaffolds Based on Di- and Tetraethynylethene," *Eur. J. Org. Chem.* **2004**, 2959-2972.
- M. B. Nielsen\*, F. Diederich\*, "Conjugated Oligoenynes Based on the Diethynylethene Unit," *Chem. Rev.* **2005**, *105*, 1837-1867.
- M. B. Nielsen\*, S. L. Broman, M. Å. Petersen, A. S. Andersson, T. S. Jensen, K. Kilså, A. Kadziola, "New Routes to Functionalized Dihydroazulene Photoswitches," *Pure Appl. Chem.* **2010**, *82*, 843-852.
- K. Jennum, M. B. Nielsen\*, "Tetrathiafulvalene Based Cruciform Molecules," *Chem. Lett.* **2011**, *40*, 662-667.
- M. B. Nielsen\*, "Molecular Scaffolding with Tetrathiafulvalene – Design and Synthesis of New Molecules for Molecular Electronics," *Phosphorus, Sulfur, and Silicon and the Related Elements* **2011**, *186*, 1055-1073.
- S. B. Nielsen\*, M. B. Nielsen\*, A. Rubio\*, "Spectroscopy of Nitrophenolates *in vacuo*: Effect of Spacer, Configuration, and Microsolvation on the Charge-Transfer Excitation Energy," *Acc. Chem. Res.* **2014**, *47*, 1417-1425.
- S. L. Broman, M. B. Nielsen\*, "Dihydroazulene: from controlling photochromism to molecular electronics devices," *Phys. Chem. Chem. Phys.* **2014**, *16*, 21172-21182.
- M. Cacciarini\*, S. L. Broman, M. B. Nielsen\*, "Synthetic protocols for the key functionalizations of the photochromic dihydroazulene scaffold," *Arkivoc* **2014**, *i*, 249-263.
- M. Jevric\*, M. B. Nielsen\*, "Synthetic Strategies for Oligoenynes," *Asian J. Org. Chem.* **2015**, *4*, 286-295.
- M. B. Nielsen\*, "Molecular Switches," in *Handbook of Single Molecule Electronics* (Ed. K. Moth-Poulsen), Pan Stanford Publishing, **2015**, 233-261.
- C. R. Parker, M. B. Nielsen\*, "Cross-Conjugation in Expanded Systems," in *Cross-Conjugation: Modern Dendralene, Radialene and Fulvene Chemistry* (Eds. H. Hopf, M. S. Sherburn), Wiley-VCH, **2016**, 337-363.
- M. B. Nielsen\*, "Sonogashira-Like Coupling Reactions with Phosphine-Gold(I) Alkynyl Complexes," *Synthesis* **2016**, *48*, 2732-2738.

CHAPTER  
1

CHAPTER  
1

CHAPTER  
6

CHAPTER  
5 CHAPTER  
6

CHAPTER  
5 CHAPTER  
6

CHAPTER  
2

CHAPTER  
4

CHAPTER  
6

CHAPTER  
6

CHAPTER  
5

CHAPTER  
2 CHAPTER  
3

CHAPTER  
6

# CONTENTS

<b>Preface .....</b>	<b>i</b>
<b>Abstract .....</b>	<b>ii</b>
<b>Abstract in Danish (Resumé på dansk) .....</b>	<b>iii</b>
<b>List of Abbreviations .....</b>	<b>iv</b>
<b>Publications .....</b>	<b>vi</b>
<b>1. Introduction .....</b>	<b>1</b>
<b>2. Optical Properties .....</b>	<b>19</b>
<b>3. Redox Properties .....</b>	<b>37</b>
<b>4. Chemical Reactivity .....</b>	<b>51</b>
<b>5. Single-Molecule Conductance Studies .....</b>	<b>67</b>
<b>6. Synthetic Methods .....</b>	<b>81</b>
<b>7. Concluding Remarks .....</b>	<b>107</b>

# INTRODUCTION

## 1.1 Introduction

$\pi$ -Conjugated molecules are important for their optical and redox properties, which are a consequence of their delocalized  $\pi$ -electrons. Chlorophylls and carotenes are thus strong chromophores employed as light-harvesters in Nature and hence involved in the very first step of photosynthesis. In materials science and supramolecular chemistry, development of organic dyes, light-harvesters, fluorophores, molecular sensors, photoswitches, nonlinear optical and conducting materials strongly relies on  $\pi$ -conjugated molecules and polymers with tailored HOMO-LUMO gaps, redox potentials, geometries, and stabilities.<sup>1</sup> Establishment of structure-property relationships by systematic studies of a series of molecules provides knowledge that can be employed to design a next generation of  $\pi$ -conjugated molecules with desired properties.

Two fundamentally different kinds of conjugation exist. Linear conjugation in a molecule corresponds to alternating single and double bonds (or triple bonds). A cross-conjugated molecule has a double bond branching off from the main chain. Thus, one double bond is a bifurcation point with one atom being geminally substituted. These two different bond connectivities are illustrated in Figure 1.1.

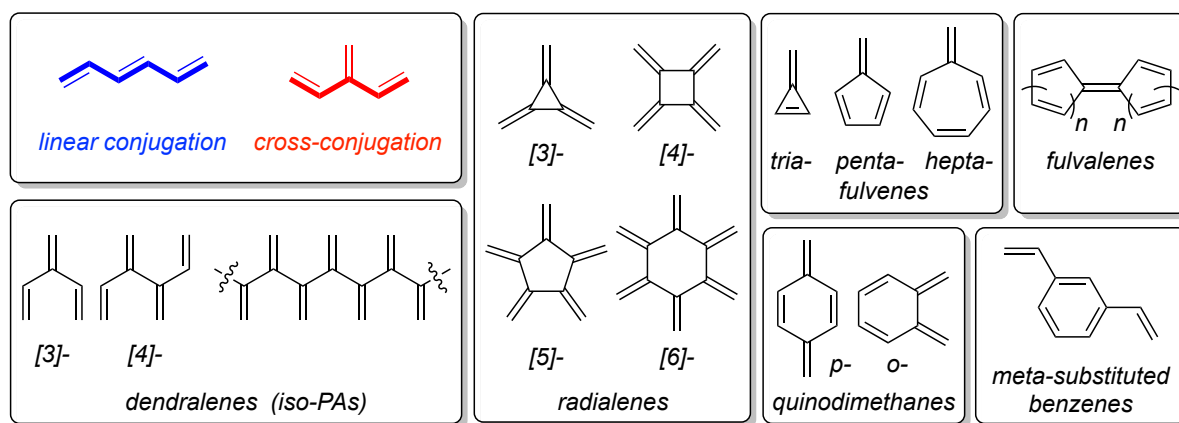


**Figure 1.1.** Arrangements of double bonds in linear vs cross-conjugation, and an overview of the most important classes of cross-conjugated molecules.

Cross-conjugated oligoenes can be divided in several classes<sup>2,3</sup> as exemplified in Figure 1.1:

- Dendralenes*, which are acyclic oligoenes;<sup>4</sup>
- Radialenes*, which are cyclic oligoenes where all double bonds are exocyclic and there are as many double bonds as possible (all-*exo*-methylenecycloalkanes; but the



name is also generally used for polycyclic systems with the maximum number of exocyclic double bonds, *e.g.* naphtharadialene containing one fused, endocyclic, double bond between two 6-membered rings);<sup>5</sup>

iv) Fulvenes, which are cyclic molecules with endocyclic double bonds and one exocyclic one (hence containing an odd number of carbon atoms in the ring);<sup>6</sup>

v) *Fulvalenes*, which contain two fulvene rings connected via one common exocyclic double bond;<sup>7</sup>

iii) *Quinoid structures*, such as quinodimethanes;<sup>8</sup>

vi) *meta-Substituted benzene rings*.

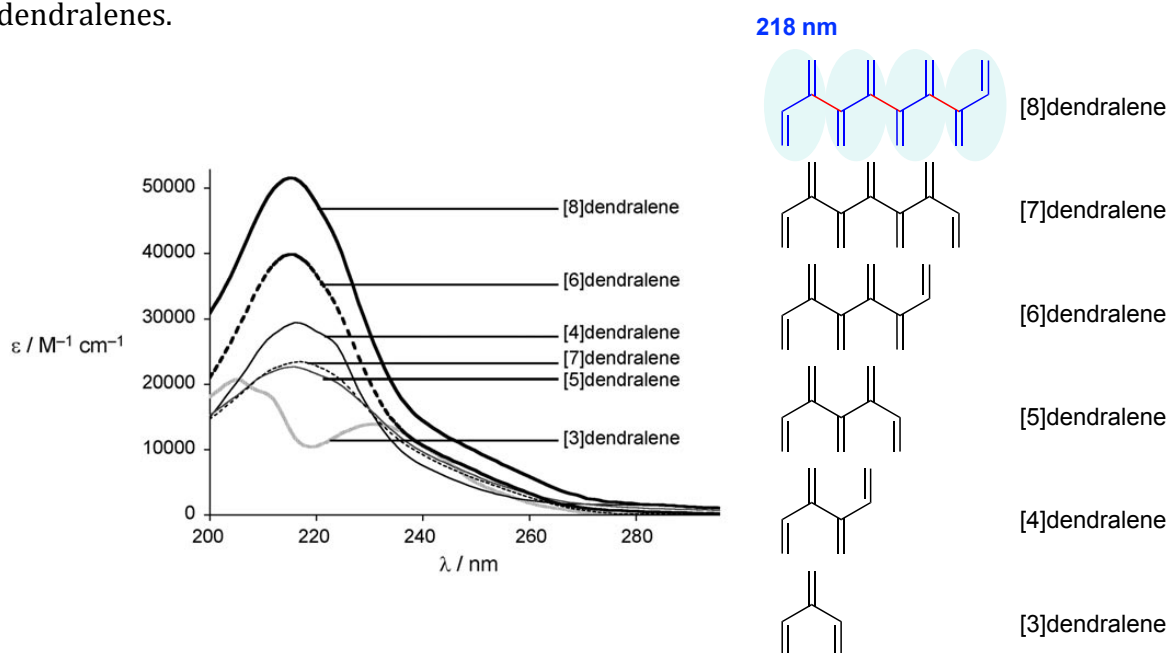
There are several combinations of the above classes, and larger cyclic structures that both have endocyclic and exocyclic double bonds have been termed *radiaannulenes*<sup>9</sup> as they are mixtures of radialenes and annulenes, where the latter only have endocyclic double bonds. Carbon atoms can be substituted for heteroatoms in the structures, and double bonds can be substituted for triple bonds, or the structures can be expanded by insertion of unsaturated units, such as aromatic rings and triple bonds. The name “*carbo-mer*” has been introduced by Chauvin and co-workers for molecules, which are obtained by insertion of C<sub>2</sub> units into all the bonds of a parent structure.<sup>10</sup> Usually, however, “partial *carbo-mers*” are studied in which the insertion of C<sub>2</sub> units is only applied over a selection of the molecule. For example, a “ring *carbo-mer*” corresponds to insertion of C<sub>2</sub> units into all bonds of the parent ring structure.

Synthesis of acyclic and cyclic  $\pi$ -systems benefits from the large arsenal of metal-catalyzed reactions available today for making carbon-carbon bonds between two sp<sup>2</sup>-hybridized carbon atoms, between two sp-hybridized carbon atoms, or between an sp<sup>2</sup>- and an sp-hybridized carbon atom, such as the Glaser-Eglinton-Hay, Heck, Negishi, Stille, Sonogashira, and Suzuki couplings.<sup>11</sup> My work is strongly synthesis-driven and as will become apparent in the forthcoming chapters, such coupling reactions have been crucial for achieving most of our target molecules.

## 1.2 Dendralenes and Radialenes

Let us first consider the optical properties of the simplest cross-conjugated oligoenes, the dendralenes, in comparison to the corresponding linearly conjugated oligoenes. These classes of compounds are also called *iso*-poly(acetylene)s (*iso*-PAs) and poly(acetylene)s (PAs), respectively. For the linearly conjugated PAs, the longest-wavelength absorption maximum increases when proceeding from the triene to the decaene by ca. 25 nm for each alkene unit added.<sup>12</sup> On the contrary, Paddon-Row, Sherburn, and co-workers have shown that the [4]- to [8]dendralenes exhibit almost the same absorption maximum around 215-217 nm (in hexane),<sup>13</sup> which is close to that

of butadiene (217.5 nm in ethanol and 218.5 nm in cyclohexane<sup>14</sup>). The smaller [3]dendralene (3-methylene-1,4-pentadiene) behaves slightly different, exhibiting absorption maxima at 206 and 231 nm in hexane. Electron diffraction studies indicate that this molecule is non-planar, taking an *anti*, *skew* conformation with a dihedral angle of 40° between the planes of the *anti*-butadiene part and the vinyl group.<sup>15</sup> The absorption spectra of the series of dendralenes are shown in Figure 1.2 (an absorption tail to the strong absorption around 215-217 nm should be noted for all the compounds). Calculations reveal that even-numbered dendralenes can be described as planar *s-trans* butadiene units where each butadiene unit is almost orthogonal to the adjacent ones, which is in line with the similar absorption maximum to that of butadiene. The effective conjugation length thus corresponds to two monomer (ethylene) units. From these studies, it is clear that  $\pi$ -electron delocalization in cross-conjugated dendralenes is less efficient than in linearly conjugated oligoenes. Another interesting observation can be made from Figure 1.2 in regard to the molar absorptivities.<sup>13</sup> For dendralenes with an even number of ethylene units, the molar absorptivity increases by ca. 5.000 M<sup>-1</sup> cm<sup>-1</sup> per unit, while dendralenes with an uneven number of ethylene units have lower molar absorptivities than could be expected. Thus, the [4]dendralene has a higher molar absorptivity than the [5]- and [7]dendralenes. In regard to chemical reactivity, there is also a significant difference between “odd” and “even” dendralenes, the former being more reactive as well as more selective in cycloaddition reactions.<sup>16</sup> Thus, mono-cycloadducts can be isolated in high yields from “odd” dendralenes, while complex mixtures result from the “even” dendralenes.

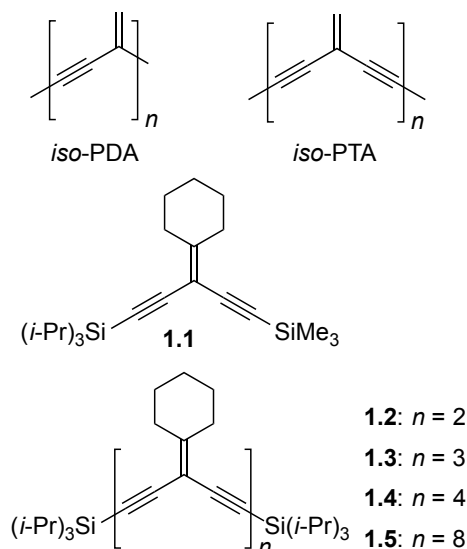
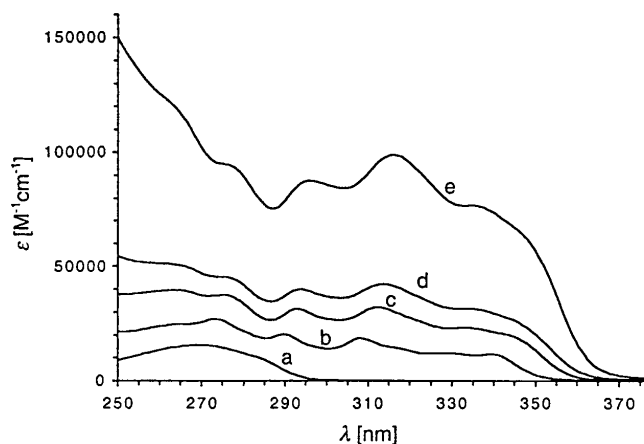


**Figure 1.2.** Left: UV-Vis absorption spectra of dendralenes in hexane. Right: Structures of dendralenes. Reproduced from Ref. 13 with permission from John Wiley and Sons.

In contrast to [3]dendralene, the cyclic [3]radialene is a planar molecule<sup>17</sup> (isomeric with benzene, but not aromatic), and in this case extended conjugation results in a redshifted absorption maximum of 289 nm (gas phase).<sup>18</sup> It is worth noting that any two double bonds of the [3]radialene are linearly conjugated, while this is not the case for the [3]dendralene. Hummelen and co-workers<sup>19</sup> have introduced the term *omniconjugation* to describe such molecules that have linearly conjugated pathways between all connected moieties. The [4]radialene is also planar<sup>20</sup> and exhibits an absorption maximum at 296 nm in ethanol (with minor, further redshifted absorptions at 312 and 325 nm).<sup>21</sup> The larger [6]radialene is assumed instead to take a chair conformation (observed for hexakis(ethylidene)cyclohexane<sup>22</sup>) and accordingly exhibits an absorption maximum at 220 nm (in hexane) similar to that of butadiene.<sup>23</sup>

The less efficient  $\pi$ -electron delocalization in cross-conjugated, acyclic oligoenes is also found in alkyne-expanded systems, such as the *iso*-poly(diacetylene) (*iso*-PDA) and *iso*-poly(triacetylene) (*iso*-PTA) oligomer families (Figure 1.3). Cross-conjugation seems, however, to extend over more units than in the simple dendralenes. *iso*-PDA derivatives with dimethyl substituents and trialkylsilyl end-caps were studied in detail by Tykwinski and co-workers.<sup>24</sup> For these oligomers the cut-off absorption is concomitantly redshifted when proceeding in a sequence from the dimer (cut-off at ca. 320) to the nonamer (cut-off at ca. 345 nm). Saturation in absorption redshift seems to be met at the nonamer length, and the effective conjugation length of *iso*-PDAs thus corresponds to 9 monomer repeat units. In 1995 Diederich and co-workers<sup>25</sup> introduced *iso*-PTAs with trialkylsilyl-protected tetraethynylethene monomer units (TEE; 3,4-diethynylhepta-3-en-1,5-diyne), which were the first series of expanded dendralenes reported. Later Diederich and this author<sup>26</sup> introduced the *iso*-PTAs **1.1-1.5** (Figure 1.3) with peripheral cyclohexylidene groups rather than ethynyl substituents on the alkene units, which are structurally closer to the parent *iso*-PTAs (having no substituents). The UV-Vis absorption spectra of these compounds are shown in Figure 1.4. The cut-off absorption is also redshifted in this series of expanded dendralenes, and it increases from ca. 355 nm in the dimer **1.2** to 375 nm in the octamer **1.5**. It is not straightforward to extrapolate the effective conjugation length in the *iso*-PTA series, but a value around 10 repeat units seems a good suggestion.

By extrapolation of the oligomer data, the lowest-energy absorptions (corresponding to  $\lambda_{\text{max}}$ ) can be estimated for the corresponding linearly and cross-conjugated polymers. These data are shown for comparison in Table 1.1. It transpires that the cross-conjugated polymers have significantly larger HOMO-LUMO gaps than the corresponding linearly conjugated polymers, signaling the less efficient  $\pi$ -electron delocalization in the former ones.

**Figure 1.3.** Expanded dendralenes.**Figure 1.4.** UV-Vis absorption spectra of **1.1** (a), **1.2** (b), **1.3** (c), **1.4** (d), and **1.5** (e) in chloroform. Reproduced from Ref. 26 with permission from John Wiley and Sons.**Table 1.1.** Estimated lowest-energy absorptions ( $E_{\text{max}}$ ; based on  $\lambda_{\text{max}}$ ) for polymers obtained by extrapolation of oligomer data. PA = poly(acetylene); PDA = poly(diacetylene); PTA = poly(triacetylene).

Polymer	$E_{\text{max}} / \text{eV}$	Polymer	$E_{\text{max}} / \text{eV}$
$E\text{-PA}$	1.8 <sup>a)</sup>	$iso\text{-PA}$	5.6 <sup>d)</sup>
$E\text{-PDA}$	2.3 <sup>b)</sup>	$iso\text{-PDA}$	3.9 <sup>e)</sup>
$E\text{-PTA}$	2.8 <sup>c)</sup>	$iso\text{-PTA}$	3.5 <sup>f)</sup>

a) Ref. 27. b) Ref. 28. c) Ref. 29. d) Refs. 13, 14. e) Ref. 24; based on the wavelength at  $\epsilon_{\text{max}}/2$  at the lower energy tail of the absorption band ( $\epsilon$  = molar absorptivity). f) Ref. 26.

Important information can also be gained from the redox properties of cross-conjugated molecules.<sup>30</sup> Radialenes often behave as multistep redox systems,<sup>5b</sup> for which formation of oxidized or reduced species usually depends on the electronic character of the peripheral substituent groups. For example, the [3]radialene **1.6** (Figure 1.5) with peripheral cyano substituents is readily reduced to its radical anion and dianion.<sup>31</sup> Perethynylated and buta-1,3-diynyl-expanded radialenes with generic structure **1.7** (cyclic oligomers comprised of  $n+2$  TEE repeat units) exhibit an exceptional ability to accommodate electrons as shown by Diederich, Gross, this author, and co-workers,<sup>30, 32</sup> and for the [3]- and [4]radialenes this ability was

explained in a detailed theoretical study by Chauvin and co-workers<sup>33</sup> by a gain of aromaticity upon reduction (Figure 1.6). Interestingly, the expanded [6]radialene of **1.7** ( $n = 4$ ) adopts a chair-like conformation, according to X-ray crystallography (Figure 1.7),<sup>32b</sup> like the non-expanded [6]radialene.<sup>22</sup> In addition, it is noteworthy that the all-carbon core of this radialene contains 60 carbon atoms like Buckminsterfullerene. On another note, Buckminsterfullerene itself contains [5]radialene structural units as illustrated in Figure 1.8.

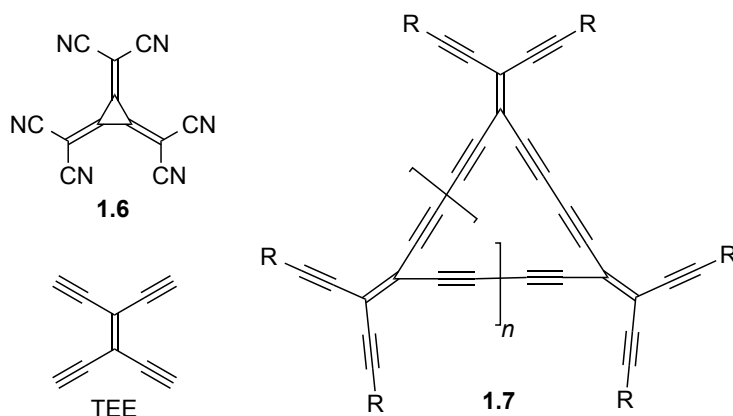


**Figure 1.5.** Radialenes like **1.6** and **1.7** ( $n = 1-4, 6$ ; R = triisopropylsilyl or aryl) are excellent electron acceptors. Radialenes **1.7** are comprised of tetraethynylethene (TEE) units



**Figure 1.6.** The dianion of a buta-1,3-dien-1,4-diyl expanded [3]radialene is a  $14 \pi_z$  Hückel aromatic system, and its aromatic character was supported by calculations as shown by Chauvin, Brøndsted Nielsen, Diederich *et al.*<sup>33</sup> Reproduced from Ref. 33 with permission from John Wiley and Sons.



**Figure 1.7.** The cyclic core of a buta-1,3-dien-1,4-diyl [6]radialene (**1.7**,  $n = 4$ , R = 3,5-dimethylphenyl) adopts a chair-like conformation as shown on this illustration by Brøndsted Nielsen, Diederich *et al.*<sup>32b</sup> Reproduced from Ref. 32b with permission from John Wiley and Sons.

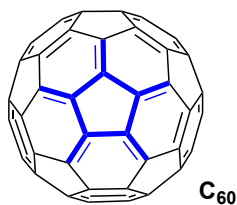


**Figure 1.8.** [5]Radialene structural units can be identified in Buckminsterfullerene,  $C_{60}$ ; one such unit is highlighted in blue.

Cross-conjugated 1,1-diethynylethenes do not undergo the Bergman cyclization characteristic of linearly conjugated *cis*-1,2-diethynylethenes.<sup>34</sup> However, upon reduction a cyclization becomes possible. Thus, Hopf, Rabinovitz, and co-workers<sup>35</sup> found from NMR experiments that the dialkynyl-substituted fluorene/dibenzofulvene **1.8** underwent conversion to the dianionic cycloaromatization product **1.9** upon treatment with potassium in THF- $d_8$  (Figure 1.9). In contrast, under thermal conditions **1.8** was found to undergo a Hopf cyclization to form the fused ring system **1.10** (Figure 1.9).<sup>35, 36</sup>

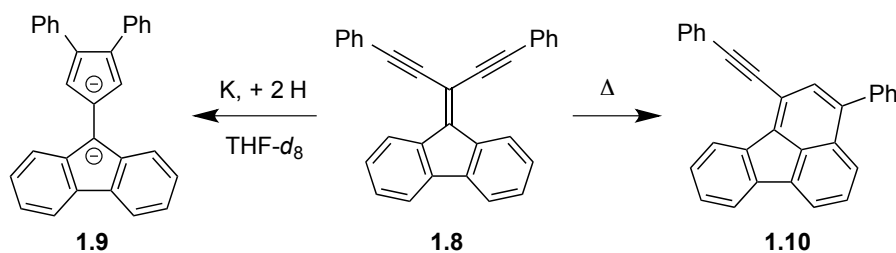


**Figure 1.9.** Reactions of cross-conjugated 1,1-diethynylethenes.

### 1.3 Fulvenes and Fulvalenes

One important characteristic of fulvenes is their dipole moments, which can be enhanced by incorporation of functional groups. Thus, functionalization of triafulvenes and heptafulvenes with acceptor groups at the exocyclic carbon and functionalization of pentafulvenes with donor groups promote polarized resonance forms containing aromatic cyclopropenium, tropylium, and cyclopentadienyl anion rings, respectively (Figure 1.10). The contributions of such resonance forms to the resonance hybrids are supported by the fact that the dipole moment of the triafulvene derivative **1.11** is 7.9 D in dioxane,<sup>37</sup> that of the heptafulvene derivative **1.12** is 7.5 D in dioxane,<sup>38</sup> and that of the pentafulvene derivative **1.13** is 4.5 D.<sup>39</sup> Heptafulvene was first synthesized by Doering and Wiley in 1960,<sup>40</sup> but it was not sufficiently stable for isolation (only stable in solution). Nozoe and co-workers introduced the two cyano groups at the exocyclic fulvene carbon, and this compound (**1.12**) was isolated as stable, orange crystals.<sup>41</sup>

For the fulvalene structure **1.14**, connecting penta- and heptafulvenes via a common exocyclic bond, polarized resonance structures with two aromatic rings can be drawn; this molecule has a dipole moment of 2.1 D.<sup>42</sup> The dipole moments provide fulvenes with unique chemical reactivity. For a recent review on fulvenes in cycloaddition reactions, the reader is referred to Ref. 43.

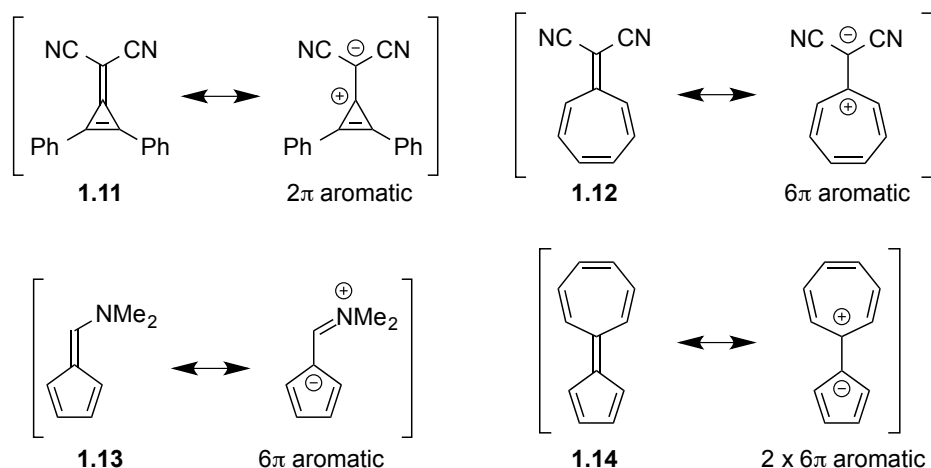


**Figure 1.10.** Functionalization of triafulvene (**1.11**) and heptafulvene (**1.12**) with electron-withdrawing cyano groups and pentafulvene (**1.13**) with an electron-donating dimethylamino group promotes polarized aromatic resonance forms. The fulvalene **1.14** has resonance forms with two aromatic rings.

Polarization of heptafulvene also plays a role for the ability of the dicyano-functionalized vinylheptafulvene (VHF) **1.15** to undergo an electrocyclic ring-closure reaction to form the dihydroazulene (DHA) derivative **1.16** as first reported by Daub and co-workers<sup>44</sup> (Figure 1.11). The rate of this ring-closure reaction is strongly enhanced in polar solvents,<sup>45</sup> and I have shown<sup>46</sup> an empirical relation between the natural logarithm of the rate constant ( $k$ ) for the ring-closure and the Dimroth-Reichardt  $E_T(30)$  solvent polarity parameter<sup>47</sup> (Figure 1.12). These results indicate a polar transition state with tropylium character in the seven-membered ring and negative charge at the dicyanovinyl unit. I have achieved additional support for this by detailed kinetics studies on DHA derivatives with donor/acceptor substitution in either the seven-membered ring or at the vinyl group, providing linear-free-energy (Hammett) correlations.<sup>48</sup> DHA **1.16** has a longest-wavelength absorption maximum at 353 nm in acetonitrile, and upon irradiation at this wavelength it undergoes a ring-opening reaction to form VHF **1.15**, which has a longest-wavelength absorption maximum at 470 nm. The DHA/VHF system is therefore characterized as a so-called T-type photochrome (only undergoing photoisomerization in one direction).<sup>49</sup> This dissertation will cover tuning of the DHA-VHF properties in more detail in Chapters 2, 4, and 5, including conductance switching in molecular electronics junctions.

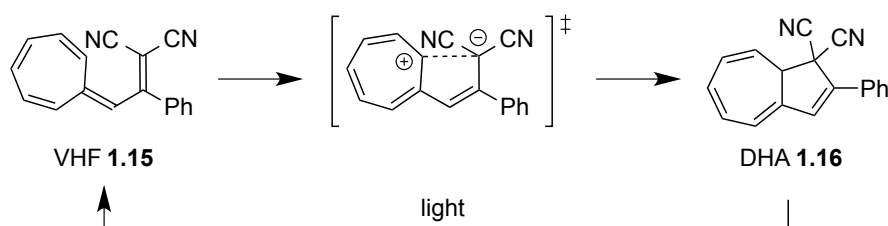


**Figure 1.11.** Thermal and light-induced switching between VHF and DHA derivatives.

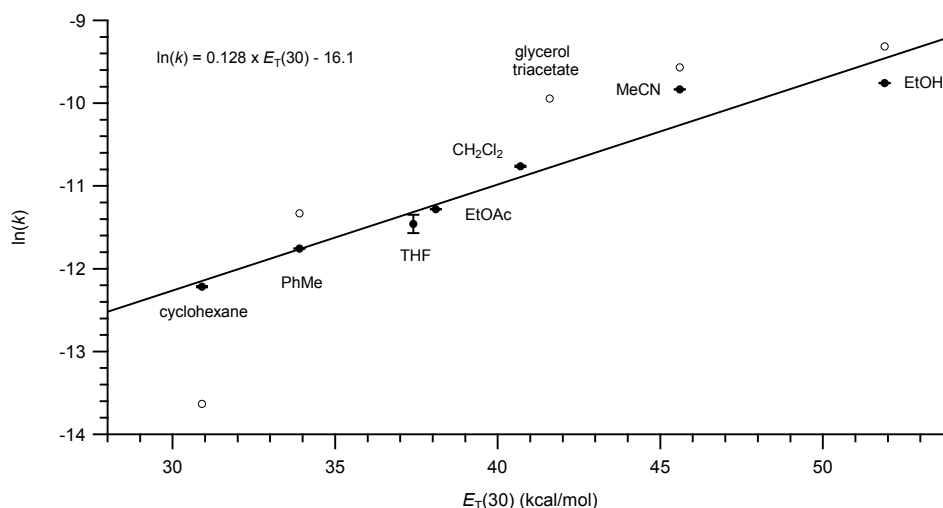


**Figure 1.12.** Dependency of the rate constant  $k$  for VHF to DHA ring-closure as a function of the solvent polarity parameter  $E_T(30)$ . Solid circles correspond to data from my laboratory (Ref. 46), while the open circles correspond to data from Ref. 45. The best straight line describing my own data is inserted. Figure reproduced from Ref. 46 (*Archive for Organic Chemistry*).

## 1.4 Heterofulvalenes and Quinoid Structures

Fulvalenes with carbon atoms substituted for heteroatoms present an important class of redox-active molecules. The most prominent representative of this class is tetrathiafulvalene (TTF; Figure 1.13),<sup>50</sup> which undergoes two reversible and sequential one-electron oxidations, first generating a radical cation and then a dication with two aromatic 1,3-dithiolium rings (a so-called Weitz type redox system<sup>51</sup>). While the radical cation is completely planar, the two rings of the dication are rotated out of coplanarity.<sup>52</sup> The four identical protons of the dication exhibit a  $^1\text{H}$ -NMR chemical shift at 9.51 ppm in  $\text{CD}_3\text{CN}$  (perchlorate salt),<sup>52</sup> which is close to that of the  $\text{CH}=\text{CH}$  protons in 1,3-dithiolium (9.67 ppm in  $\text{CD}_3\text{CN}$ ; tetrafluoroborate salt).<sup>53</sup> The aromatic isomerization stabilization energy of the TTF dication has been calculated by Sauer and *me*<sup>54</sup> to  $-35.7 \text{ kcal mol}^{-1}$  based on the isomerization reaction shown in Figure 1.14. This corresponds to an aromatic stabilization energy of each ring of  $-17.8 \text{ kcal mol}^{-1}$ , which is close to the value of  $-16.3 \text{ kcal mol}^{-1}$  obtained for 1,3-dithiolium. The redox properties of TTF can be finely tuned by peripheral substitution or by incorporation of a  $\pi$ -extended spacer between the two dithiole rings. In this dissertation I will show examples from my work on both these modifications. For example, the fusion of TTF



and an alkyne-expanded *p*-quinodimethane derivative (Wurster type redox system<sup>51</sup>) has provided molecules that can gain aromaticity upon either oxidation or reduction.<sup>55</sup> The gain of aromaticity upon reduction of such molecules resembles the situation for the cross-conjugated 7,7,8,8-tetracyanoquinodimethane (TCNQ) shown in Figure 1.15, which together with TTF was shown by Ferraris *et al.*<sup>56</sup> in 1973 to form the first organic complex (TTF-TCNQ donor-acceptor complex) with metallic properties, and therefore referred to as an organic metal.

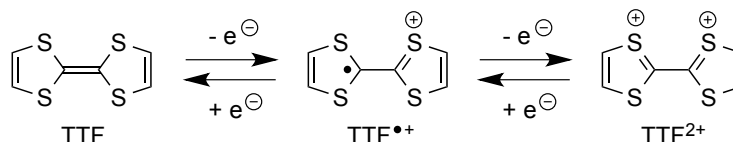


**Figure 1.13.** Reversible oxidations of tetrathiafulvalene (TTF).

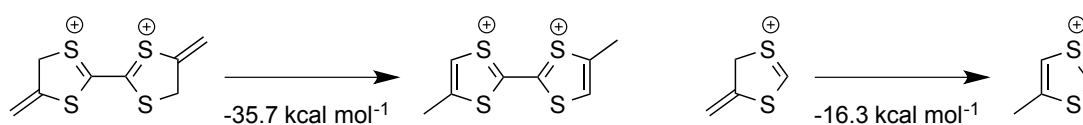


**Figure 1.14.** Reactions used for calculating the isomerization stabilization energies of  $\text{TTF}^{2+}$  and 1,3-dithiolium.

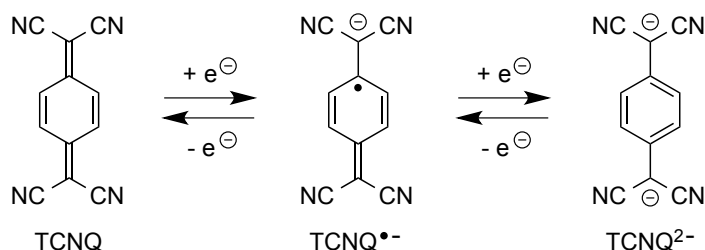


**Figure 1.15.** Reversible reductions of 7,7,8,8-tetracyanoquinodimethane (TCNQ).

The reversible oxidations of TTF are usually not displayed by the related 1,4-dithiafulvenes (DTFs) containing a hydrogen atom at the exocyclic fulvene carbon. Thus, such compounds often undergo dimerization upon oxidation as illustrated in Figure 1.16 for a general DTF derivative.<sup>57</sup> A subsequent loss of two protons generates an extended TTF (ext-TTF), a vinylogous TTF.

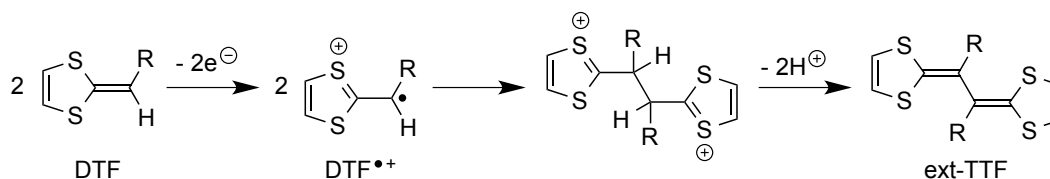
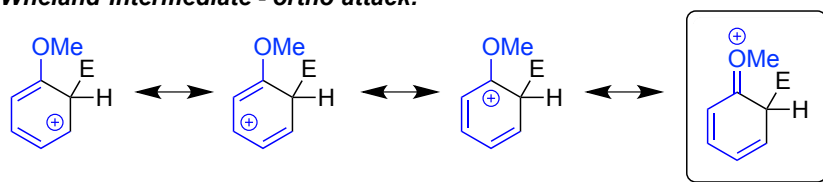


**Figure 1.16.** General scheme for formation of an extended TTF (ext-TTF) by radical dimerization of a dithiafulvene (DTF) derivative upon oxidation followed by loss of two protons.

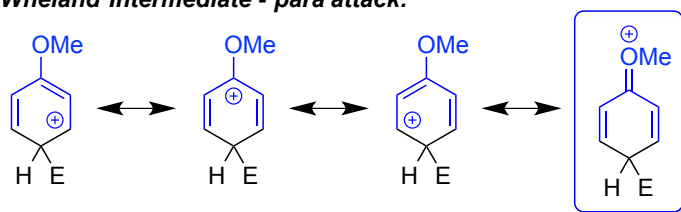
### 1.5 *meta*-Substituted Aromatics

Although *meta*-substituted aromatic compounds may not adhere strictly to the definition of cross-conjugation, I have decided to put them into this category. Indeed, it is convenient to consider the *meta* configuration as cross-conjugated in regard to molecular properties, such as chemical reactivity and optical properties. For example, the regioselectivity induced by *ortho*-*para*- and *meta*-directing groups in electrophilic aromatic substitution is basically explained from Kekulé structures and rooted in the most important consequence of cross-conjugation, namely the lack of a resonance form where electrons are delocalized between two double bonds connected to the bifurcation point. Consider for example anisole, a benzene ring functionalized with an electron-donating methoxy group. The Wheland intermediate obtained after attack by an electrophile has one additional resonance form when the electrophile has attacked in either *ortho* or *para* positions than in the *meta* position (Figure 1.17).

**Wheland Intermediate - *ortho* attack:**



**Wheland Intermediate - *para* attack:**



**Wheland Intermediate - *meta* attack:**

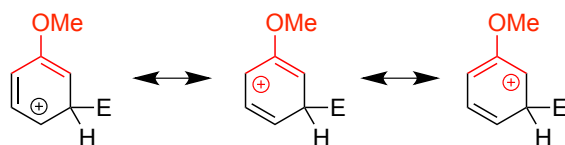


**Figure 1.17.** Wheland intermediates for attack of an electrophile ( $E^+$ ) at either *ortho*, *para*, or *meta* positions of anisole. Cross-conjugation will not allow delocalization of the positive charge onto the methoxy group in the Wheland intermediate resulting from the *meta* attack.

The difference in acidity of substituted phenols also illustrates the effect of linear vs cross-conjugation. Thus, *p*-nitrophenol with a  $pK_a$  value of 7.15 is a stronger acid than *m*-nitrophenol with a  $pK_a$  value of 8.36<sup>58</sup> due to the mesomeric delocalization of the negative charge of the phenolate anion onto the nitro group when located in the *para* position. We shall in the next chapter see how linear vs cross-conjugation also

influences the charge-transfer absorption maxima of various nitrophenolate derivatives.

The less efficient  $\pi$ -electron delocalization via cross-conjugation also has implications for the single-molecule conductance and hence for the design of molecular wires for molecular electronics applications. Thus, theoretical work by Ratner and co-workers<sup>59</sup> has shown that cross-conjugated molecular wires conduct current less efficiently than related linearly conjugated molecules due to quantum interference effects.<sup>60</sup> This difference has also been proven experimentally. For example, the influence of anchoring of molecules via either *meta*- or *para*-phenylene spacers between two gold electrodes has been studied for various molecules (Figure 1.18). The conductance of the linearly conjugated molecular wire **1.17** was determined to be almost two orders of magnitude higher than that of the cross-conjugated molecular wire **1.18** (having the same conjugated anthracene core) although the distance (number of bonds) between the two sulfur electrode anchoring groups are longer in **1.17** than in **1.18**.<sup>61</sup> In another study, it was found that linearly conjugated molecules **1.19** and **1.20** transmitted current at least one order of magnitude more efficiently than the cross-conjugated ones **1.21** and **1.22**; here anchoring to the electrodes is assumed to occur via the thiophene sulfur atoms.<sup>62</sup>

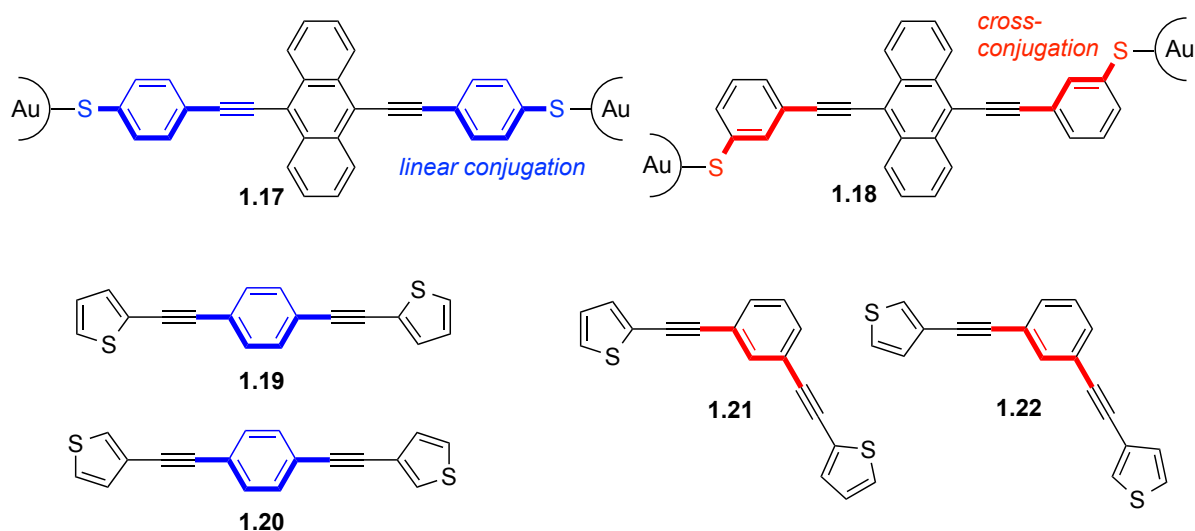


**Figure 1.18.** Molecular wires that have been subjected to single-molecule conductance studies in junctions. The linearly conjugated molecules exhibited significantly higher conductances than the related cross-conjugated ones.

The different conductivities of linearly and cross-conjugated molecules can be conveniently employed for designing molecular switches. An example of one such system is shown in Figure 1.19.<sup>63</sup> The dithienylethene photoswitch **1.23** undergoes an electrocyclic photoisomerization to the closed dihydrodithienobenzene **1.24**. Molecule

**1.24** is comprised of a large linearly conjugated system, while molecule **1.23** is cross-conjugated along the backbone of the molecule. Molecule **1.24** exhibits a redshifted longest-wavelength absorption (visible region) relative to that of **1.23** (UV region). It should be emphasized, however, that this redshift is not only the result of linear vs cross-conjugation, but also a result of forcing the double bonds into co-planarity in the locked isomer **1.24**. The system was anchored via the acetyl-protected thiolate groups between electrodes or nanoparticles in various devices.<sup>63</sup> Reversible conductance switchings were observed in these devices between a low-conducting *off state* (isomer **1.23**) and a high-conducting *on state* (isomer **1.24**). The conversion in one direction (from **1.23** to **1.24**) was achieved by UV light, while conversion in the opposite direction was achieved by visible light, reflecting the different absorption maxima of the two isomers. Importantly, anchoring of the molecules to electrodes occurred via acetyl-protected thiols at *meta* positions to the dithienylethene system. The reason for this chosen configuration (rather than *para*) was to achieve a weak electronic coupling of the molecule to the electrodes to avoid quenching of the molecular photoactivity in the junction by the electrodes.

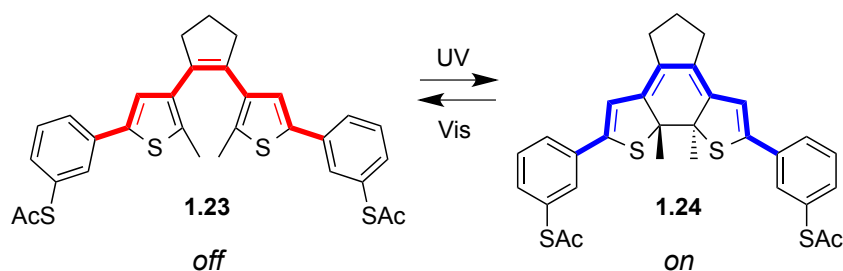


**Figure 1.19.** Light-induced conductance switching between cross-conjugated (*off*) and linearly conjugated (*on*) isomers (anchored via the sulfur end-groups between electrodes).

*The following chapters of this dissertation will show how my research has contributed to an understanding of the consequences of cross-conjugation for communication between electron donors and acceptors via studies of the optical properties of bridged donor-acceptor chromophores, for the optical properties of various large  $\pi$ -conjugated systems, for the redox-properties of tetrathiafulvalene and extended tetrathiafulvalene derivatives, for the redox properties of expanded radiannulene macrocycles, for the electrocyclic ring-closure reaction of substituted vinylheptafulvenes, for interconversions between benzo-fused dihydroazulenes and vinylheptafulvenes (introducing quinoid character in the one isomer), and finally for the single-molecule conductances of various molecular wires. The dissertation will thus include examples based on the parent classes introduced in Figure 1.1 and expanded versions thereof. The research has been driven by my development of synthetic protocols for achieving these advanced  $\pi$ -conjugated scaffolds, relying in particular on finding optimum conditions for making carbon-carbon bonds by metal-catalyzed coupling reactions,- conditions that do not only promote the coupling reactions but conditions under which substrates and products do not decompose. Each chapter will show selected synthetic examples, while Chapter 6 is dedicated to a more in-depth coverage of synthetic protocols for preparing and functionalizing cross-conjugated molecules.*

---

## References

1. M. B. Nielsen (Ed.), *Organic Synthesis and Molecular Engineering*, Wiley, **2014**.
2. H. Hopf, M. S. Sherburn (Eds.), *Cross-Conjugation: Modern Dendralene, Radialene and Fulvene Chemistry*, Wiley-VCH, **2016**.
3. I have in my "definition" extended the cross-conjugated compound classes relative to those listed in Ref. 2 by the quinodimethanes, fulvalenes, and *meta*-substituted aromatics.
4. a) H. Hopf, *Angew. Chem. Int. Ed. Engl.* **1984**, *23*, 947-958; b) H. Hopf, *Angew. Chem. Int. Ed.* **2001**, *40*, 705-707.
5. a) H. Hart, A. Teuerstein, M. Jeffares, W.-J. Hu Kung, D. L. Ward, *J. Org. Chem.* **1980**, *45*, 3731-3735; b) H. Hopf, G. Maas, *Angew. Chem. Int. Ed. Engl.* **1982**, *31*, 931-954.
6. a) J. H. Day, *Chem. Rev.* **1953**, *53*, 167-189; b) K. Hafner, K. H. Häfner, C. König, M. Kreuder, G. Ploss, G. Schulz, E. Sturm, K. H. Vöpel, *Angew. Chem. Int. Ed.* **1963**, *2*, 123-134; c) E. D. Bergmann, *Chem. Rev.* **1968**, *68*, 41-84; d) T. Kawase, H. Kurata, "Recent Developments in Fulvene and Heterofulvene Chemistry," in *Cross-Conjugation: Modern Dendralene, Radialene and Fulvene Chemistry* (Eds. H. Hopf, M. S. Sherburn), Wiley-VCH, **2016**, pp. 145-247.
7. B. Halton, *Eur. J. Org. Chem.* **2005**, 3391-3414.
8. P.-Y. Michellys, H. Pellissier, M. Santelli, *Org. Prep. Proc. Int.* **1996**, *28*, 545-608.
9. a) F. Mitzel, C. Boudon, J.-P. Gisselbrecht, P. Seiler, M. Gross, F. Diederich, *Helv. Chim. Acta* **2004**, *87*, 1130-1157; b) G. Chen, L. Wang, D. W. Thompson, Y. Zhao, *Org. Lett.* **2008**, *10*, 657-660; c) G. Chen, L. Dawe, L. Wang, Y. Zhao, *Org. Lett.* **2009**, *11*, 2736-2739; d) M. Ghomali, M. N. Chaur, M. Wilde, M. J. Ferguson, R. McDonald, L. Echegoyen, R. R. Tykwinski, *Chem. Commun.* **2009**, 3038-3040; e) Y.-L. Wu, F. Bures, P. D. Jarowski, W. B. Schweizer, C. Boudon, J.-P. Gisselbrecht, F. Diederich, *Chem. Eur. J.* **2010**, *16*, 9592-9605.
10. V. Maraval, R. Chauvin, *Chem. Rev.* **2006**, *106*, 5317-5343.
11. For reviews on metal-catalyzed carbon-carbon coupling reactions, see: a) E. I. Negishi, *Acc. Chem. Res.* **1982**, *15*, 340-348; b) J. K. Stille, *Angew. Chem. Int. Ed. Engl.* **1986**, *25*, 508-523; c) T. N. Mitchell, *Synthesis* **1992**, 803-815; d) E. Erdik, *Tetrahedron* **1992**, *48*, 9577-9648; e) A. De Meijere, F. E. Meyer, *Angew. Chem. Int. Ed. Engl.* **1994**, *33*, 2379-2411; f) A. Suzuki, *J. Organomet. Chem.* **1999**, *576*, 147-168; g) I. P. Beltskaya, A. V. Cheprakov, *Chem. Rev.* **2000**, *100*, 3009-3066; h) P. Siemsen, R. C. Livingston, F. Diederich, *Angew. Chem. Int. Ed.* **2000**, *39*, 2632-2657; i) F. Beilina, A. Carpita, R. Rossi, *Synthesis* **2004**, 2419-2440; j) R. Chinchilla, C. Najera, *Chem. Rev.* **2007**, *107*, 874-922; k) R. Chinchilla, C. Nájera, *Chem. Soc. Rev.* **2011**, *40*, 5048-5121.
12. F. Sondheimer, D. A. Ben-Efraim, R. Wolovsky, *J. Am. Chem. Soc.* **1961**, *83*, 1675-1681.
13. A. D. Payne, G. Bojase, M. N. Paddon-Row, M. S. Sherburn, *Angew. Chem. Int. Ed.* **2009**, *48*, 4836-4839.
14. W. F. Forbes, R. Shilton, *J. Org. Chem.* **1959**, *24*, 436-438.
15. A. Almenningen, A. Gatial, D. S. B. Grace, H. Hopf, P. Klæboe, F. Lehrich, C. J. Nielsen, D. L. Powell, M. Trættemberg, *Acta Chem. Scand.* **1988**, *A 42*, 634-650.
16. a) M. N. Paddon-Row, M. S. Sherburn, *Chem. Commun.* **2012**, *48*, 832-834; b) C. G. Newton, M. S. Sherburn, "Cross-Conjugation in Synthesis," in *Cross-Conjugation: Modern Dendralene*,

- 
- Radialene and Fulvene Chemistry* (Eds. H. Hopf, M. S. Sherburn), Wiley-VCH, **2016**, pp. 337-363.
17. a) E. A. Dorko, J. L. Hencher, S. H. Bauer, *Tetrahedron* **1968**, *24*, 2425-2434; b) J. C. Burr, Jr., E. A. Dorko, J. A. Merritt, *J. Chem. Phys.* **1966**, *45*, 3877-3879; c) K. H. Rhee, F. A. Miller, *Spectrochim. Acta Part A* **1971**, *27*, 1-10; d) E. A. Dorko, R. Scheps, S. A. Rice, *Z. Phys. Chem. (Munich)* **1974**, *78*, 568-571.
  18. T. Bally, E. Haselbach, *Helv. Chim. Acta* **1978**, *61*, 754-761.
  19. M. H. van der Veen, M. T. Rispens, H. J. Tonkman, J. C. Hummelen, *Adv. Funct. Mater.* **2004**, *14*, 215-223.
  20. F. A. Miller, F. R. Brown, K. H. Rhee, *Spectrochim. Acta Part A* **1972**, *28*, 1467-1478.
  21. G. W. Griffin, L. I. Peterson, *J. Am. Chem. Soc.* **1963**, *85*, 2268-2273.
  22. W. March, J. D. Dunitz, *Helv. Chim. Acta* **1975**, *58*, 707-712.
  23. P. Schiess, M. Heitzmann, *Helv. Chim. Acta* **1978**, *61*, 844-847.
  24. a) S. Eisler, R. R. Tykwinski, *Angew. Chem. Int. Ed.* **1999**, *38*, 1940-1943; b) Y. Zhao, R. R. Tykwinski, *J. Am. Chem. Soc.* **1999**, *121*, 458-459; c) S. Eisler, R. McDonald, G. R. Loppnow, R. R. Tykwinski, *J. Am. Chem. Soc.* **2000**, *122*, 6917-6928; d) Y. Zhao, K. Campbell, R. R. Tykwinski, *J. Org. Chem.* **2002**, *67*, 336-344.
  25. A. M. Boldi, J. Anthony, V. Gramlich, C. B. Knobler, C. Boudon, J.-P. Gisselbrecht, M. Gross, F. Diederich, *Helv. Chim. Acta* **1995**, *78*, 779-796.
  26. E. Burri, F. Diederich, M. B. Nielsen, *Helv. Chim. Acta* **2002**, *85*, 2169-2182.
  27. G. Wenz, M. A. Müller, M. Schmidt, G. Wegner, *Macromolecules* **1984**, *17*, 837-850.
  28. a) F. Wudl, S. P. Bitler, *J. Am. Chem. Soc.* **1986**, *108*, 4685-4687; b) R. Giesa, R. C. Schulz, *Polym. Int.* **1994**, *33*, 43-60.
  29. a) R. E. Martin, U. Gubler, J. Cornil, M. Balakina, C. Boudon, J.-P. Gisselbrecht, F. Diederich, P. Günter, M. Gross, J.-L. Brédas, *Chem. Eur. J.* **2000**, *6*, 3622-3635; b) M. J. Edelmann, M. A. Estermann, V. Gramlich, F. Diederich, *Helv. Chim. Acta* **2001**, *84*, 473-480; c) Y. Takayama, C. Delas, K. Muraoka, M. Uemura, F. Sato, *J. Am. Chem. Soc.* **2003**, *125*, 14163-14167.
  30. a) J.-P. Gisselbrecht, N. N. P. Moonen, C. Boudon, M. B. Nielsen, F. Diederich, M. Gross, *Eur. J. Org. Chem.* **2004**, 2959-2972; b) M. B. Nielsen, F. Diederich, *Chem. Rev.* **2005**, *105*, 1837-1867.
  31. a) T. Fukunaga, M. D. Gordon, P. J. Krusic, *J. Am. Chem. Soc.* **1976**, *98*, 611-613; b) J. Mirek, A. Buda, *Z. Naturforsch. A* **1984**, *39*, 386-390.
  32. a) J. Anthony, A. M. Boldi, C. Boudon, J.-P. Gisselbrecht, M. Gross, P. Seiler, C. B. Knobler, F. Diederich, *Helv. Chim. Acta* **1995**, *78*, 797-817; b) M. B. Nielsen, M. Schreiber, Y. G. Baek, P. Seiler, S. Lecomte, C. Boudon, R. R. Tykwinski, J.-P. Gisselbrecht, V. Gramlich, P. J. Skinner, C. Bosshard, P. Günter, M. Gross, F. Diederich, *Chem. Eur. J.* **2001**, *7*, 3263-3280.
  33. C. Lepetit, M. B. Nielsen, F. Diederich, R. Chauvin, *Chem. Eur. J.* **2003**, *9*, 5056-5066.
  34. a) R. R. Jones, R. G. Bergman, *J. Am. Chem. Soc.* **1972**, *94*, 660-661; b) R. G. Bergman, *Acc. Chem. Res.* **1973**, *6*, 25-31; c) T. P. Lockhardt, P. B. Commita, R. G. Bergman, *J. Am. Chem. Soc.* **1981**, *103*, 4082-4090.
  35. L. Eshdat, H. Berger, H. Hopf, M. Rabinovitz, *J. Am. Chem. Soc.* **2002**, *124*, 3822-3823.

36. H. Hopf, H. Berger, G. Zimmermann, U. Nüchter, P. G. Jones, I. Dix, *Angew. Chem. Int. Ed. Engl.* **1997**, *36*, 1187-1190.
37. E. D. Bergmann, I. Agranat, *J. Am. Chem. Soc.* **1964**, *86*, 3587-3589.
38. M. Yamakama, H. Watanabe, T. Mukai, T. Nozoe, M. Kubo, *J. Am. Chem. Soc.* **1960**, *82*, 5665-5667.
39. K. Hafner, K. H. Häfner, C. König, M. Kreuder, G. Ploss, G. Schulz, E. Sturm, K. H. Vöpel, *Angew. Chem.* **1963**, *75*, 35-46.
40. W. von E. Doering, D. W. Wiley, *Tetrahedron* **1960**, *11*, 1384-1390.
41. T. Nozoe, T. Mukai, K. Osaka, *Bull. Chem. Soc. Jpn.* **1961**, *34*, 1384-1390.
42. R. Hollenstein, A. Mooser, M. Neuenschwander, W. von Philipsborn, *Angew. Chem.* **1974**, *86*, 595-596.
43. B.-C. Hong, "Constructing Molecular Complexity and Diversity by Cycloaddition Reactions of Fulvenes," in *Cross-Conjugation: Modern Dendralene, Radialene and Fulvene Chemistry* (Eds. H. Hopf, M. S. Sherburn), Wiley-VCH, **2016**, pp. 249-299.
44. a) J. Daub, T. Knöchel, A. Mannschreck, *Angew. Chem. Int. Ed. Engl.* **1984**, *23*, 960-961; b) S. Gierisch, J. Daub, *Chem. Ber.* **1989**, *122*, 69-75.
45. H. Görner, C. Fischer, S. Gierisch, J. Daub, *J. Phys. Chem.* **1993**, *97*, 4110-4117.
46. S. L. Broman, S. L. Brand, C. R. Parker, M. Å. Petersen, C. G. Tortzen, A. Kadziola, K. Kilså, M. B. Nielsen, *Arkivoc* **2011**, *ix*, 51-67.
47. C. Reichardt, *Solvents and Solvent Effects in Organic Chemistry*, VCH, Weinheim, **1988**.
48. a) S. L. Broman, M. Å. Petersen, C. Tortzen, A. Kadziola, K. Kilså, M. B. Nielsen, *J. Am. Chem. Soc.* **2010**, *132*, 9165-9174; b) M. Å. Petersen, S. L. Broman, K. Kilså, A. Kadziola, M. B. Nielsen, *Eur. J. Org. Chem.* **2011**, 1033-1039; c) S. L. Broman, M. Jevric, M. B. Nielsen, *Chem. Eur. J.* **2013**, *19*, 9542-9548.
49. For glossary of terms used in photochemistry (IUPAC recommendations), see: T. Braslavsky, *Pure Appl. Chem.* **2007**, *79*, 293-465.
50. M. Bendikov, F. Wudl, D. F. Perepichka, *Chem. Rev.* **2004**, *104*, 4891-4945.
51. For an overview of Wurster and Weitz redox systems, see: K. Deuchert, S. Hünig, *Angew. Chem. Int. Ed. Engl.* **1978**, *17*, 875-886.
52. P. R. Ashton, V. Balzani, J. Becher, A. Credi, M. C. T. Fyfe, G. Mattersteig, S. Menzer, M. B. Nielsen, F. M. Raymo, J. F. Stoddart, M. Venturi, D. J. Williams, *J. Am. Chem. Soc.* **1999**, *121*, 3951-3957.
53. F. Wudl, M. L. Kaplan, E. J. Hufnagel, E. W. Southwick, Jr., *J. Org. Chem.* **1974**, *39*, 3608-3609.
54. M. B. Nielsen, S. P. A. Sauer, *Chem. Phys. Lett.* **2008**, *453*, 136-139.
55. K. Lincke, A. F. Frellsen, C. R. Parker, A. D. Bond, O. Hammerich, M. B. Nielsen, *Angew. Chem. Int. Ed.* **2012**, *51*, 6099-6102.
56. J. Ferraris, D. O. Cowan, V. V. Walatka, Jr., J. H. Perlstein, *J. Am. Chem. Soc.* **1973**, *95*, 948-949.
57. a) M. Sallé, A. Belyasmine, A. Gorgues, M. Jubault, N. Soyer, *Tetrahedron Lett.* **1991**, *32*, 2897-2900; b) R. Carlier, P. Hapiot, D. Lorcy, A. Robert, A. Tallec, *Electrochim. Acta.* **2001**, *46*, 3269-3277; c) P. Frère, P. J. Skabara, *Chem. Soc. Rev.* **2005**, *34*, 69-98; d) G. Chen, I. Mahmud, L. N. Dawe, D. Lee, Y. Zhao, *J. Org. Chem.* **2011**, *76*, 2701-2715.



- 58 E. P. Serjeant, B. Dempsey, *Ionisation Constants of Organic Acids in Aqueous Solution. International Union of Pure and Applied Chemistry (IUPAC). IUPAC Chemical Data Series No. 23*, **1979**, New York, Pergamon Press, Inc.
59. a) G. C. Solomon, D. Q. Andrews, R. P. Van Duyne, M. A. Ratner, *J. Am. Chem. Soc.* **2008**, *130*, 7788-7789; b) G. C. Solomon, J. P. Bergfield, C. A. Stafford, M. A. Ratner, *Beilstein J. Nanotechnol.* **2011**, *2*, 862-871.
60. For a discussion of quantum interference effects, see: G. C. Solomon, "Cross-Conjugation and Quantum Interference," in *Cross-Conjugation: Modern Dendralene, Radialene and Fulvene Chemistry* (Eds. H. Hopf, M. S. Sherburn), Wiley-VCH, **2016**, pp. 397-412.
61. M. Mayor, H. B. Weber, J. Reichert, M. Elbing, C. von Hänish, D. Beckmann, M. Fischer, *Angew. Chem. Int. Ed.* **2003**, *42*, 5834-5838.
62. C. R. Arroyo, S. Tarkuc, R. Frisenda, J. S. Seldenthuis, C. H. M. Woerde, R. Eelkema, F. C. Grozema, H. S. J. van der Zant, *Angew. Chem. Int. Ed.* **2013**, *52*, 3152-3155.
63. a) A. J. Kronemeijer, H. B. Akkerman, T. Kudernac, B. J. van Wees, B. L. Feringa, P. Blom, B. de Boer, *B. Adv. Mater.* **2008**, *20*, 1467-1473; b) J. S. van der Molen, J. Liao, T. Kudernac, J. S. Agustsson, L. Bernard, M. Calame, B. J. van Wees, B. L. Feringa, C. Schönenberger, *Nano Lett.* **2009**, *9*, 76-80.

# OPTICAL PROPERTIES

## 2.1 Introduction

This chapter will elucidate the consequences of cross-conjugation in regard to electronic absorption properties of various nitrophenolate derivatives, extended tetrathiafulvalenes (TTFs), and dihydroazulene/vinylheptafulvene (DHA/VHF) systems. The nonlinear optical properties of tetraethynylethene (TEE) scaffolds will also be covered. Some of the results have been previously reviewed by me together with co-workers.<sup>1</sup>

UV-Vis absorption spectroscopy was already introduced in the previous chapter as a convenient way of evaluating the efficiency of conjugation in dendralenes and expanded dendralenes. However, some care has to be taken when using this method for donor-acceptor (D-A) systems from the position of their charge-transfer (CT) absorption bands. When studying D-A compounds, it is important to keep in mind that efficient electronic communication between D and A groups corresponds to a high degree of charge-transfer in the ground state, and this should lead to a blueshifted absorption maximum relative to a D-A system for which the coupling is weak. In other words, efficient  $\pi$ -electron delocalization across a bridge in D-bridge-A systems (strong mixing of D's HOMO and A's LUMO) should have the "opposite effect" as the one in symmetrical oligoenes, namely a blueshifted absorption. This principle is illustrated schematically in Figure 2.1. However, an increase in the HOMO energy of D or a decrease in the LUMO energy of A owing to extended conjugation of these individual units will of course lower the CT energy.

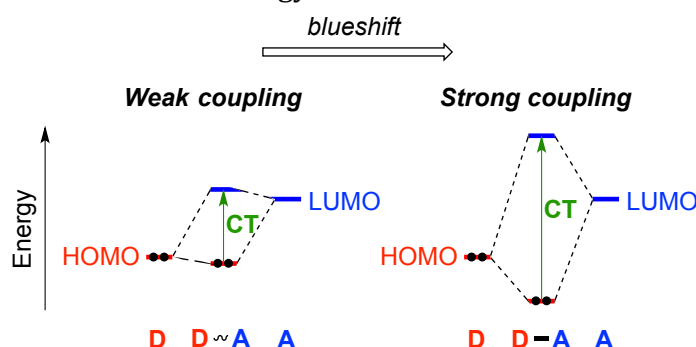
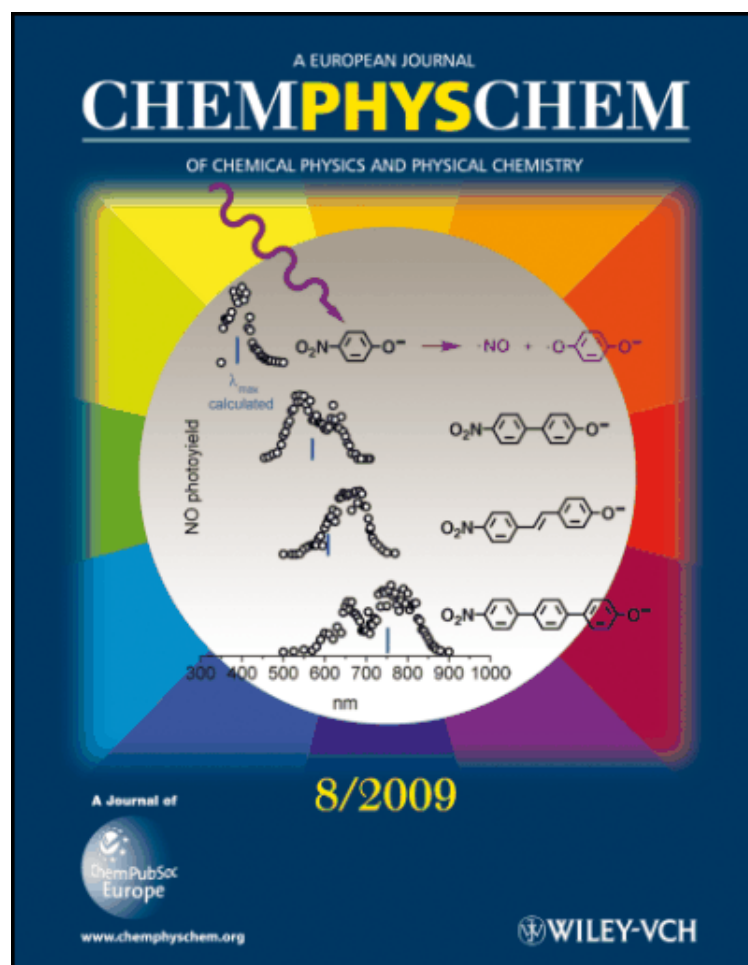


**Figure 2.1.** Schematic illustration of the charge-transfer (CT) energies of donor-acceptor (D-A) systems with weak (left) and strong (right) coupling between D and A units.

The position of the CT absorption can, however, be perturbed by solvents or counter ions so that the intrinsic properties are masked. It is therefore of interest to compare results from solution and gas phase. I shall in this chapter present several gas-

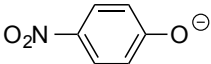
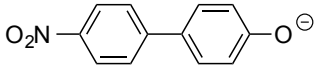
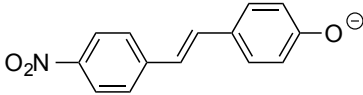
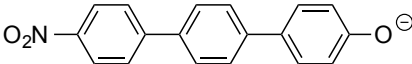
phase absorption data, which were all obtained by Prof. Steen Brøndsted Nielsen at Aarhus University, employing state-of-the-art equipment for action spectroscopy studies on large and ionic compounds that are transferred to the gas phase by electrospray ionization.<sup>2</sup>

To illustrate the complications sometimes resulting from solution studies, it is instructive to compare the data we achieved for the longest-wavelength absorptions of nitrophenolates **2.1-2.4** from studies in solution (sodium salts) and in gas phase (anions only) (Figure 2.2 and Table 2.1).<sup>3</sup> The gas phase data show that the absorption is concomitantly redshifted from **2.1** to **2.4**, while this is not the case in solution (MeCN or MeOH) as **2.4** exhibits a blueshifted absorption relative to that of both **2.2** and **2.3**. If one were to use the solution data to explain the intrinsic optical properties of these  $\pi$ -extended nitrophenolates, one would not only need to take solvation into account but also counter ion effects (sodium ions)! Solvatochromism is a strong indication of CT character of an absorption, and, indeed, the CT maxima of **2.1-2.4** vary significantly between the two solvents MeCN and MeOH.



**Figure 2.2.** Gas phase absorption spectra of various nitrophenolate derivatives. Work resulting from collaboration between Steen Brøndsted Nielsen (Aarhus University) and me. Reproduced from Ref. 3 with permission from John Wiley and Sons.

**Table 2.1.** Longest-wavelength absorption maxima of extended nitrophenolates in solution (MeCN or MeOH; sodium salts – obtained by deprotonation of the corresponding phenols by NaOMe) and in the gas phase.

Nitrophenolate		MeCN	MeOH	Gas phase
		$\lambda_{\max}$ / nm	$\lambda_{\max}$ / nm	$\lambda_{\max}$ / nm
	<b>2.1</b>	430	387	392
	<b>2.2</b>	507	406	541
	<b>2.3</b>	543	435	660
	<b>2.4</b>	466	377	775

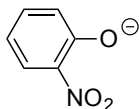
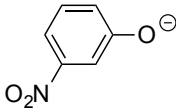
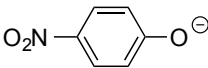
In cases where the communication between D and A is very poor, the CT band may be too weak to be confidently assigned or completely absent, and one thus has to take care not to mistakenly assign a higher-energy absorption band to the CT band. Calculations are helpful in such cases and were used to confirm the gas-phase absorption maxima presented in Table 2.1 as CT transitions (also supported by the solvatochromic behavior). The calculational data presented in this chapter were obtained by Prof. Angel Rubio at University of San Sebastián, Spain. The results presented in this chapter also come from other collaborations, mentioned in the relevant paragraphs below.

## 2.2 *ortho*-, *meta*-, and *para*-Nitrophenolate Chromophores

The *o*-, *m*- and *p*-nitrophenolates (**2.5**, **2.6**, **2.1**) are sort of text book examples of donor-acceptor chromophores and very well suited for elucidating the influence of *ortho*-, *meta*-, *para*-substitution patterns. Their CT absorptions were investigated in solution and gas phase, and the measured maxima are listed in Table 2.2.<sup>4</sup> The individual absorption maxima differ between the two phases due to solvation and counter ion effects, but we see that in both phases the values increase in the same sequence, **2.1** (*para*) → **2.5** (*ortho*) → **2.6** (*meta*); this sequence was also obtained in the parallel calculational study by Rubio. The absorption maximum of the cross-conjugated *meta* isomer is thus in both phases significantly redshifted relative to those of the two other isomers. This reflects the fact that electronic communication between the donor group ( $O^-$ ) and the acceptor group ( $NO_2$ ) is very poor in a *meta*

configuration; no resonance form can be drawn where the negative charge on oxygen is moved to the nitro group. This corresponds to the weak coupling regime illustrated in Figure 2.1 to the left.

**Table 2.2.** Longest-wavelength absorption maxima of *o*-/*m*-/*p*-nitrophenolates in solution (MeCN; sodium salts – obtained by deprotonation of the corresponding phenols by NaOt-Bu) and in the gas phase.

Nitrophenolate		Solution (MeCN)	Gas phase
		$\lambda_{\text{max}} / \text{nm}$	$\lambda_{\text{max}} / \text{nm}$
	<b>2.5</b>	443	399
	<b>2.6</b>	473	532
	<b>2.1</b>	430	392

### 2.3 Diethynylethene-Extended Nitrophenolates

To elucidate the influence of 1,1-/1,2-diethynylethene bridges between a phenol (phenolate) donor and nitrophenyl acceptor, we prepared the linearly conjugated compound **2.7** (*E* isomer) according to Figure 2.3 and the cross-conjugated compound **2.8** according to Figure 2.4.<sup>5</sup> The C<sub>2</sub> units of the diethynylethene bridges are convenient in regard to allowing co-planarity of the aryl groups and the  $\pi$ -conjugated bridge.

The readily available alkyne **2.9**<sup>6</sup> and the vinylic bromide **2.10**<sup>7</sup> were subjected to a Sonogashira coupling<sup>8</sup> affording the *E*-diethynylethene **2.11**. We have devised a simple route to the starting material **2.10** by subjecting 3-(4-nitrophenyl)propionaldehyde to a Ramirez dibromoolefination<sup>9</sup> (treatment with CBr<sub>4</sub> and PPh<sub>3</sub>) followed by a reduction of the resulting vinylic dibromide by diethylphosphite at 50 °C.<sup>7</sup> Compound **2.11** was then treated with K<sub>2</sub>CO<sub>3</sub> in MeOH/CH<sub>2</sub>Cl<sub>2</sub> to afford the target molecule **2.7**. The first step in the synthesis of the cross-conjugated counterpart is again a Sonogashira coupling, this time between alkyne **2.12** and the triflate **2.13** for which a synthesis had been developed by Eisler and Tykwinski.<sup>10</sup> The product **2.14** was subjected to protodesilylation, and the resulting terminal alkyne **2.15** was then treated with the aryl iodide **2.16** under Sonogashira conditions, furnishing compound **2.17**. Cleavage of the ester group then gave the target molecule **2.8**.

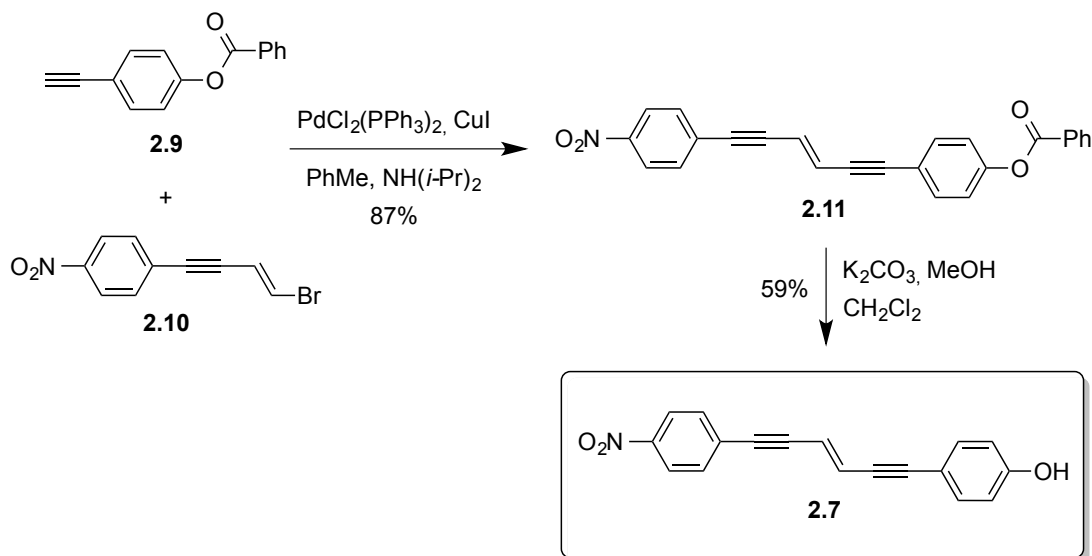


**Figure 2.3.** Synthesis of linearly conjugated diethynylethene with donor-acceptor substitution.

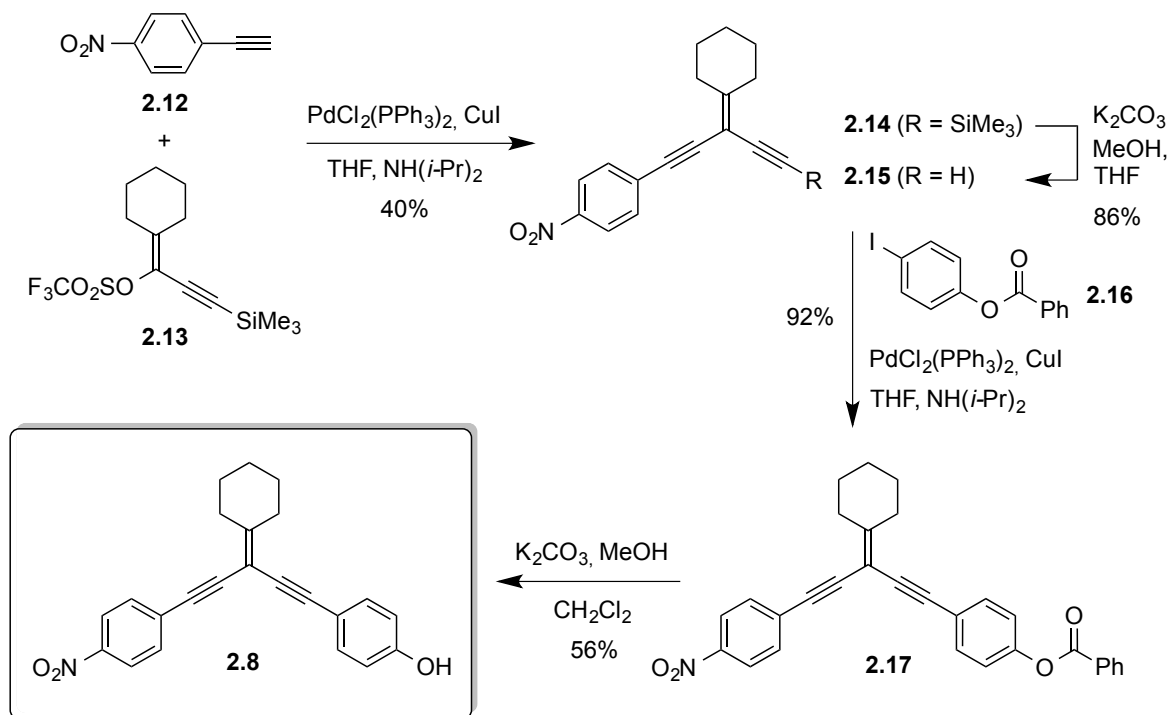


**Figure 2.4.** Synthesis of cross-conjugated diethynylethene with donor-acceptor substitution.

The neutral phenols **2.7** and **2.8** exhibit longest-wavelength absorptions at 368 nm and 346 nm in MeOH, while the corresponding phenolates (achieved by treatment with NaOMe) absorb at 416 nm and 312 / 336 nm, respectively.<sup>5</sup> The unexpected blueshift in the absorption of **2.8** upon deprotonation seems to indicate that the CT absorption is absent in the spectrum. In fact, for the phenolate of **2.8** coupled cluster (CC2) calculations give absorption maxima at 886 nm (oscillator strength of 0.06) and 499 nm (oscillator strength of 0.35). Thus, the longest-wavelength absorption has a very small oscillator strength, which signals that the donor and acceptor parts are very

weakly coupled. This is also evident when looking at the HOMO and LUMO orbitals, which are largely separated between the donor and acceptor ends (Figure 2.5). For the phenolate of the linearly conjugated **2.7** the calculations give absorption maxima at 736 nm (oscillator strength of 1.90) and 420 nm (oscillator strength of 0.38 nm). For this anion the oscillator strengths are much larger and, indeed, there is good “overlap between” (*i.e.*, same atoms sharing) the HOMO and LUMO of this compound (Figure 2.5). Importantly, the calculations also reveal that the cross-conjugated donor-acceptor phenolate does indeed exhibit a redshifted CT absorption maximum relative to the linearly conjugated one (886 nm vs 736 nm); it is just too weak to be observed experimentally.

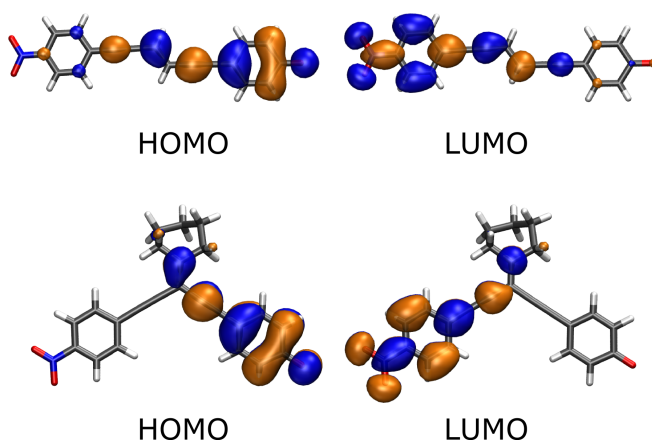


**Figure 2.5.** Frontier orbitals of the phenolates of **2.7** (top) and **2.8** (bottom) obtained by the coupled cluster (CC2) method. Reproduced from Ref. 5 with permission from John Wiley and Sons.

The conclusion that the smallest degree of donor-acceptor coupling in the ground state furnishes cross-conjugated D-A molecules with the most redshifted absorption is also in agreement with studies conducted by Diederich and co-workers<sup>11</sup> on 1,1- and 1,2-diethynylethenes substituted with 4-(*N,N*-dimethylamino)phenyl groups at each of the two terminal alkyne positions and two cyano groups at the central ethylene unit.

## 2.4 Extended Tetrathiafulvalenes (TTFs)

It is also possible to extract information on cross-conjugation from the absorption properties of extended TTFs. Thus, we prepared the two extended TTFs **2.18** and **2.19** (Figure 2.6)<sup>12</sup> by Sonogashira couplings using the acetylenic dithiafulvene (DTF) building block **2.20**,<sup>13</sup> 1,4-diiodobenzene (**2.21**), and the DTF building block **2.22**<sup>12</sup> as precursors. Compound **2.19**, which can be considered as an expanded [3]dendralene, has longest-wavelength absorption maxima (394/415 nm in CH<sub>2</sub>Cl<sub>2</sub>) very similar to those of the extended TTF **2.18**. Thus, the electron delocalization across the central cross-conjugated DTF unit is insignificant in **2.19**.

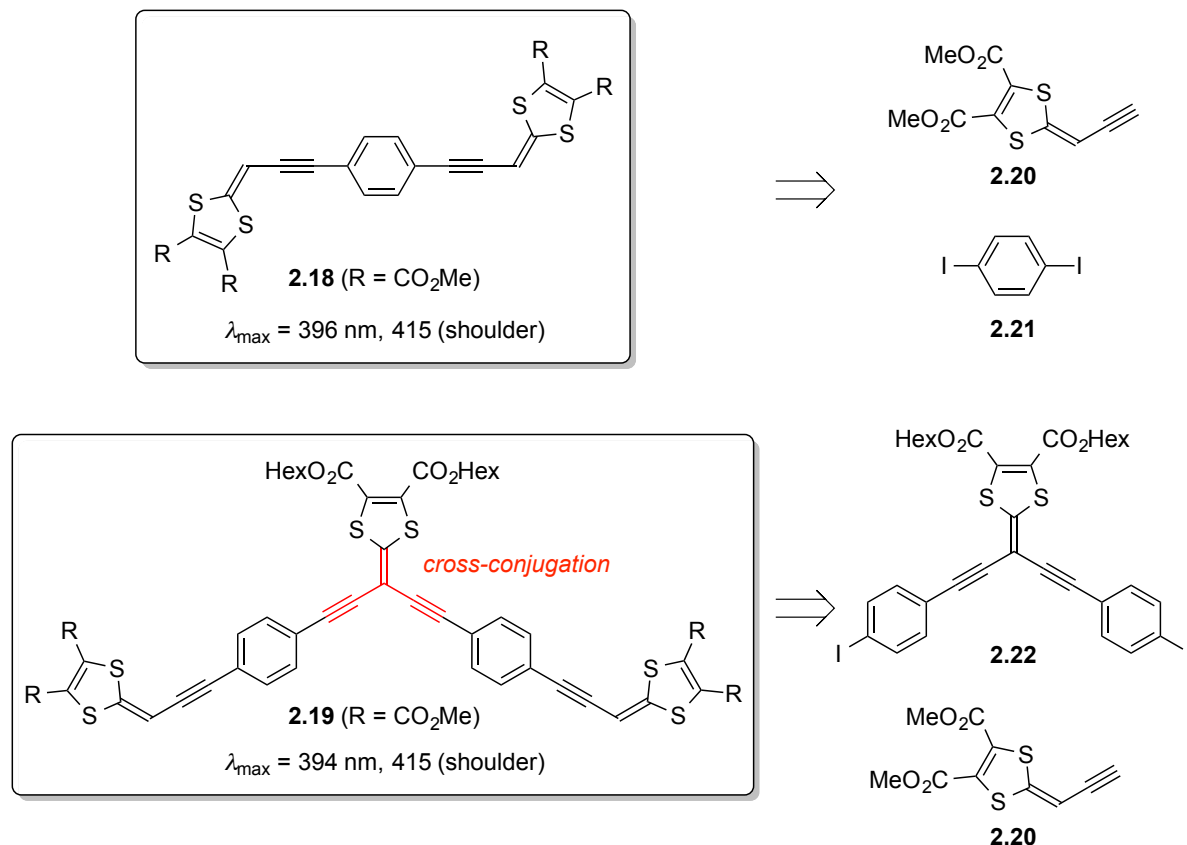


**Figure 2.6.** Extended TTFs (prepared from the shown precursors subjected to Sonogashira coupling conditions) and their longest-wavelength absorption maxima in  $\text{CH}_2\text{Cl}_2$ .

It is also interesting to compare the longest-wavelength absorptions of compounds **2.23** and **2.24** (Figure 2.7), which we prepared by triethylphosphite-mediated reactions between 4,5-bis(methylthio)-1,3-dithiol-2-thione and terephthalaldehyde and benzene-1,3,5-tricarbaldehyde, respectively (see Chapter 6).<sup>14, 15</sup> The linearly conjugated *p*-phenylene-extended TTF **2.23** has a redshifted absorption maximum (424 nm in  $\text{CH}_2\text{Cl}_2$ ) relative to that of the *meta*-substituted and cross-conjugated tris-DTF **2.24** (371 nm in  $\text{CH}_2\text{Cl}_2$ ) although the latter is a much larger chromophore.

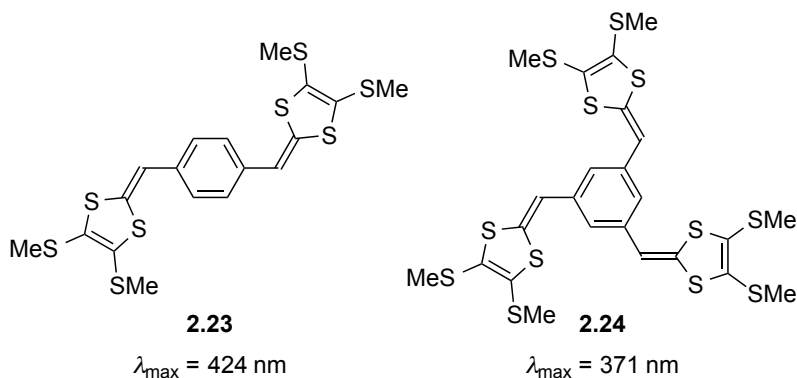


**Figure 2.7.** Extended TTFs and their longest-wavelength absorption maxima in  $\text{CH}_2\text{Cl}_2$ .



Bryce and co-workers<sup>16</sup> studied the compounds **2.25-2.27** shown in Figure 2.8. The [3]- and [4]dendralenes **2.26** and **2.27** only showed minor absorption redshifts relative to the absorption of the extended TTF **2.25**, which is in line with results described above from my lab.

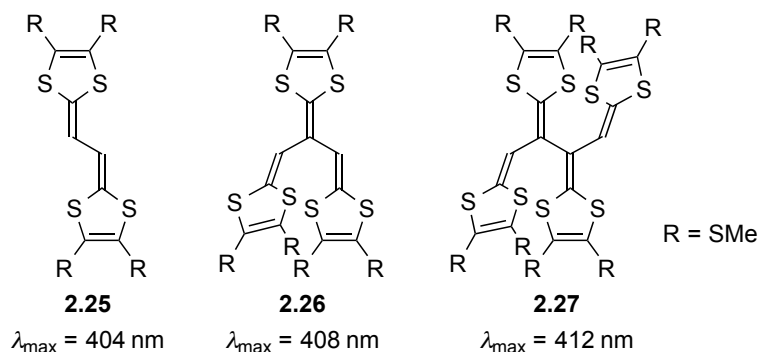


**Figure 2.8.** Dendralene-like TTFs and their longest-wavelength absorption maxima in  $\text{CH}_2\text{Cl}_2$ .  
Work by Bryce and co-workers.<sup>16</sup>

## 2.5 Functionalized Dihydroazulenes (DHAs)

The dihydroazulene/vinylheptafulvene (DHA/VHF) photo-/thermoswitch has several positions available for tuning of optical properties. We developed the first regioselective protocol for functionalizing DHA at C-7 by the bromination – elimination – cross-coupling protocol outlined in Figure 2.9.<sup>17</sup> As starting material, we employed DHA **2.28**, for which we have developed a large-scale synthesis, with acetophenone (which is the source of the phenyl substituent at C-2 in the final product), malononitrile, and tropylium tetrafluoroborate as starting materials.<sup>18</sup> Due to the stereocenter at C-8a, **2.28** is formed as a racemic mixture. It was converted to the dibromide **2.29**, formed as a racemic mixture of two enantiomers (two new stereocenters are formed, and the conversion is hence stereospecific), and then regioselective elimination of HBr provided the bromo-substituted DHA **2.30**. This compound is rather unstable, but can be subjected to a Sonogashira reaction with triisopropylsilylacetylene, affording the product **2.31**. This functionalization has little influence on the optical properties since DHA **2.31** exhibits a longest-wavelength absorption maximum close to that of **2.28** at 353 nm in MeCN. This indifference in absorption maxima can be explained by a combination of two factors: *i*) the alkyne unit is cross-conjugated to the largest part of the  $\pi$ -system (C-2 – C-6); *ii*) the C-7 – C-8 bond deviates significantly from co-planarity with the remaining part of the  $\pi$ -system (C-2 – C-6) as revealed by X-ray crystallographic analysis (Figure 2.10).

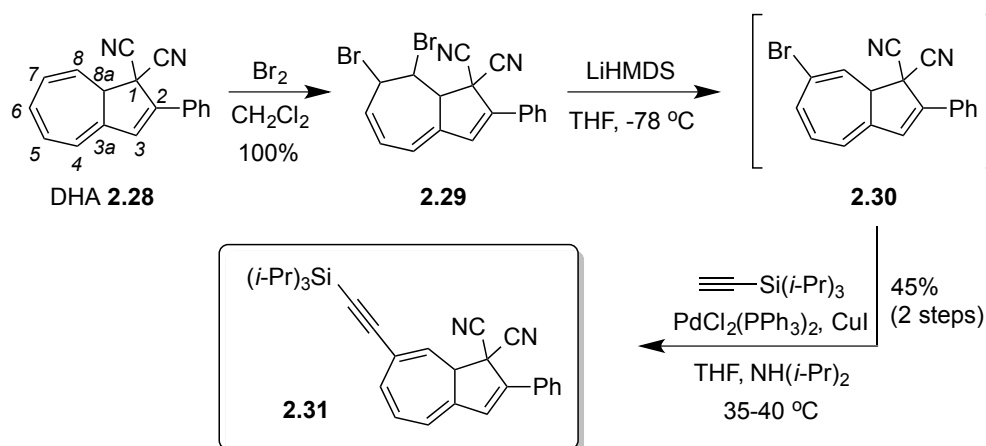


**Figure 2.9.** Regioselective functionalization of DHA at position C-7. Numbering of the DHA core is shown at the structure of **2.28**. LiHMDS = lithium hexamethyldisilazide.

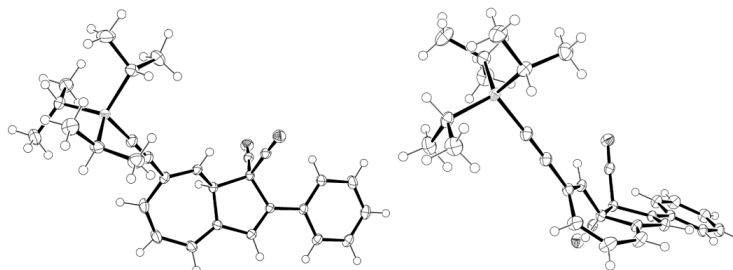


**Figure 2.10.** Two different views of the molecular structure of DHA **2.31** solved by X-ray crystallography. Reproduced from Ref. 17 with permission from John Wiley and Sons.

Upon irradiation of DHA **2.31** in MeCN at 355 nm, it undergoes a ring-opening reaction to form a mixture of the VHF isomers *Z*-**2.32** and *E*-**2.32** (Figure 2.11).<sup>17</sup> These VHF isomers have absorption maxima at 477 nm as shown in Figure 2.12. We have shown that isomerization between these VHF isomers can occur both thermally and photochemically.<sup>19</sup> X-Ray crystallographic analysis of the related VHF **2.34** provides a bond length of the exocyclic heptafulvene bond of 1.39 Å (Figure 2.13),<sup>20</sup> and it thus has significant single bond character, which assumingly is further promoted in a polar solvent (providing a zwitterionic structure). In the dark, the mixture of VHF isomers *Z/E*-**2.32** undergoes ring-closure to reform the dihydroazulene scaffold. Yet, the product after one such cycle shows a redshifted absorption maximum at 376 nm (Figure 2.12).<sup>17</sup> By <sup>1</sup>H-NMR spectroscopy we could confirm that a 1:2 mixture of two DHA isomers were present, the original DHA **2.31** and in majority the isomer **2.33** where the alkyne substituent has moved to position C-6 (Figure 2.11). Now the alkyne is in linear conjugation with the larger part of the nearly planar chromophore part, and therefore the molecule has a redshifted absorption maximum, estimated to be ca. 381 nm. DHA **2.33** is also photoactive, and by choosing a longer wavelength of irradiation (430 nm) where **2.31** hardly absorbs, the ratio between **2.31** and **2.33** could be

changed to ca. 5.5:4.5 after 3 cycles; an infinite number of cycles should ultimately regenerate the pure isomer **2.31**. Finally, it deserves mention that the isomerization is strongly solvent dependent. Performing the light/heat cycles of **2.31** in cyclohexane leads to no generation of **2.33**, which supports the importance of a polar solvent for promoting the zwitterionic resonance form shown in Figure 2.11.

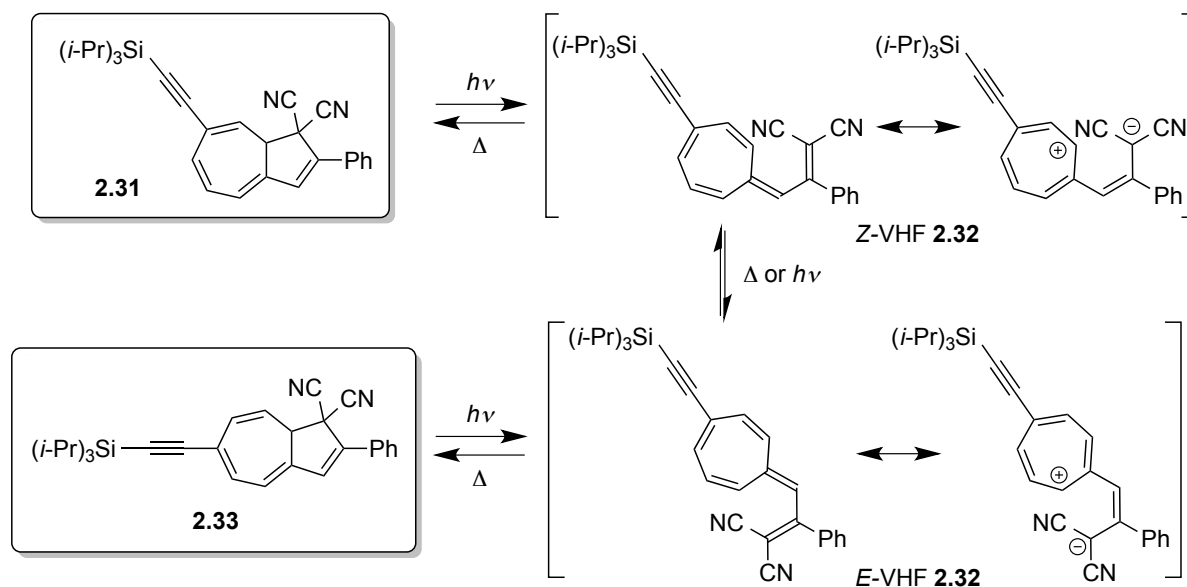


**Figure 2.11.** Isomerization between C-7 and C-6 substituted DHAs via light-induced ring-opening followed by thermal ring-closure cycle.

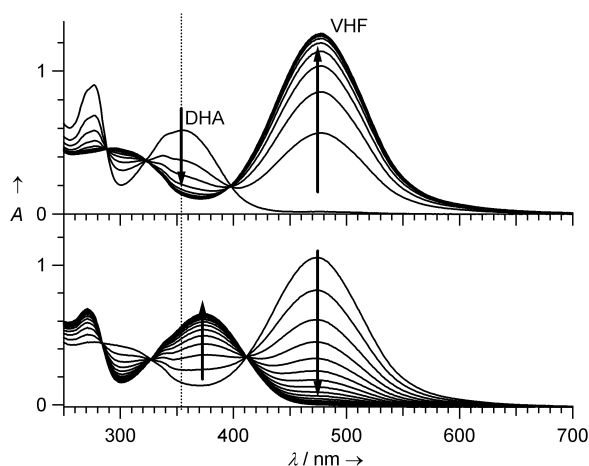


**Figure 2.12.** Top: Spectral evolution during irradiation of DHA **2.31** in MeCN with 353-nm light, forming Z/E-VHF **2.32**. Bottom: Spectral evolution during thermal back-reaction of Z/E-VHF **2.32** monitored at 70°C (2 min steps), forming a mixture of DHAs **2.31** and **2.33**. The DHA absorption redshifts after one cycle. Reproduced from Ref. 17 with permission from John Wiley and Sons.

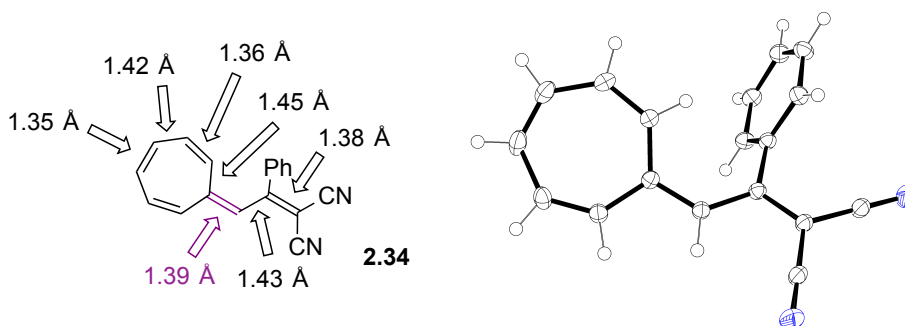


**Figure 2.13.** Molecular structure and selected bond lengths of VHF **2.34** (*s-trans* conformer) according to X-ray crystallographic analysis. Reproduced from Ref. 20 (*Beilstein Journal of Organic Chemistry*).

We have made a large selection of C-7 arylethynyl- and aryl-substituted derivatives by Sonogashira and Suzuki couplings. These compounds showed similar behavior to that of DHA **2.31**.<sup>21</sup> Yet, the absorption maxima can be strongly influenced by donor/acceptor substitution. Thus, placing a 4-(*N,N*-dimethylamino)phenyl substituent at the seven-membered ring (compounds **2.35-2.37**) results in redshifted absorption maxima of the C-6 substituted DHA and of the *Z/E*-VHFs (Figures 2.14 and 2.15).<sup>21b</sup>

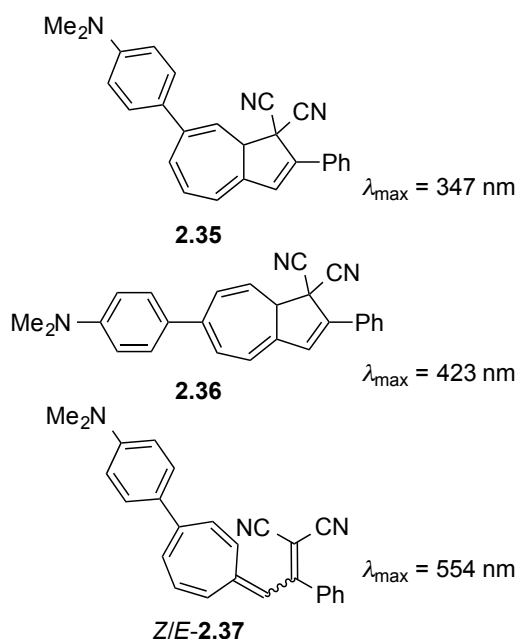


**Figure 2.14.** Absorption maxima of donor-functionalized and isomeric DHAs and VHFs in MeCN. DHA **2.34** was prepared by the bromination – elimination – cross-coupling (Suzuki) protocol.



**Figure 2.15.** The colors of DHA and VHF depend on the position and character of substituent groups as illustrated here by a color circle. The DHA color varies between yellow and orange. Protonation/deprotonation of the anilino group by acid/base changes the VHF color between violet and red. Reproduced from Ref. 21b with permission from John Wiley and Sons.

## 2.6 Non-Linear Optical Properties of Tetraethynylethene–Tetrathiafulvalene (TEE–TTF) Scaffolds

Diederich, Günter, and co-workers<sup>22</sup> have shown that donor-acceptor substituted tetraethynylethenes (TEEs) exhibit excellent third-order nonlinear optical (NLO) properties. An important take-home-message from their work is that placing an anilino donor and *p*-nitrophenyl acceptor in a linearly conjugated pathway as in compound **2.38** (Figure 2.16) provides a much higher value of the second hyperpolarizability than when these aryl substituents are placed in a cross-conjugated arrangement as in **2.39**. The planarity of arylated TEE scaffolds allows for efficient p-orbital overlap. Thus, Hopf and co-workers<sup>23</sup> have shown from X-ray crystallographic analysis that tetrakis(phenylethynyl)ethylene is planar. Instead, the smaller tetraphenylethylene is not planar due to steric interactions according to studies by Hoekstra and Vos.<sup>24</sup>

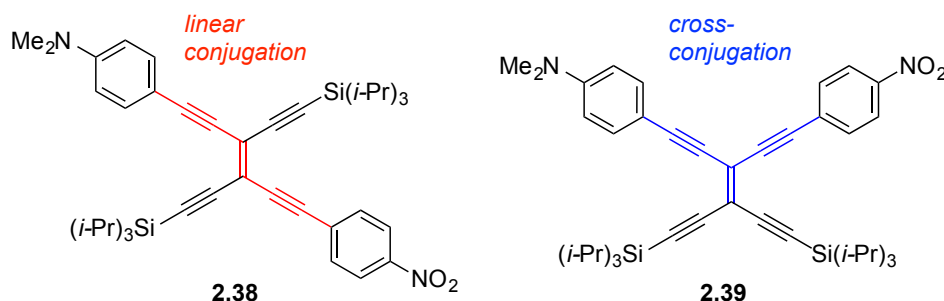


**Figure 2.16.** Arylated TEEs prepared and studied by Diederich, Günter, and co-workers.<sup>22</sup>

We became interested in studying the influence of functionalizing the TEE core with TTF donor groups, and we therefore devised a synthetic protocol for TEE-TTF **2.40** (containing hexyl substituents to assure solubility) shown in Figure 2.17.<sup>25</sup> First, the TTF derivative **2.41**<sup>26</sup> was converted to the iodo-substituted TTF **2.42** via a monolithiation followed by iodination. A Sonogashira coupling with trimethylsilylacetylene then afforded the product **2.43**. After desilylation, the terminal alkyne intermediate **2.44** was subjected to Sonogashira couplings with the vinylic dibromide **2.45** (the synthesis of which was also developed by us<sup>7</sup>) under two different conditions (*methods A and B*), both affording the target molecule **2.40**. These conditions involved Pd catalyst systems based on the bulky and electron-rich phosphine ligand P(*t*-Bu)<sub>3</sub>, which was shown by Hundertmark *et al.*<sup>27, 28</sup> to promote coupling of less reactive halides (arylbromides). Initial attempts of using the simpler PPh<sub>3</sub> ligand did not provide any TEE-TTF product. In addition, the reaction mixture was subjected to ultrasound (at ca. 30 °C), which we have shown is a very efficient and gentle method of promoting Sonogashira couplings, for which the products are sensitive to elevated temperature.<sup>29, 30</sup> To my knowledge, our paper in 2004<sup>29</sup> was the first to employ successfully ultrasound for the Sonogashira reaction (in the synthesis of

a TEE-extended TTF in a coupling between **2.20** and (3-(dibromomethylene)penta-1,4-diyne-1,5-diyl)bis(trimethylsilane), described in the next chapter), but other papers using ultrasound for Sonogashira reactions followed shortly after.<sup>31</sup>

The third-order NLO properties of **2.40** were studied by Prof. Ivan Biaggio at LeHigh University in Bethlehem, USA. The rotational average of the third-order polarizability of **2.40** was determined to  $\gamma_{\text{rot}} = 9 \pm 3 \times 10^{-48} \text{ m}^5 \text{V}^{-2}$ .<sup>25</sup> Its NLO properties thus resemble those of related tetraaryl-substituted TEEs, such as **2.46** (Figure 2.18) with  $\gamma_{\text{rot}} = 11.6 \pm 0.6 \times 10^{-48} \text{ m}^5 \text{V}^{-2}$ .<sup>32</sup> Compound **2.40** is oxidized reversibly in two two-electron oxidation steps. The NLO properties of the di- and tetracations have unfortunately not been investigated, but it is likely that they are strongly dependent on the oxidation state as the TTF units are converted from donor into acceptor units upon oxidation. This conversion can be followed by spectroelectrochemistry. UV-Vis spectroelectrochemical studies were performed *in-house* (together with Prof. K. Kilså). The neutral molecule exhibits a broad CT absorption band at  $\lambda_{\text{max}}$  661 nm, extending beyond 850 nm. Calculations reveal that the HOMO is mainly on the TTF units, while the LUMO is distributed over the nitrophenyl groups and the TEE core. Generation of the two TTF radical cations provides longest-wavelength absorption bands at  $\lambda_{\text{max}} = 438$  and 678 nm (Figure 2.19), characteristic for the intrinsic absorptions of the TTF radical cation.<sup>33</sup> Upon further oxidation, the longest-wavelength absorption is blueshifted to a broad absorption around 550 nm due to formation of TTF dications.

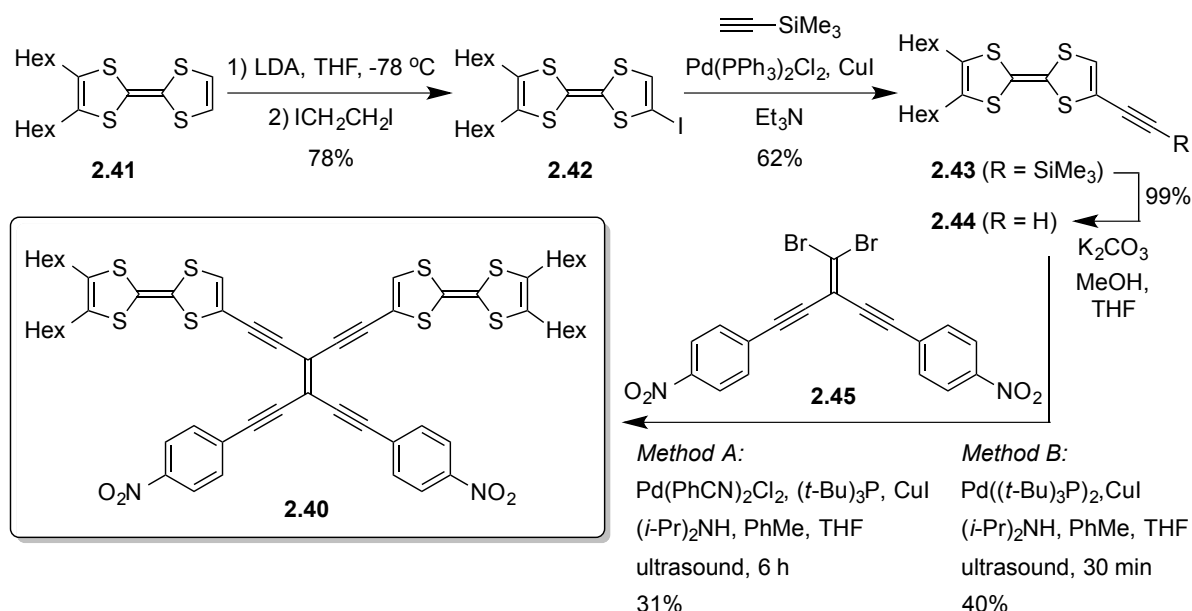


**Figure 2.17.** Synthesis of TEE-TTF scaffold. LDA = lithium diisopropylamide.

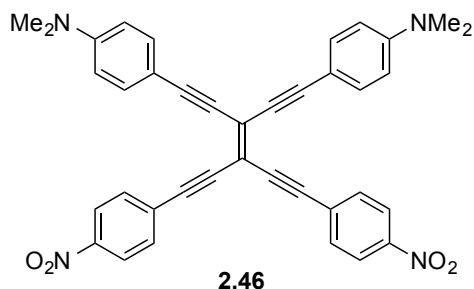


**Figure 2.18.** Tetraaryl-substituted donor-acceptor TEE.

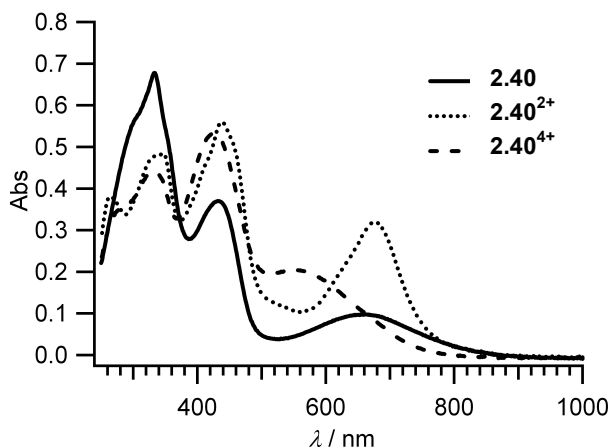


**Figure 2.19.** UV-Vis absorption spectra of **2.40** in neutral, dicationic, and tetracationic forms in  $\text{CH}_2\text{Cl}_2$  (+ 0.15 M  $\text{Bu}_4\text{NPF}_6$ ) obtained by spectroelectrochemistry. Adapted with permission from Ref. 25 (A. S. Andersson, L. Kerndrup, A. Ø. Madsen, K. Kilså, M. B. Nielsen, P. R. La Porta, I. Biaggio, *J. Org. Chem.* **2009**, 74, 375-382). Copyright (2009) American Chemical Society.

## 2.7 Conclusions

My work on donor-acceptor chromophores has shown how redshifted charge-transfer absorptions are obtained by decoupling the donor and acceptor units by a cross-conjugated bridge. Interpretations of experimental solution and gas phase absorption data were supported by calculations. In some cases decoupling between donor and acceptor ends is so strong that the CT absorption is not seen in the experimental spectrum.

Studies on a selection of expanded dendralene-like structures based on dithiafulvene units have shown that conjugation is not efficiently transmitted through the dithiafulvene bifurcation point (*i.e.*, the exocyclic fulvene carbon). In addition, placing dithiafulvenyl substituents in either *meta* or *para* configurations relative to each other at a benzene ring has strong implications for the optical properties, the *para* configuration exhibiting a significantly redshifted absorption maximum. Synthetically, we have found that ultrasound is a very convenient method of promoting Sonogashira couplings of substrates and products that are sensitive to elevated heating for prolonged times, and that dithiafulvenes can be made by phosphite-mediated couplings between benzaldehyde derivatives and 1,3-dithiol-2-thiones. Phosphite-mediated carbon-carbon double bond formation employed to achieved large two-dimensional “H-cruciform” shaped structures will be covered in a later chapter (Chapter 6).

The optical properties of the DHA photoswitch can be tuned by substituents anchored via either  $\text{sp}$ - or  $\text{sp}^2$ -hybridized carbon atoms. While little influence is seen when adding a substituent at position C-7, being in cross-conjugation (and out of co-

planarity) with the largest part of the chromophore, a significant redshift is observed when moving the substituent to position C-6. Isomerization between these two DHA regioisomers is observed upon ring-opening/closure cycles in a polar solvent like acetonitrile, in which isomerization between the *Z/E* isomeric VHF (open forms) occurs. This isomerization is explained by a significant contribution of a zwitterionic resonance form to the resonance hybrid describing VHF. As explained in the previous chapter, this is in line with the faster VHF to DHA ring-closure reaction in polar solvents than in nonpolar ones. Synthetically, we developed an efficient bromination – elimination – cross-coupling protocol for regioselectively functionalizing DHA at position C-7.

The TEE molecule comprises several linearly and cross-conjugated pathways between its alkyne units and is an excellent scaffold for construction of donor-acceptor molecules with high third-order nonlinearities as shown in the pioneering work of Diederich, Günter, and co-workers. We have together with Biaggio shown that such excellent NLO properties are maintained by incorporation of two redox-active TTF substituents instead of two aryl donor units at a TEE scaffold. The three redox states of TTF (0, +1, +2) render such molecules interesting for NLO materials whose properties may be controlled by the TTF oxidation states. Indeed, the donor properties are lost upon generation of the two TTF dication units, and, according to spectroelectrochemical studies, this tetracation species no longer exhibits the low-energy CT absorption as the neutral chromophore.

Finally, one additional comment on optical properties deserves mention. While I have shown examples in this chapter of direct charge-transfer excitations in donor-acceptor systems based mainly on my own work, another type is photoinduced charge separation where the donor unit is locally excited and thereafter transfers an electron to the acceptor unit. This is the key process in photovoltaic devices. Wasielewski and co-workers<sup>34</sup> have studied the influence of cross-conjugation vs linear conjugation for such a process in compounds **2.47-2.49** (Figure 2.20), containing the 3,5-dimethyl-4-(9-anthracenyl)julodinine donor and the naphthalene-1,8:4,5-bis(dicarboximide) acceptor. Interestingly, the photoinduced charge separation through the cross-conjugated 1,1-diphenylethylene bridge in **2.47** occurred 30 times slower than through the linearly conjugated *trans*-stilbene bridge present in **2.48**. In fact, the rate was comparable to that observed for **2.49** containing a diphenylmethane bridge, corresponding to broken conjugation between the donor and acceptor units. Presumably, the  $\sigma$ -system also comprises the primary charge separation pathway in the cross-conjugated compound.



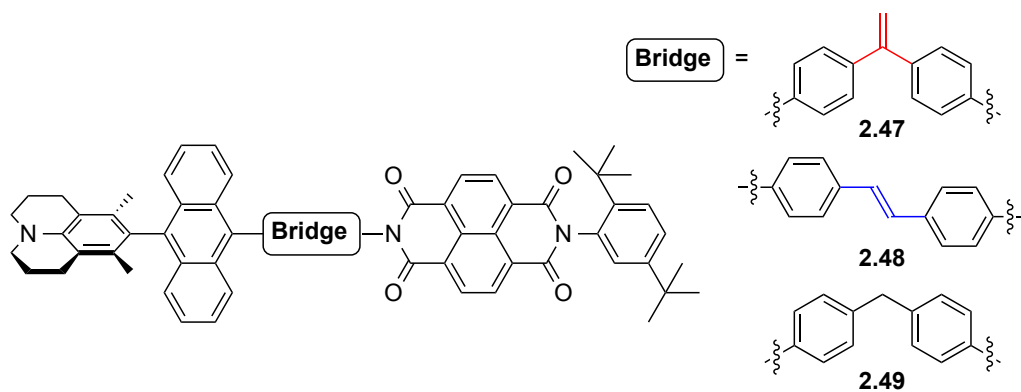


**Figure 2.20.** Compounds for which the influence of the bridging unit in regard to photoinduced charge separation has been studied by Wasielewski and co-workers.<sup>34</sup>

---

## References

1. a) S. B. Nielsen, M. B. Nielsen, A. Rubio, *Acc. Chem. Res.* **2014**, *47*, 1417-1425; b) C. R. Parker, M. B. Nielsen, "Cross-Conjugation in Expanded Systems," in *Cross-Conjugation: Modern Dendralene, Radialene and Fulvene Chemistry* (Eds. H. Hopf, M. S. Sherburn), Wiley-VCH, **2016**, pp. 337-363.
2. For details on the instrumentation, see: Ref. 1a.
3. M.-B. S. Kirketerp, M. Å. Petersen, M. Wanko, L. A. E. Leal, H. Zettergren, F. M. Raymo, A. Rubio, M. B. Nielsen, S. B. Nielsen, *ChemPhysChem* **2009**, *10*, 1207-1209.
4. M. Wanko, J. Houmøller, K. Støchkel, M.-B. S. Kirketerp, M. Å. Petersen, M. B. Nielsen, S. B. Nielsen, A. Rubio, *Phys. Chem. Chem. Phys.* **2012**, *14*, 12905-12911.
5. M. A. Christensen, E. A. Della Pia, J. Houmøller, S. Thomsen, M. Wanko, A. D. Bond, A. Rubio, S. B. Nielsen, M. B. Nielsen, *Eur. J. Org. Chem.* **2014**, 2044-2052.
6. Kotljarewskii, Bardamowa, *Izvestiya Sibirskogo Otdeleniya Akademii Nauk SSSR, Seriya Khimicheskikh Nauk* **1964**, 2073.
7. A. S. Andersson, K. Qvortrup, E. R. Torbensen, J.-P. Mayer, J.-P. Gisselbrecht, C. Boudon, M. Gross, A. Kadziola, K. Kilså, M. B. Nielsen, *Eur. J. Org. Chem.* **2005**, 3660-3671.
8. K. Sonogashira, Y. Tohda, N. Hagihara, *Tetrahedron Lett.* **1975**, *16*, 4467-4470.
9. N. B. Desai, N. B. McKelvie, F. Ramirez, *J. Am. Chem. Soc.* **1962**, *84*, 1745-1747.
10. S. Eisler, R. R. Tykwinski, *Angew. Chem. Int. Ed.* **1999**, *38*, 1940-1943.
11. a) N. N. P. Moonen, R. Gist, C. Boudon, J.-P. Gisselbrecht, P. Seiler, T. Kawai, A. Kishioka, M. Gross, M. Irie, F. Diederich, *Org. Biomol. Chem.* **2003**, *1*, 2032-2034; b) N. N. P. Moonen, F. Diederich, *Org. Biomol. Chem.* **2004**, *2*, 2263-2266.
12. M. B. Nielsen, J. C. Petersen, N. Thorup, M. Jessing, A. S. Andersson, A. S. Jepsen, J.-P. Gisselbrecht, C. Boudon, M. Gross, *J. Mater. Chem.* **2005**, *15*, 2599-2605.
13. a) M. B. Nielsen, N. N. P. Moonen, C. Boudon, J.-P. Gisselbrecht, P. Seiler, M. Gross, F. Diederich, *Chem. Commun.* **2001**, 1848-1849; b) M. B. Nielsen, N. F. Utesch, N. N. P. Moonen, C. Boudon, J.-P. Gisselbrecht, S. Concilio, S. P. Piatto, P. Seiler, P. Günter, M. Gross, F. Diederich, *Chem. Eur. J.* **2002**, *8*, 3601-3613.
14. S. S. Schou, C. R. Parker, K. Lincke, K. Jennum, J. Vibenholt, A. Kadziola, M. B. Nielsen, *Synlett* **2013**, *24*, 231-235.
15. Sallé and co-workers prepared related phenylene-extended TTFs using Horner-Wadsworth-Emmons reactions: M. Sallé, A. Belyasmine, A. Gorgues, M. Jubault, N. Soyer, *Tetrahedron Lett.* **1991**, *32*, 2897-2900.
16. M. R. Bryce, M. A. Coffin, P. J. Skabara, A. J. Moore, A. S. Batsanov, J. A. K. Howard, *Chem. Eur. J.* **2000**, *6*, 1955-1962.
17. M. Å. Petersen, S. L. Broman, A. Kadziola, K. Kilså, M. B. Nielsen, *Eur. J. Org. Chem.* **2009**, 2733-2736.
18. S. L. Broman, S. L. Brand, C. R. Parker, M. Å. Petersen, C. G. Tortzen, A. Kadziola, K. Kilså, M. B. Nielsen, *Arkivoc* **2011**, *ix*, 51-67.
19. O. Schalk, S. L. Broman, M. Å. Petersen, D. V. Khakhulin, R. Y. Brogaard, M. B. Nielsen, A. E. Boguslavskiy, A. Stalow, T. I. Sølling, *J. Phys. Chem. A* **2013**, *117*, 3340-3347.

- 
20. V. Mazzanti, M. Cacciarini, S. L. Broman, C. R. Parker, M. Schau-Magnussen, A. D. Bond, M. B. Nielsen, *Beilstein J. Org. Chem.* **2012**, *8*, 958-966.
  21. a) S. L. Broman, M. Å. Petersen, C. Tortzen, A. Kadziola, K. Kilså, M. B. Nielsen, *J. Am. Chem. Soc.* **2010**, *132*, 9165-9174; b) M. Å. Petersen, S. L. Broman, K. Kilså, A. Kadziola, M. B. Nielsen, *Eur. J. Org. Chem.* **2011**, 1033-1039.
  22. R. R. Tykwinski, U. Gubler, R. E. Martin, F. Diederich, C. Bosshard, P. Günter, *J. Phys. Chem. B* **1998**, *102*, 4451-4465.
  23. H. Hopf, M. Kreutzer, P. G. Jones, *Chem. Ber.* **1991**, *124*, 1471-1475.
  24. A. Hoekstra, A. Vos, *Acta Crystallogr. B* **1975**, *31*, 1716-1721.
  25. A. S. Andersson, L. Kerndrup, A. Ø. Madsen, K. Kilså, M. B. Nielsen, P. R. La Porta, I. Biaggio, *J. Org. Chem.* **2009**, *74*, 375-382.
  26. A. S. Andersson, K. Kilså, T. Hassenkam, J.-P. Gisselbrecht, C. Boudon, M. Gross, M. B. Nielsen, F. Diederich, *Chem. Eur. J.* **2006**, *12*, 8451-8459.
  27. T. Hundertmark, A. F. Littke, S. L. Buchwald, G. C. Fu, *Org. Lett.* **2000**, *2*, 1729-1731.
  28. For a review on electron-rich phosphines in organic synthesis, see: J. Valentine, H. Donald, J. H. Hillhouse, *Synthesis* **2003**, 2437-2460.
  29. K. Qvortrup, A. S. Andersson, J.-P. Mayer, A. S. Jepsen, M. B. Nielsen, *Synlett* **2004**, 2818-2820.
  30. For reviews on applications of sonochemistry, see: a) T. J. Mason, *Chem. Soc. Rev.* **1997**, *26*, 443-451; b) G. Cravotto, E. C. Gaudino, P. Cintas, *Chem. Soc. Rev.* **2013**, *42*, 7521-7534; c) G. Chatel, D. R. MacFarlane, *Chem. Soc. Rev.* **2014**, *43*, 8132-8149.
  31. a) A. R. Gholap, K. Venkatasen, R. Pasricha, T. Daniel, R. J. Lahoti, K. V. Srinivasan, *J. Org. Chem.* **2005**, *70*, 4869-4872; b) S. S. Palimkar, P. H. Kumar, R. L. Lahoti, K. V. Srinivasan, *Tetrahedron* **2006**, *62*, 5109-5115; c) N. Fu, Y. Zhang, D. Yang, B. Chen, X. Wu, *Catalysis Comm.* **2008**, *9*, 976-979.
  32. a) R. Spreiter, C. Bosshard, G. Knöpfle, P. Günter, R. R. Tykwinski, M. Schreiber, F. Diederich, *J. Phys. Chem. B* **1998**, *102*, 4451-4465; b) U. Gubler, C. Bosshard, *Adv. Polym. Sci.* **2002**, *158*, 123-191.
  33. a) V. Khodorkovsky, L. Shapiro, P. Krief, A. Shames, G. Mabon, A. Gorgues, M. Giffard, *Chem. Commun.* **2001**, 2736-2737; b) M.-B. S. Kirketerp, L. A. E. Leal, D. Varsano, A. Rubio, T. J. D. Jørgensen, K. Kilså, M. B. Nielsen, S. B. Nielsen, *Chem. Commun.* **2011**, *47*, 6900-6902.
  34. A. B. Ricks, G. C. Solomon, M. T. Colvin, A. M. Scott, K. Chen, M. A. Ratner, M. R. Wasielewski, *J. Am. Chem. Soc.* **2010**, *132*, 15427-15434.

# REDOX PROPERTIES

## 3.1 Introduction

I shall now turn to how cross-conjugation influences redox properties of organic molecules. This work is based on our acetylenic scaffolds of tetrathiafulvalenes (TTFs), and parts of it were recently included in a chapter by Parker and me in a book by Hopf and Sherburn on cross-conjugation.<sup>1,2</sup> As mentioned in Chapter 1, TTF undergoes two reversible oxidations, whereby the cross-conjugated molecule is converted into two 1,3-dithiolium rings. We shall see how the readiness of oxidation changes when inserting a  $\pi$ -conjugated bridge between two the dithiafulvene (DTF) units or when linking two TTF units by acyclic or cyclic acetylenic scaffolds. As cyclic units, alkyne-expanded, cross-conjugated quinoid structures (also termed radiaannulenes) will be introduced, which exhibit a remarkable ability to accommodate electrons upon reduction. Electrochemical experiments were performed at Université Louis Pasteur in Strasbourg (Prof. Maurice Gross, Dr. Jean-Paul Gisselbrecht, Dr. Corinne Boudon) or at University of Copenhagen (Prof. Ole Hammerich).

## 3.2 Extended Tetrathiafulvalenes

We have developed synthetic protocols for extended TTFs **3.1** and **3.2** with di- and tetraethynylethene spacers, which connect the DTF units in either linearly or cross-conjugated (Figures 3.1 and 3.2).

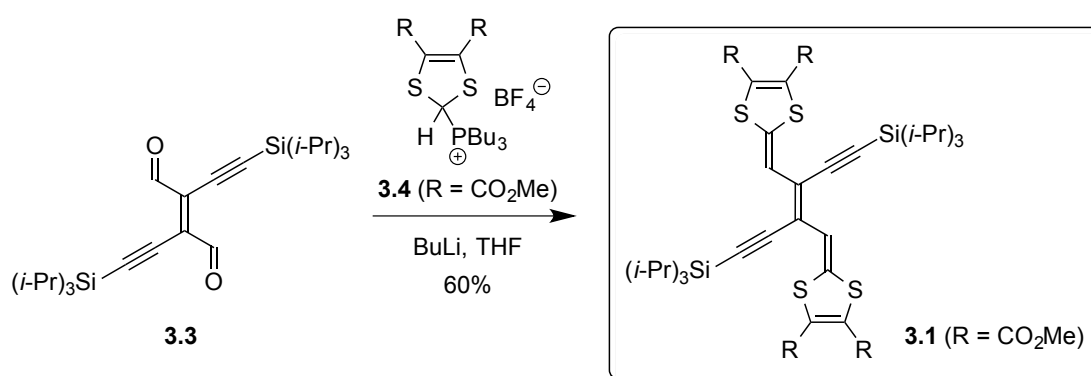


**Figure 3.1.** Synthesis of linearly conjugated extended TTF with a central diethynylethene unit.

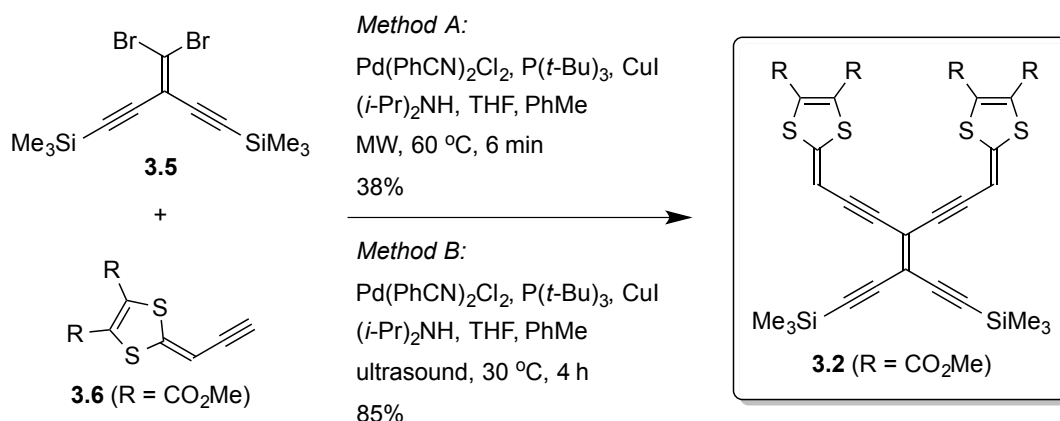


**Figure 3.2.** Synthesis of cross-conjugated extended TTF with a central tetraethynylethene (TEE) unit. MW = microwave heating.

Synthesis of the linearly conjugated **3.1**<sup>3</sup> was accomplished in a Wittig reaction between the dialdehyde **3.3**<sup>4</sup> and the ylide generated from the phosphonium salt **3.4**<sup>5</sup>. The cross-conjugated TEE-TTF **3.2**<sup>6</sup> was achieved in a Sonogashira reaction between the vinylic dibromide **3.5**<sup>4</sup> and the acetylenic DTF building block **3.6**<sup>7</sup>. Synthesis of arylated TEEs is usually achieved between **3.5** (or related structures with triisopropylsilyl protecting groups) and donor- or acceptor-functionalized arylacetylenes using the simple catalyst system  $\text{Pd}(\text{PPh}_3)_2\text{Cl}_2/\text{CuI}$  and an amine base.<sup>8</sup> Yet, such conditions failed completely to give any of the desired product **3.2**. Therefore, we turned to the catalyst system  $\text{Pd}(\text{PhCN})_2\text{Cl}_2/\text{P}(t\text{-Bu})_3/\text{CuI}$  reported by Hundertmark *et al.*<sup>9</sup> for room-temperature reactions of arylbromides. At the same time, we subjected the reaction mixture to microwave heating at 60 °C for 6 min (*Method A*), which, gratifyingly gave the product **3.2** in a yield of 38%. The yield was further increased to 85% by replacing the microwave heating with ultrasonication for 6 h at ca. 30 °C (*Method B*). Employing ultrasound provides particularly gentle conditions for Sonogashira reactions for which products or substrates are sensitive to elevated temperature; other examples were covered in the previous chapter.

The redox properties of **3.1** and **3.2** were studied by Dr. Jean-Paul Gisselbrecht, Dr. Corinne Boudon, and Prof. Maurice Gross at Université Louis Pasteur in Strasbourg.<sup>3</sup> Compound **3.1** exhibited two reversible one-electron oxidations at +0.18 and +0.39 V vs  $\text{Fc}/\text{Fc}^+$  in  $\text{CH}_2\text{Cl}_2$  (+ 0.1 M  $\text{Bu}_4\text{NPF}_6$ ), while compound **3.2** exhibited an irreversible oxidation at +0.71 V vs  $\text{Fc}/\text{Fc}^+$ . Thus, we see that it is more difficult to oxidize the cross-conjugated compound **3.2**. The dication of **3.1** can be described by a closed-shell resonance form, while this is not possible for the dication of **3.2**, which must have two unpaired electrons (Figure 3.3). This inability to delocalize the unpaired electron(s) is likely the reason for the irreversible oxidation of **3.2**; presumably, it

undergoes intermolecular dimerization reactions as observed for other DTF compounds (see Chapter 1; Figure 1.16).<sup>10</sup>

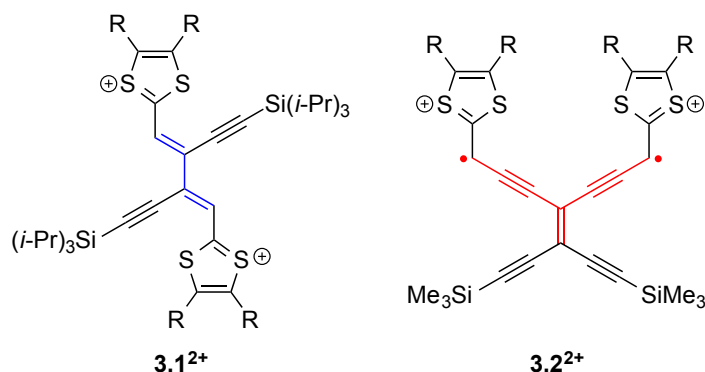


**Figure 3.3.** Dication structures of **3.1** and **3.2**.

The higher oxidation potential experienced by **3.2** may not solely be a result of cross-conjugation as there is also the electron-withdrawing effect of the alkyne units to take into account. Nevertheless, the oxidation still occurs at higher potential than for the extended TTF **3.7** with a linearly conjugated spacer and ethynyl substituents at the exocyclic DTF carbons (Figure 3.4; compound synthesized by me via a Glaser-Hay dimerization reaction during post-doctoral stay with Prof. François Diederich at ETH-Zürich<sup>7</sup>); this compound shows a first, reversible one-electron oxidation at +0.64 V vs Fc/Fc<sup>+</sup> (and a second reversible one-electron oxidation at +0.76 V vs Fc/Fc<sup>+</sup>).

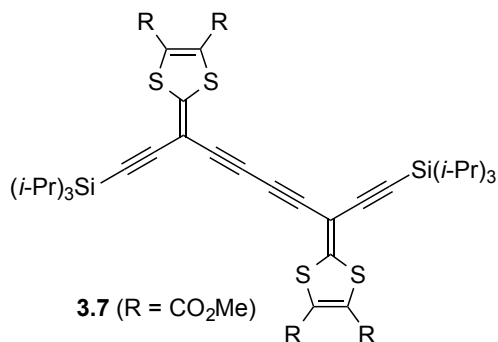


**Figure 3.4.** Buta-1,3-diene-1,4-diyl extended TTF with ethynyl substituents at the exocyclic DTF carbons.

### 3.3 Combining Weitz and Wurster Type Redox Systems

A *Weitz type redox system* consists of two rings separated by a vinylene spacer and is aromatic in the oxidized form.<sup>11</sup> TTF and *N,N'*-dimethyl-4,4'-bipyridinium are examples of such redox systems. A *Wurster type system* consists of a central ring with two end-groups and is aromatic in the reduced form. Wurster's blue (*N,N,N',N'*-tetramethylphenylenediamine), TCNQ, and *p*-benzoquinone are examples of such redox systems. We became interested to combine Weitz and Wurster type systems in one

molecule in order to achieve a system that can exist in multiple aromatic redox states. As Wurster type systems we employed the quinoid structures shown in Figure 3.5 (top; systems A and B), which can also be termed radiannulenes as they contain both endo- and exocyclic double bonds.<sup>12</sup> Kuwatani and Ueda<sup>13</sup> had previously prepared the *Sworski-type*<sup>14</sup> dehydroannulene **3.8** and shown by NMR spectroscopic studies that it exhibits a diatropic ring-current. We reasoned that similar linearly conjugated and Hückel  $14\pi$ -aromatic systems could be achieved by reduction of cross-conjugated systems A and B. The two endocyclic double bonds offer sites for fusion of TTF units, and our synthesis of a combined system is shown in Figure 3.6. Selective removal of the trimethylsilyl groups of the TEE derivative **3.9**<sup>4</sup> followed by a fourfold Sonogashira reaction with the TTF-diiodide **3.10** allowed us to prepare the TTF-radiannulene **3.11**.<sup>15</sup> It is isolated in a modest yield of 10%, but in Chapter 6 I shall present how the synthesis of such compounds can be improved (the yield is, however, not so poor considering the fact that the reaction involves four Sonogashira reactions). Compound **3.11** has an almost planar  $\pi$ -system as shown by X-ray crystallographic analysis (Figure 3.7).

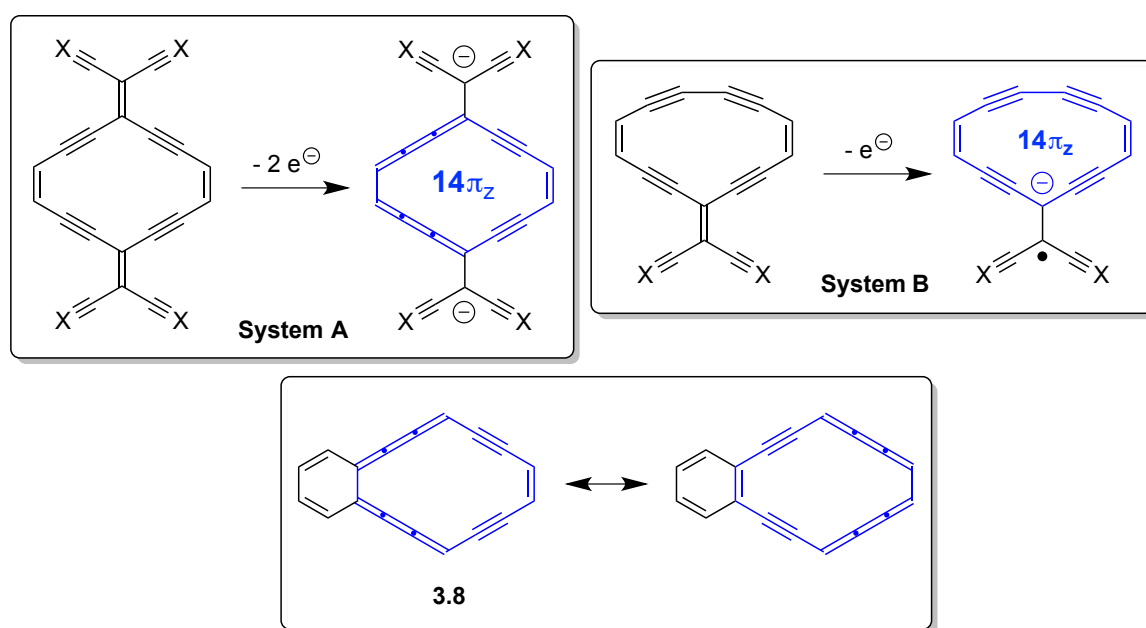


**Figure 3.5.** Top: Wurster type redox systems, which gain  $14\pi$ -aromaticity upon reduction. X can be a carbon-based group (as in our work) or another atom/group. The designation  $\pi_z$  indicates that only  $\pi$ -electrons in parallel p-orbitals are included in the electron count in these cumulenic structures. Bottom: Dehydroannulene **3.8** studied by Kuwatani and Ueda by NMR spectroscopy.<sup>13</sup>

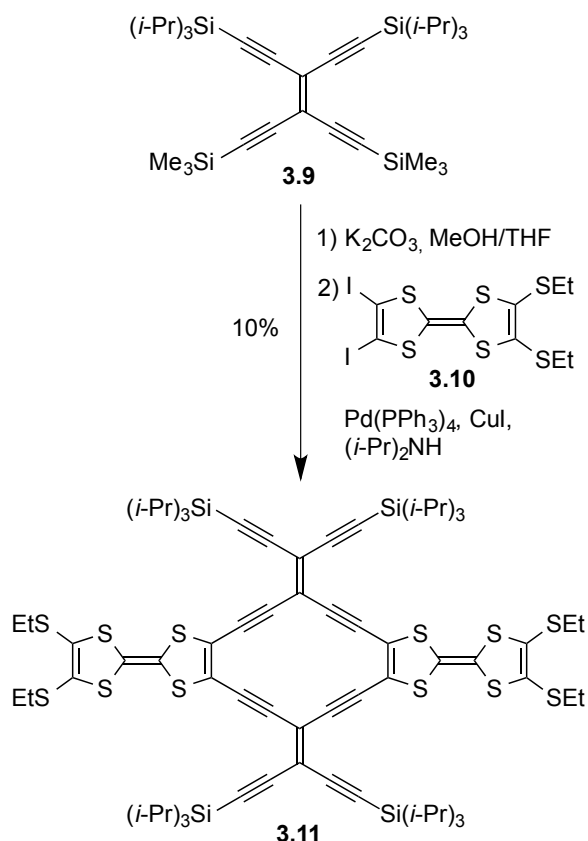


**Figure 3.6.** Synthesis of TTF-radiaannulene with system A as core.

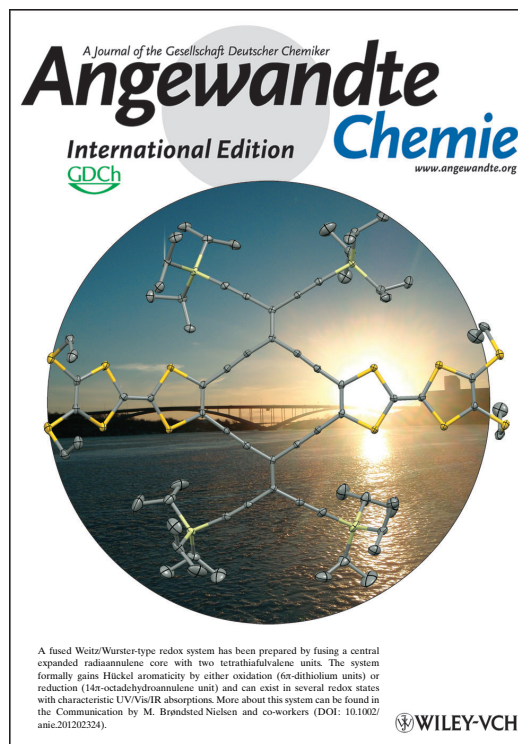


**Figure 3.7.** The  $\pi$ -system of **3.11** is almost planar according to X-ray crystallographic analysis. Reproduced from Ref. 15 with permission from John Wiley and Sons.

In addition, we prepared the TTF-radiaannulene based on system B in a stepwise manner as shown in Figure 3.8.<sup>16</sup> Compound **3.12** was subjected to Sonogashira couplings with trimethylsilylacetylene, and the trimethylsilyl groups of the product **3.13** were then removed by the action of potassium carbonate in methanol/tetrahydrofuran, and the resulting intermediate was subsequently subjected to an oxidative Glaser-Hay homo-coupling to provide the TTF-radiaannulene **3.14**. The cyclic core of this compound is almost planar according to X-ray crystallography (Figure 3.9), but the two TTF units are slightly bent. The buta-1,3-diyne-1,4-diyl bridging unit is bent from linearity, with a  $\text{C}_{\text{TTF}}\text{-C}\equiv\text{C}$  angle of  $166^\circ$  and a  $\text{C}\equiv\text{C}\text{-C}$  angle of  $170^\circ$ .



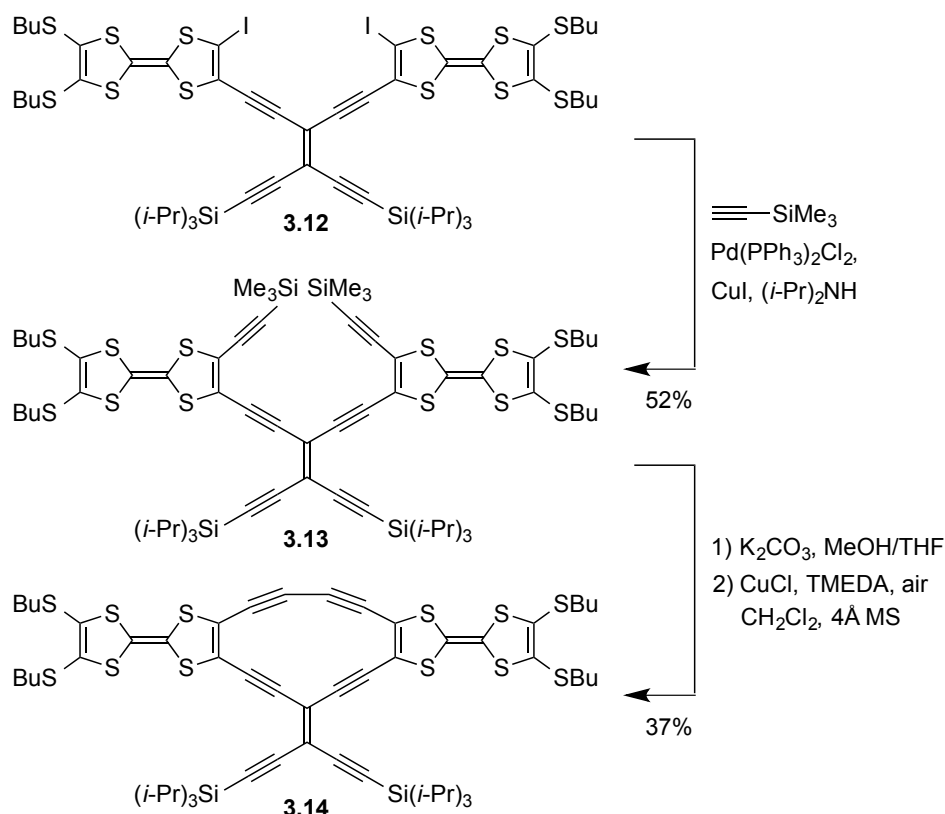


**Figure 3.8.** Synthesis of TTF-radiaannulene with system B as core. TMEDA = *N,N,N',N'*-tetramethylethylenediamine; MS = molecular sieves.

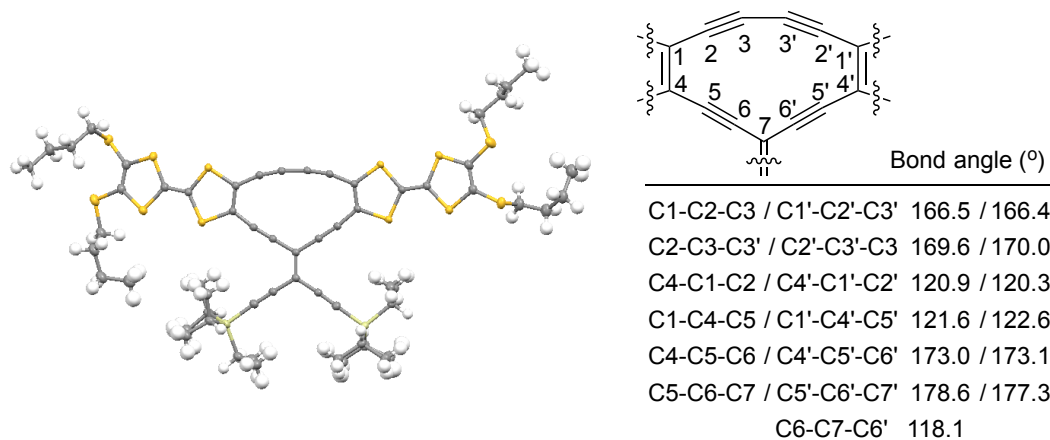


**Figure 3.9.** The  $\pi$ -system of **3.14** is almost planar according to X-ray crystallographic analysis (left). Bond angles of the cyclic core are listed to the right. Reproduced from Ref. 16 (*Beilstein Journal of Organic Chemistry*).

The cyclic voltammograms showing the reductions of TTF-radiaannulenes **3.11** and **3.14** are included in Figure 3.10.<sup>15, 16</sup> Both these compounds undergo reversible one-electron reductions to their radical anions (red curves). Further one-electron reduction to the dianions also occurs almost reversibly – the dianions are, however, sufficiently basic to produce minor amounts of monoprotonation products, and the oxidation of these is observed during the reverse scan. The first and second reductions occur at half-wave potentials of -1.16 V and -1.52 V vs  $\text{Fc}/\text{Fc}^+$  for **3.11** and at -1.12 V and -1.51 V for **3.14**. These potentials are remarkably smaller than that required to

reduce the acyclic TEE-TTF compound **3.15** shown in Figure 3.11 (here oxidations are shown, not reductions), which is reduced at -1.70 V vs Fc/Fc<sup>+</sup>. The easy reductions of the TTF-radiaannulenes indicate that a gain of aromaticity upon reduction plays an important role as suggested above, and the radiaannulene cores are thus Wurster type redox systems. Nucleus independent chemical shift (NICS) calculations on **3.11** in neutral and dianionic forms support this interpretation – the NICS(0) $\pi_{zz}$  value becomes more negative when proceeding from neutral (-8.4 ppm) to dianion (-33.2 ppm). NICS indices correspond to the negative of the magnetic shielding tensor field computed at a chosen point in the vicinity of the molecule, typically at ring centers (indicated by the number 0) or above, and was introduced by Schleyer and co-workers<sup>17</sup> as a convenient magnetic criterion for aromaticity – the more negative value, the more aromatic. During bulk electrolysis of **3.11** (performed in connection to spectroelectrochemical studies), its dianion underwent conversion to an unidentified product. This reaction of the dianion into another product was evidenced by UV-Vis and IR spectroscopies recorded during electrolysis, and formation of the dianion was irreversible under these conditions. Possibly, but pure speculation, anionic cycloaromatizations of the external, cross-conjugated diethynylethene units occur – as reported by Hopf, Rabinovitz, and co-workers<sup>18</sup> for a benzofulvene derivative (see Figure 1.9 of Chapter 1). The radical anion of **3.11** was instead formed reversibly under the bulk electrolysis conditions.

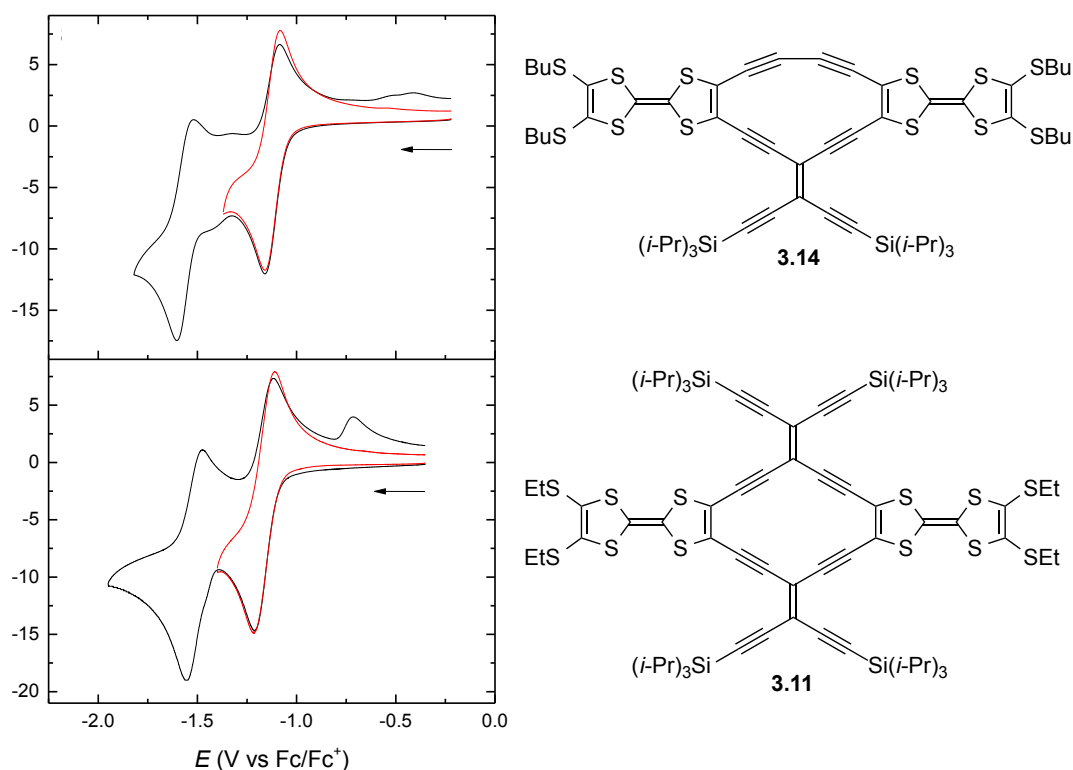


**Figure 3.10.** Cyclic voltammograms for the reduction of TTF-radiaannulenes in  $\text{CH}_2\text{Cl}_2$  (0.1 M  $\text{Bu}_4\text{NPF}_6$ ) at a glassy carbon electrode with a scan rate of  $0.1 \text{ V s}^{-1}$ . The reduction stopping at the radical anion state is shown in red color. Reproduced from Ref. 16 (*Beilstein Journal of Organic Chemistry*).

The oxidations of the TTF-radiaannulenes and the related TEE-TTFs **3.15** and **3.16** are shown in Figure 3.11. For the acyclic compounds, the two TTF units are oxidized in two two-electron steps, which means that they behave as independent redox centers, no matter whether the bridging unit is cross-conjugated (**3.15**) or linearly conjugated (**3.16**). In contrast, the first oxidation wave is split into two one-electron oxidations for both TTF-radiaannulenes, which indicates two interacting TTF units. In addition, spectroelectrochemical studies revealed a broad intervalence charge transfer absorption around 2300 nm for the monocations of these compounds (mixed valence TTF/TTF<sup>•+</sup>). *In all, the following redox states can be observed during electrochemical reduction/oxidation of the two TTF-radiaannulenes: -2, -1, 0, +1, +2, +4.*

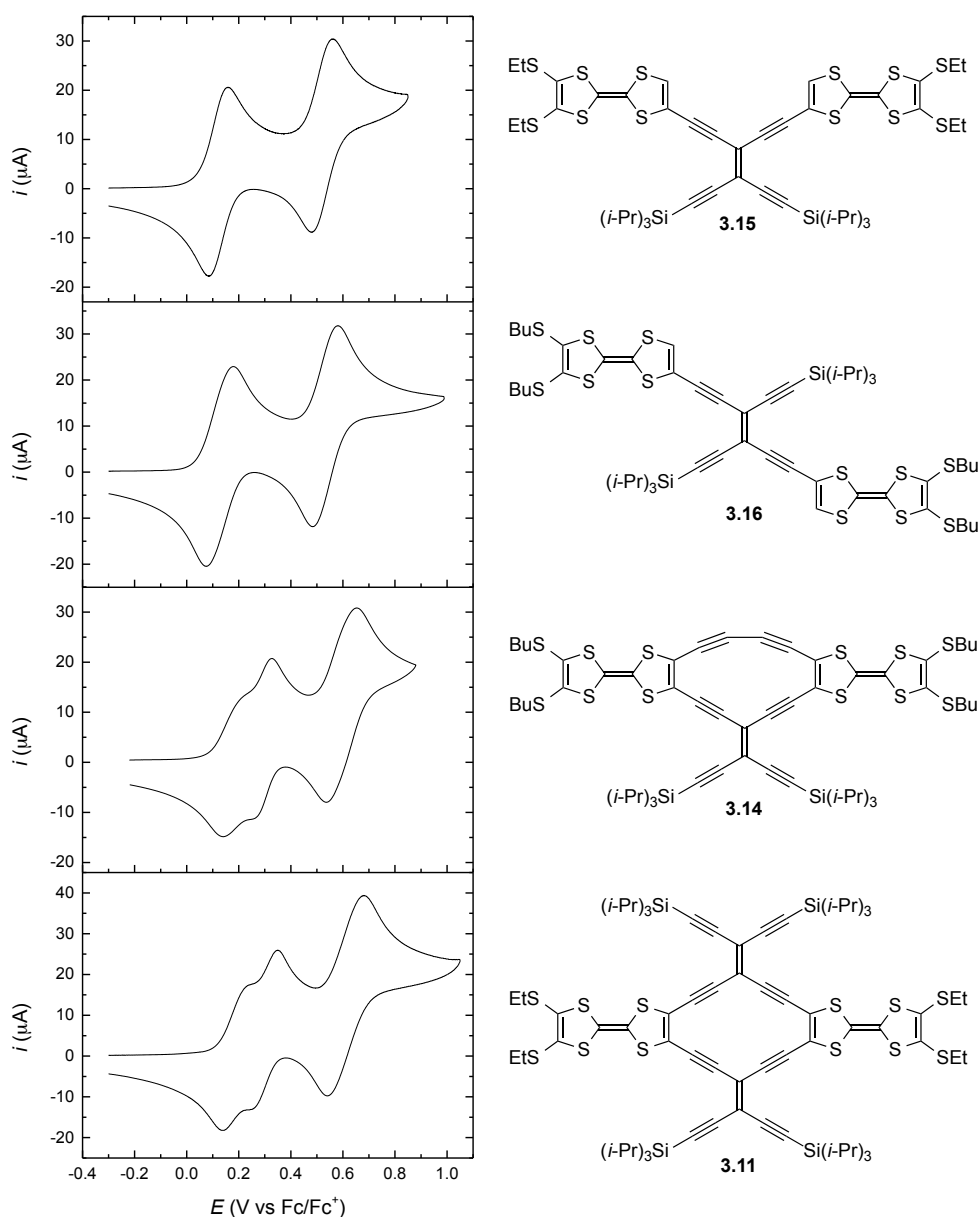


**Figure 3.11.** Cyclic voltammograms for the oxidation of bis-TTFs with various bridging units in CH<sub>2</sub>Cl<sub>2</sub> (0.1 M Bu<sub>4</sub>NPF<sub>6</sub>) at a glassy carbon electrode with a scan rate of 0.1 V s<sup>-1</sup>. Reproduced from Ref. 16 (*Beilstein Journal of Organic Chemistry*).

### 3.4 Indenofluorene-Extended TTFs

Together with Prof. Michael M. Haley at University of Oregon, Eugene, we have prepared and studied a selection of indenofluorene- and thienoacene-extended TTFs.<sup>19</sup> The synthesis of two of these compounds are shown in Figure 3.12, both containing two central thienothiophene units.<sup>19b</sup> A Horner-Wadsworth-Emmons reaction between dione **3.17** and phosphonate ester **3.18** gave the extended TTF **3.19**, while a similar reaction between **3.20** and **3.18** gave the extended TTF **3.21**, which is a structural isomer of **3.19**. The structures were confirmed by X-ray crystallography, revealing completely planar  $\pi$ -systems (Figure 3.13). The electrochemistry of these compounds was strongly concentration dependent as evident from the differential pulse voltammograms shown in Figure 3.14. Thus, the first oxidation peak is very broad, and at high concentrations even two peaks can be seen. This behavior signals that the radical cations strongly associate, forming mixed valence (neutral•cation) and  $\pi$ -dimer (cation•cation) complexes. These compounds are particularly interesting as tectons for redox-controlled self-assembly. By diluting the samples to the 2-10  $\mu$ M range, we were able to estimate the formal oxidation potentials from the differential pulse voltammograms and obtain the following values: +0.32 and +0.60 V vs. Fc/Fc<sup>+</sup> for **3.19** and +0.09 and +0.33 V vs. Fc/Fc<sup>+</sup> for **3.21**. It transpires that **3.19** is significantly more difficult to oxidize than **3.21**. This difference can be explained by the different conjugation pathways between the two DTF units – in **3.19** they are cross-conjugated while they are linearly conjugated in **3.21**. Thus, for the dication of **3.21** a closed-shell resonance form can be drawn, while this is not possible for **3.19** (Figure 3.15).

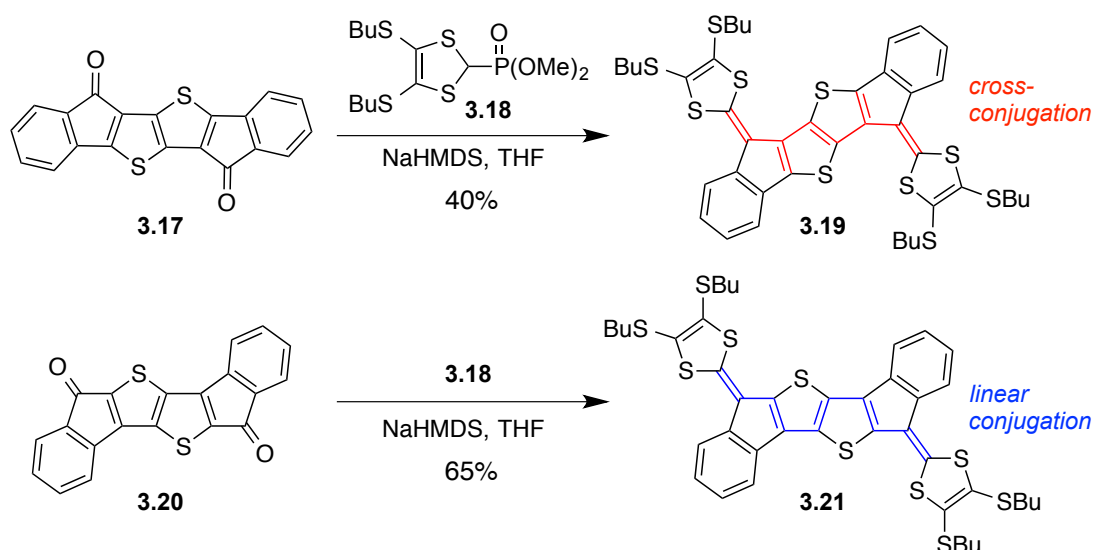


**Figure 3.12.** Synthesis of extended TTFs with thienoacene cores. NaHMDS = sodium hexamethyldisilazide.

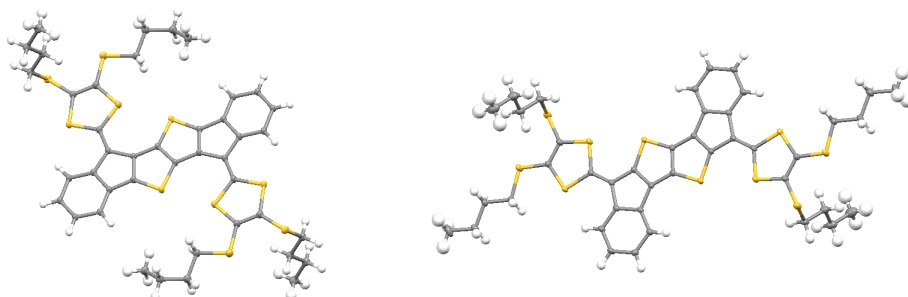


**Figure 3.13.** Molecular structures of **3.19** (left) and **3.21** (right) obtained by X-ray crystallography. Reproduced from Ref. 19b [M. A. Christensen, G. E. Rudebusch, C. R. Parker, C. L. Andersen, A. Kadziola, M. M. Haley, O. Hammerich, M. B. Nielsen, *RSC Adv.* **2015**, *5*, 49748-49751] - Reproduced by permission of The Royal Society of Chemistry.

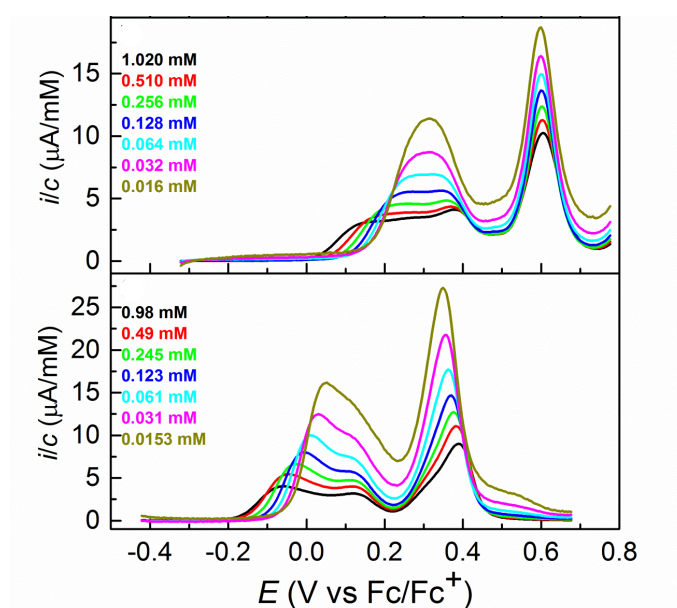


**Figure 3.14.** Differential pulse voltammograms of **3.19** (top) and **3.20** (bottom) at different concentrations measured at a glassy carbon working electrode in  $\text{CH}_2\text{Cl}_2$  (0.1 M  $\text{Bu}_4\text{NPF}_6$ ). Reproduced from Ref. 19b [M. A. Christensen, G. E. Rudebusch, C. R. Parker, C. L. Andersen, A. Kadziola, M. M. Haley, O. Hammerich, M. B. Nielsen, *RSC Adv.* **2015**, *5*, 49748-49751] - Reproduced by permission of The Royal Society of Chemistry.

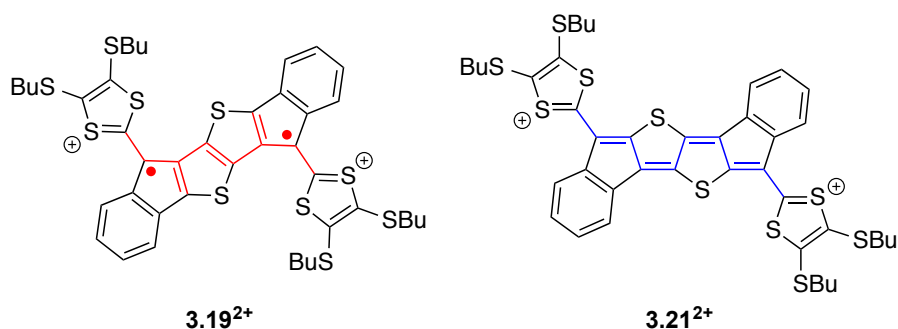


**Figure 3.15.** Dication structures of **3.19** and **3.21**.

### 3.5 Tetracenotetracene-Extended TTFs

Functionalization of polycyclic aromatic hydrocarbons (PAHs) with cross-conjugated, exocyclic DTFs units present a method to control the geometry of the PAH system via the redox state of the DTF units. Using a similar synthetic protocol as above (Horner-Wadsworth-Emmons reactions), we prepared in collaboration with Dr. Michel Frigoli at Institut Lavoisier de Versailles the “super-extended” TTF **3.22** shown in Figure 3.16.<sup>20</sup> Calculations reveal that the central core of this compound is not planar (due to steric interactions), but upon formation of the dication a planar tetraceno[2,1,12,11-*opqra*]tetracene core is formed and two 1,3-dithiolium rings, which can now freely rotate. From cyclic voltammetry it was found that **3.22** underwent a reversible two-electron oxidation to form this dication. For other examples of extended TTFs showing conformational changes upon oxidation, the reader is referred to Ref. 21.

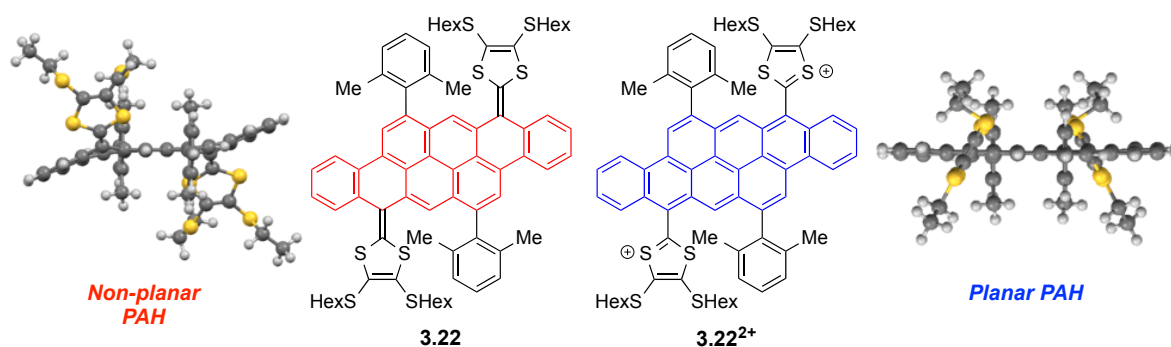


**Figure 3.16.** The redox-state of exocyclic DTF units can be employed to control the geometry of large polycyclic aromatic hydrocarbon (PAH) cores. Adapted from Ref. 20 [S. L. Broman, C. L. Andersen, T. Jousselin-Oba, M. Mansø, O. Hammerich, M. Frigoli, M. B. Nielsen, *Org. Biomol. Chem.*, In press] - Reproduced by permission of The Royal Society of Chemistry.

### 3.6 Conclusions

Separating two DTF redox centers by either cross-conjugated or linearly conjugated spacers has significant influence on the readiness of oxidation. Thus, cross-conjugated compounds are more difficult to oxidize than related, linearly conjugated ones. When the DTF unit is placed at a five-membered ring fused to other rings, co-planarity of the entire  $\pi$ -system is allowed. This co-planarity is not possible when the DTF unit is instead placed at a six-membered ring being part of an acene core, which itself is forced to deviate from planarity (see Ref. 21 for examples hereof). We employed this non-planarity in the neutral state for controlling the geometry of a large PAH (tetraceno[2,1,12,11-*opqra*]tetracene) via the oxidation state of the DTFs. Thus, upon oxidation of the cross-conjugated DTF units into 1,3-dithiolium rings, the linearly conjugated, planar PAH core is generated.

Larger alkyne-expanded quinoid structures constructed from TEE units present Wurster type redox systems, which seem to gain aromaticity upon reduction. By fusing

such systems to Weitz type redox systems (TTF), molecules that can exist in several redox states have been obtained. Interestingly, two TTF units interact when bridged by such cyclic cores as evident from stepwise oxidations and a near-infrared intervalence charge transfer absorption band of the monocation, while two TTF units behave as independent redox centers when simply bridged by one TEE unit in an acyclic structure.

## References

1. C. R. Parker, M. B. Nielsen, "Cross-Conjugation in Expanded Systems," in *Cross-Conjugation: Modern Dendralene, Radialene and Fulvene Chemistry* (Eds. H. Hopf, M. S. Sherburn), Wiley-VCH, **2016**, pp. 337-363.
2. For another coverage of cross-conjugation in redox-active TTF derivatives, see: M. Hasegawa, Y. Misaki, "Cross-Conjugation and Electronic Structure in TTF Analogs," in *Cross-Conjugation: Modern Dendralene, Radialene and Fulvene Chemistry* (Eds. H. Hopf, M. S. Sherburn), Wiley-VCH, **2016**, pp. 301-336.
3. a) M. B. Nielsen, J.-P. Gisselbrecht, N. Thorup, S. P. Piotto, C. Boudon, M. Gross, *Tetrahedron Lett.* **2003**, *44*, 6721-6723; b) A. S. Andersson, K. Qvortrup, E. R. Torbensen, J.-P. Mayer, J.-P. Gisselbrecht, C. Boudon, M. Gross, A. Kadziola, K. Kilså, M. B. Nielsen, *Eur. J. Org. Chem.* **2005**, 3660-3671.
4. J. Anthony, A. M. Boldi, Y. Rubin, M. Hobi, V. Gramlich, C. B. Knobler, P. Seiler, F. Diederich, *Helv. Chim. Acta* **1995**, *78*, 13-45.
5. M. Sato, N. C. Gonella, M. P. Cava, *J. Org. Chem.* **1979**, *44*, 930-934.
6. K. Qvortrup, A. S. Andersson, J.-P. Mayer, A. S. Jepsen, M. B. Nielsen, *Synlett* **2004**, 2818-2820.
7. a) M. B. Nielsen, N. N. P. Moonen, C. Boudon, J.-P. Gisselbrecht, P. Seiler, M. Gross, F. Diederich, *Chem. Commun.* **2001**, 1848-1849; b) M. B. Nielsen, N. F. Utesch, N. N. P. Moonen, C. Boudon, J.-P. Gisselbrecht, S. Concilio, S. P. Piotto, P. Seiler, P. Günter, M. Gross, F. Diederich, *Chem. Eur. J.* **2002**, *8*, 3601-3613.
8. a) R. R. Tykwinski, M. Schreiber, V. Gramlich, P. Seiler, F. Diederich, *Adv. Mater.* **1996**, *8*, 226-231; b) R. R. Tykwinski, M. Schreiber, R. P. Carlón, F. Diederich, V. Gramlich, *Helv. Chim. Acta* **1996**, *79*, 2249-2281.
9. T. Hundertmark, A. F. Littke, S. L. Buchwald, G. C. Fu, *Org. Lett.* **2000**, *2*, 1729-1731.
10. a) M. Sallé, A. Belyasmine, A. Gorgues, M. Jubault, N. Soyer, *Tetrahedron Lett.* **1991**, *32*, 2897-2900; b) R. Carlier, P. Hapiot, D. Lorcy, A. Robert, A. Tallec, *Electrochim. Acta.* **2001**, *46*, 3269-3277; c) P. Frère, P. J. Skabara, *Chem. Soc. Rev.* **2005**, *34*, 69-98; d) G. Chen, I. Mahmud, L. N. Dawe, D. Lee, Y. Zhao, *J. Org. Chem.* **2011**, *76*, 2701-2715.
11. For an overview of Wurster and Weitz redox systems, see: K. Deuchert, S. Hünig, *Angew. Chem. Int. Ed. Engl.* **1978**, *17*, 875-886.
12. For radiaannulene structures reported by other groups, see: a) F. Mitzel, C. Boudon, J.-P. Gisselbrecht, P. Seiler, M. Gross, F. Diederich, *Helv. Chim. Acta* **2004**, *87*, 1130-1157; b) G. Chen, L. Wang, D. W. Thompson, Y. Zhao, *Org. Lett.* **2008**, *10*, 657-660; c) G. Chen, L. Dawe, L. Wang, Y. Zhao, *Org. Lett.* **2009**, *11*, 2736-2739; d) M. Ghomali, M. N. Chaur, M. Wilde, M. J. Ferguson, R. McDonald, L. Echegoyen, R. R. Tykwinski, *Chem. Commun.* **2009**, 3038-3040; e) Y.-L. Wu, F. Bures, P. D. Jarowski, W. B. Schweizer, C. Boudon, J.-P. Gisselbrecht, F. Diederich, *Chem. Eur. J.* **2010**, *16*, 9592-9605.
13. Y. Kuwatani, I. Ueda, *Angew. Chem. Int. Ed. Engl.* **1995**, *34*, 1892-1894.
14. T. J. Sworski, *J. Chem. Phys.* **1948**, *16*, 550.
15. K. Lincke, A. F. Frellsen, C. R. Parker, A. D. Bond, O. Hammerich, M. B. Nielsen, *Angew. Chem. Int. Ed.* **2012**, *51*, 6099-6102.



- 
16. H. Jiang, V. Mazzanti, C. R. Parker, S. L. Broman, J. H. Wallberg, K. Lušpai, A. Brincko, H. G. Kjaergaard, A. Kadziola, P. Rapt, O. Hammerich, M. B. Nielsen, *Beilstein J. Org. Chem.* **2015**, *11*, 930-948.
17. a) P. v. R. Schleyer, C. Maerker, A. Dransfeld, H. Jiao, N. J. R. v. E. Hommes, *J. Am. Chem. Soc.* **1996**, *118*, 6317-6318; b) Z. Chen, C. S. Wannere, C. Corminboeuf, R. Puchta, P. v. R. Schleyer, *Chem. Rev.* **2005**, *105*, 3842-3888.
18. L. Eshdat, H. Berger, H. Hopf, M. Rabinovitz, *J. Am. Chem. Soc.* **2002**, *124*, 3822-3823.
19. a) M. A. Christensen, C. R. Parker, T. J. Sørensen, S. de Graaf, T. J. Morsing, T. Brock-Nannestad, J. Bendix, M. M. Haley, P. Rapt, A. Danilov, S. Kubatkin, O. Hammerich, M. B. Nielsen, *J. Mater. Chem. C* **2014**, *2*, 10428-10438; b) M. A. Christensen, G. E. Rudebusch, C. R. Parker, C. L. Andersen, A. Kadziola, M. M. Haley, O. Hammerich, M. B. Nielsen, *RSC Adv.* **2015**, *5*, 49748-49751.
20. S. L. Broman, C. L. Andersen, T. Jousselin-Oba, M. Mansø, O. Hammerich, M. Frigoli, M. B. Nielsen, *Org. Biomol. Chem.* **2017**, *15*, 807-811.
21. a) Y. Yamashita, T. Miyashi, *Chem. Lett.* **1988**, 661-664; b) Y. Yamashita, Y. Kobayashi, T. Miyashi, *Angew. Chem. Int. Ed. Engl.* **1989**, *28*, 1052-1053; c) M. R. Bryce, E. Fleckenstein, S. Hünig, *J. Chem. Soc., Perkin Trans 2* **1990**, 1777-1783; d) A. J. Moore, M. R. Bryce, *J. Chem. Soc., Perkin 1* **1991**, 157-168; e) N. Martín, L. Sánchez, C. Seoane, E. Ortí, P. M. Viruela, R. Viruela, *J. Org. Chem.* **1998**, *63*, 1268-1279; f) F. G. Brunetti, J. L. López, C. Atienza, N. Martín, *J. Mater. Chem.* **2012**, *22*, 4188-4205; g) E. A. Younes, Y. Zhao, *RSC Adv.* **2015**, *5*, 88821-88825.

# CHEMICAL REACTIVITY

## 4.1 Introduction

In the first chapter, the chemistry of the dendralenes in cycloaddition reactions was mentioned and the different behavior of “odd” and “even” dendralenes.<sup>1</sup> Cross-conjugation also has strong implication for the chemistry of polycyclic nonbenzenoidic  $\pi$ -electron systems (such as pentalenes, azulenes, heptalenes, and larger fused structures derived therefrom),<sup>2</sup> and in the field of asymmetric organocatalysis, cross-conjugation has found recent interest, namely in the study of enantioselective Diels-Alder reactions with cross-conjugated trienamines.<sup>3</sup>

In this chapter I will focus on my group’s work in regard to elucidating how the ring-closure of the cross-conjugated vinylheptafulvene (VHF) into a dihydroazulene (DHA) is controlled by donor-acceptor (D-A) substitution at various positions. This system was first reported by Daub and co-workers who did pioneering work in the field.<sup>4</sup> DHA undergoes photoisomerization to the meta-stable VHF that in time will return to DHA – and the system can be termed as a photo-/thermoswitch. Some of the work of Daub and our own work has been reviewed in *Phys. Chem. Chem. Phys.* by S. L. Broman and me.<sup>5</sup>

As mentioned in the introductory chapter, the rate of the VHF ring-closure reaction depends on solvent polarity, which calls for a polarized transition state (Figure 4.1).<sup>4b, 6</sup> This is further supported by the influence exerted by D and A groups as shown below. The rate of the ring-closure reaction can also reveal the influence of a functional group attached to the VHF via either a linearly or cross-conjugated linker. In other words, we can use the ring-closure reaction for probing how the electronic character of a substituent is transmitted through a cross-conjugated bridge.

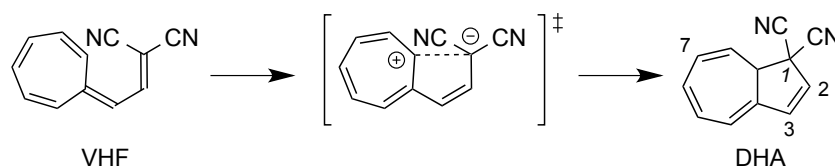


**Figure 4.1.** Thermal ring-closure reaction of VHF.

By benzannulation, the DHA-VHF isomerization is coupled to loss of aromaticity by formation of a quinoid structure. The consequences hereof will also be of focus in this chapter.

## 4.2 Donor-Acceptor Substitution at DHA Positions C-2 and C-7

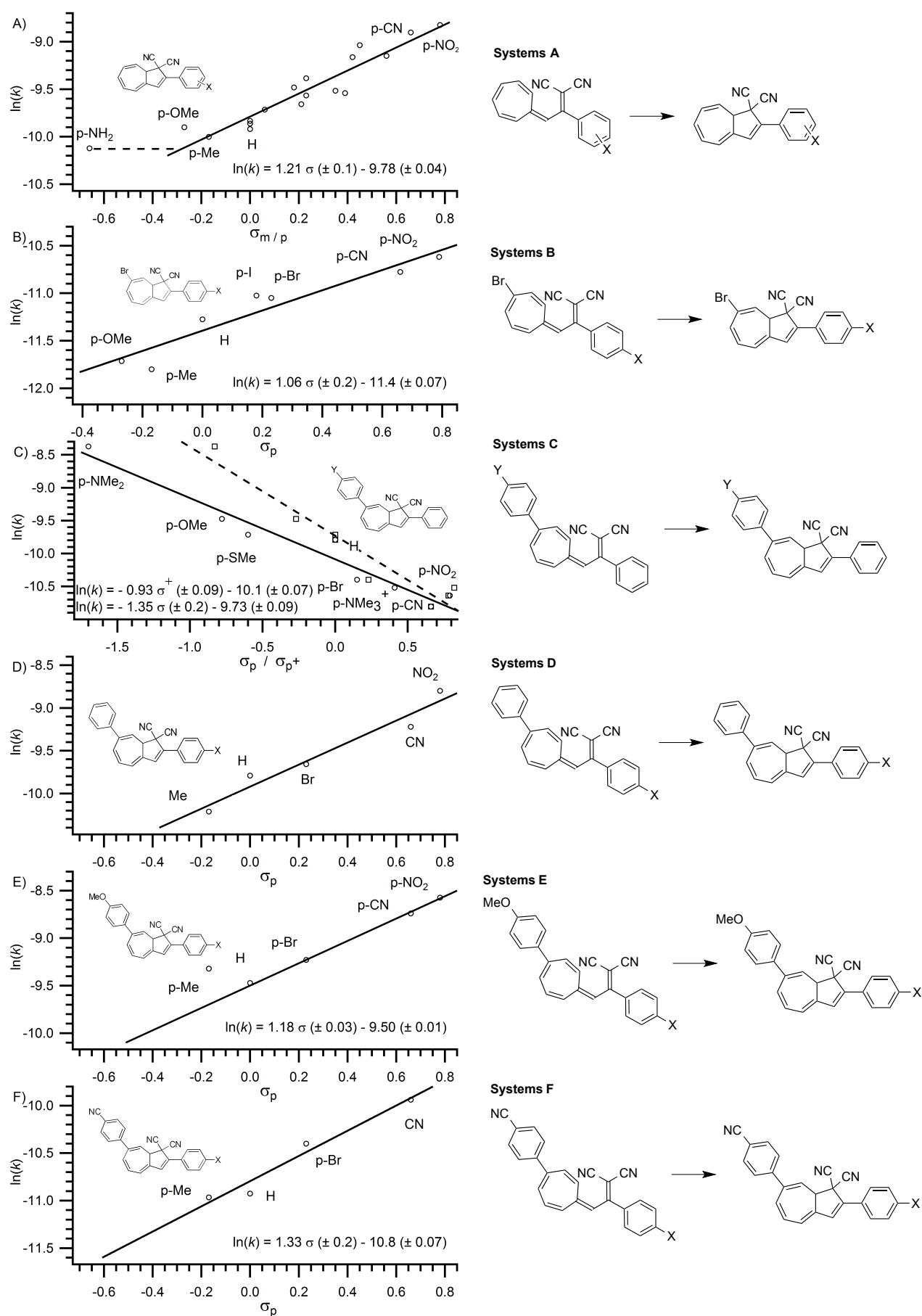
To elucidate the influence of donor and acceptor groups at positions C-2 and C-7 of DHA, we prepared a large selection of aryl-substituted derivatives.<sup>7</sup> To avoid confusion, I shall always refer to DHA atom numbers rather than to VHF atom numbers, although it is the ring-closure of VHF that is of focus in the following (*cf.*, Figure 4.1). Arylations at position C-7 were accomplished by Suzuki cross-coupling<sup>8</sup> reactions between the 7-bromo-substituted DHA and an aryl boronic acid. The DHAs were converted to VHFs by irradiation, and then the rate constants  $k$  of the first-order VHF-to-DHA back-reactions were measured in the dark at 25 °C in MeCN using UV-Vis absorption spectroscopy (by following the exponential decay in the characteristic VHF absorption around 475 nm).<sup>7a, 9</sup>

Figure 4.2 shows six different systems that were prepared and studied: for systems A, B, D, E, F, the aryl group at C-2 of DHA is changed while keeping the remaining part of the molecule constant, and for system C, the aryl group at C-7 is instead changed. For the former systems, it was found that electron-withdrawing groups enhance the reaction, while electron-donating retard it. In fact, when  $\ln k$  is plotted against Hammett substituent constants ( $\sigma_p$  for *para* substituents and  $\sigma_m$  for *meta* substituents),<sup>10</sup> linear correlations are achieved for each series. The lines have positive slopes with quite similar sizes, but the lines are parallel-displaced relative to each other. Oppositely, for system C it was found that electron-donating groups enhance the reaction, electron-withdrawing groups retard it, and again a linear-free-energy relationship (Hammett correlation) is achieved, now with negative slope (Figure 4.2). A slightly better correlation is obtained in this case by using through-conjugation substituent constants ( $\sigma_p^+$ ).

The diarylated systems C-F can conveniently be combined in one correlation as shown in Figure 4.3 where  $\ln k$  is plotted against the difference in substituent constants for the substituents placed at C-2 and C-7 of DHA.

It also deserves mention that a Hammett correlation was obtained for a series of arylethynyl-substituted systems at position C-7 of DHA (prepared using Sonogashira coupling reactions of the 7-bromo-substituted DHA).<sup>11</sup> The Hammett correlation had in this case a negative slope, which is in agreement with the resemblance of this series of compounds to system C.

# Chapter 4: Chemical Reactivity



**Figure 4.2.** Hammett correlations for VHF-to-DHA conversions in MeCN at 25 °C.  $[k] = \text{s}^{-1}$ .  
Reproduced from Ref. 9 with permission from John Wiley and Sons.

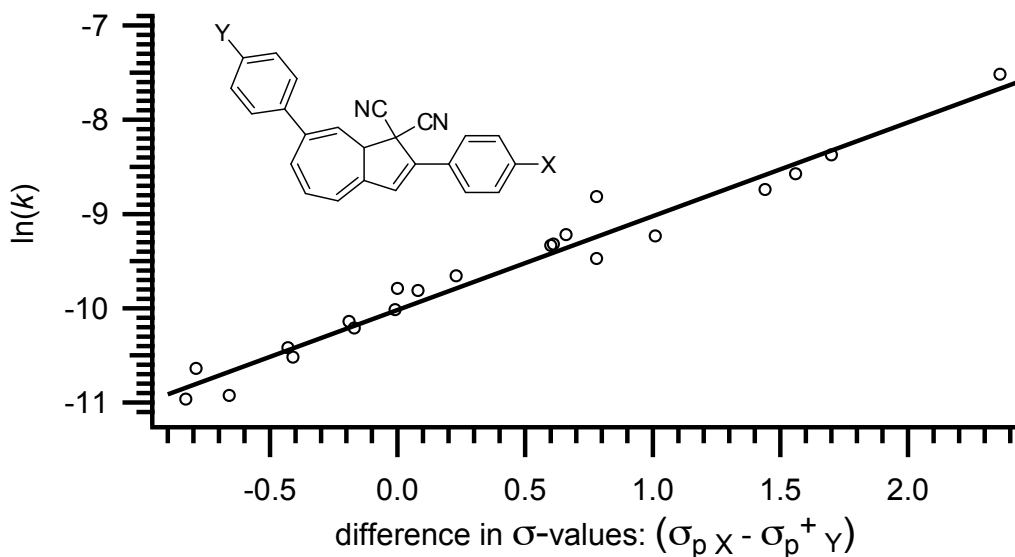


**Figure 4.3.** Hammett correlation for the VHF-to-DHA conversions based on systems C-F (MeCN, 25 °C).  $[k] = \text{s}^{-1}$ . Reproduced from Ref. 5 [S. L. Broman, M. B. Nielsen, *Phys. Chem. Chem. Phys.* **2014**, 16, 21172-21182] - Published by the PCCP Owner Societies.

By subjecting alkyne-functionalized DHAs to Copper and Ruthenium Catalyzed Azide-Alkyne Cycloadditions (CuAAC and RuAAC)<sup>12</sup> with tolylazide, we incorporated 1,4- and 1,5-disubstituted 1,2,3-triazoles at *meta* and *para* positions of the phenyl group at C-2 (Systems A).<sup>13</sup> The rate constants for the corresponding VHF to DHA ring-closures were subsequently measured. From the correlation obtained for Systems A in Figure 4.2, Hammett  $\sigma$ -constants for the triazoles in the four different substitution patterns could then be obtained by interpolations. The results are shown in Figure 4.4. The positive numbers for the  $\sigma$ -constants indicate that the triazoles are electron-withdrawing substituents. When placed in *para* positions on the phenyl group, the electron-withdrawing effect is close to that exerted by the halogens Cl and Br.<sup>10</sup> The electron-withdrawing effect is also reflected by the significant C-H acidity<sup>14</sup> and ability of 1,2,3-triazoles to engage in C-H  $\cdots$  anion hydrogen bonds.<sup>15</sup> As expected the values are close to 0 when the groups are placed in *meta* positions.

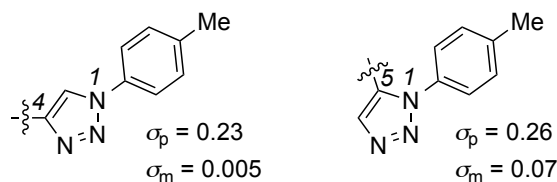


**Figure 4.4.** Hammett  $\sigma$ -constants achieved for triazoles based on the correlation obtained for Systems A.

### 4.3 Cross-Conjugated vs Linearly Conjugated Substituent at Position C-2

In the above systems A, the difference between *meta*- and *para*-substituted phenyl substituents X is clearly seen by comparing the VHF half-lives for a *m*-CN substituent group (108 min) and a *p*-CN substituent group (85 min). Thus, when placed in linear conjugation (*para*), the ring-closure reaction occurs significantly faster. To further study the influence of cross-conjugation, we decided to functionalize the DHA-VHF system with a 4-nitrophenyl via either a linearly conjugated bridge (**4.1**) or a cross-conjugated bridge (**4.2**); see Figure 4.5.<sup>16</sup> The two DHAs were prepared by a Sonogashira coupling reaction as the key step. The half-lives of the corresponding VHF's were compared to the related VHF's **4.3**<sup>4b</sup> and **4.4**<sup>17</sup> (at 25 °C in MeCN). First, we see that the 4-nitrophenyl-functionalized VHF **4.3** has the shortest half-life (79 min). Moving the 4-nitrophenyl further apart from the VHF via conjugated bridges increases the half-life, but the increase strongly depends on the nature of the bridging unit. Thus, the linearly conjugated VHF **4.1** has a half-life of 119 min, while the cross-conjugated VHF **4.2** has a longer half-life of 131 min, close to that of the 4-ethynylphenyl derivative **4.4** (137 min). The influence of the 4-nitrophenyl electron-withdrawing group is thus reduced when linked via a cross-conjugated bridge.

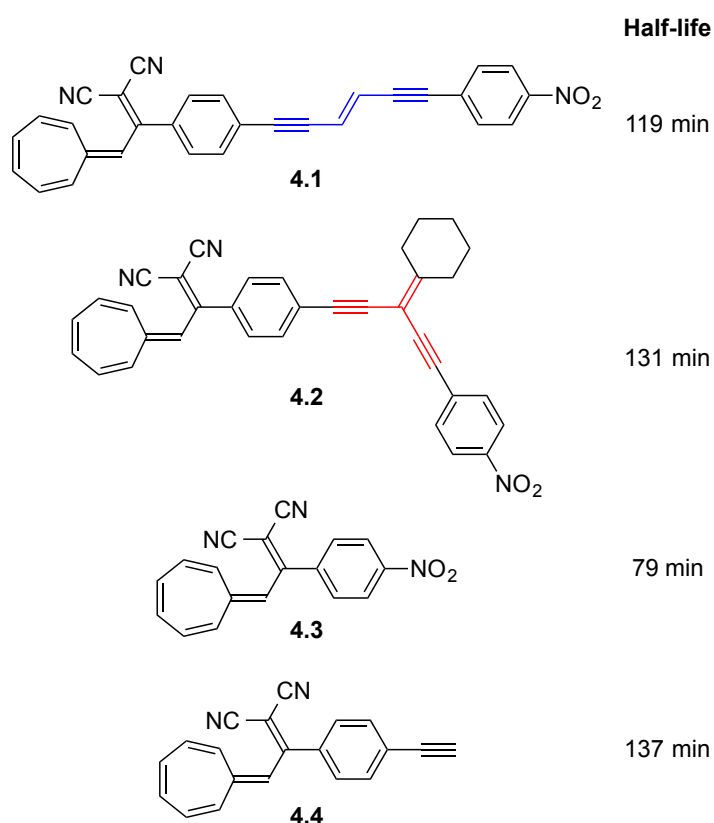


**Figure 4.5.** Half-lives for VHF-to-DHA conversions in MeCN at 25 °C.

#### 4.4 Donor-Acceptor Substitution at DHA Position C-3

Arylation at position C-3 of DHA is more challenging (see Chapter 6), but we managed to prepare two series of compounds (Systems G and H in Figure 4.6) where a substituent group is changed at this position ( $Z = \text{OMe}, \text{H}, \text{NO}_2$ ).<sup>18</sup> Interestingly, these compounds return from VHF to DHA at ultrafast rates at room temperature, and for this reason we had to conduct kinetics measurements at  $-20\text{ }^\circ\text{C}$  in EtOH. Again we achieved Hammett correlations as shown in Figure 4.6, for both series with a negative slope. Thus, at this position electron-donating groups enhance the ring-closure reaction in contrast to their influence at DHA position C-2. One reason for the ultrafast reactions can be that the VHF *s-trans/s-cis* preequilibrium is more in favor of the reactive *s-cis* conformer for these systems due to steric interactions with the aryl group. This interpretation was supported by a calculational study by Prof. Mikkelsen and co-workers at University of Copenhagen.<sup>18b</sup>

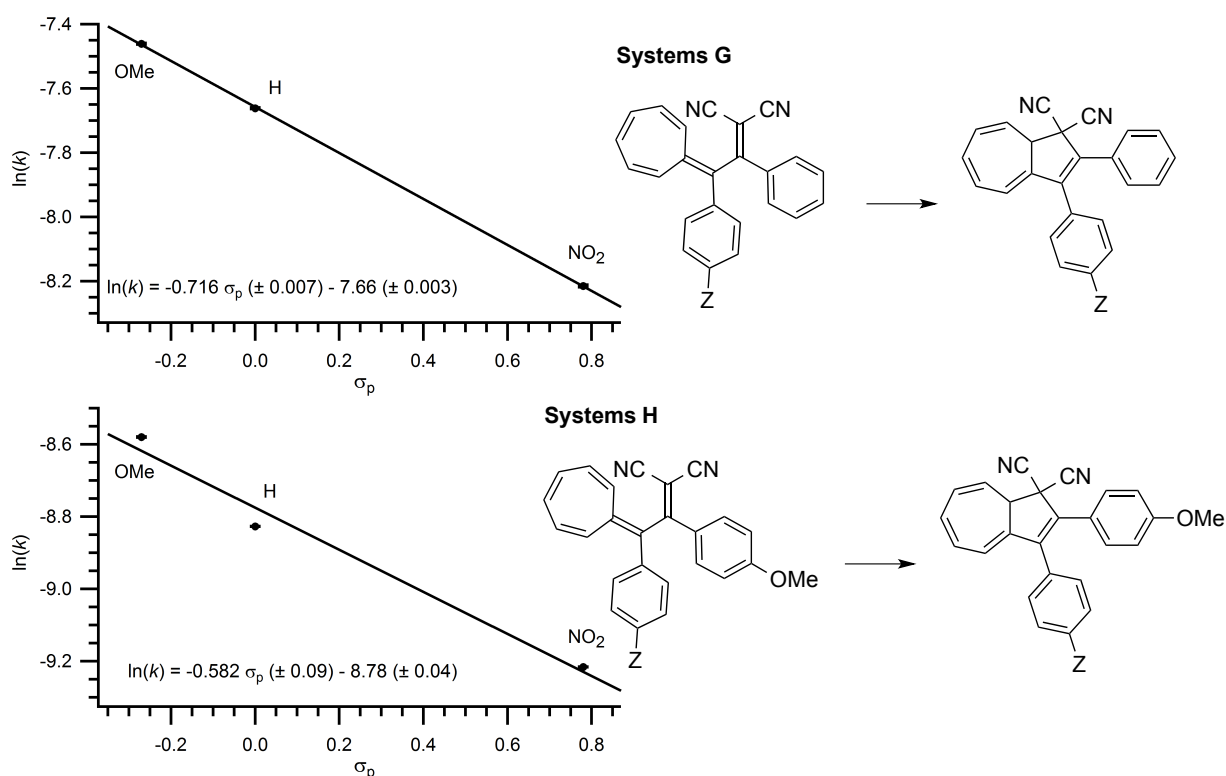


**Figure 4.6.** Hammett correlations for VHF-to-DHA conversions in EtOH at  $-20\text{ }^\circ\text{C}$ .  $[k] = \text{s}^{-1}$ . Reproduced from Ref. 18b with permission from John Wiley and Sons.

#### 4.5 Influence of Benzannulation

Another way of tuning the switching properties is to fuse a benzene ring to either the seven- or five-membered ring of DHA. Then conversion of DHA to a VHF will be accompanied by conversion of the aromatic system into a cross-conjugated *o*-quinoid structure, and the energy difference between the two isomers should accordingly be increased. For comparison, Mitchell and co-workers<sup>19</sup> have shown how the properties

of the metacyclophanediene-dihydropyrene photoswitch can be strongly tuned by benzannulation. In addition, Yang *et al.*<sup>20</sup> have shown that if the ethene bridge in dithienylethene photoswitches is made part of an aromatic system, the relative dithienylethene/dihydrodithienobenzene stabilities are altered relative to the non-benzenoid isomers.

We recently prepared DHA **4.5** (see Chapter 6 for synthesis) where a benzene ring is fused to positions C-7 and C-8 of DHA (Figure 4.7).<sup>21</sup> This DHA could not be converted to VHF by irradiation, but instead it was opened to the *Z/E*-VHF **4.6** by treatment with  $\text{AlCl}_3$  followed by water, which, however, underwent immediate ring-closure to form DHA **4.7** where the fusion has moved to the C-5 – C-6 bond of DHA. In a similar manner, DHA **4.8** was converted to VHF **4.9**,<sup>22</sup> which could not be isolated as it returned instantaneously to the aromatic DHA. Now this fast conversion is presumably not only a result of the undesirable quinoid structure of **4.9** as the VHF is also locked in the reactive *s-cis* conformation. Indeed, we have together with Prof. Jörg Daub at University of Regensburg found that when DHA **4.10** is opened to VHF **4.11**, it returns within seconds to the DHA (Figure 4.8).<sup>23</sup> Calculations reveal that the Gibbs free energy difference between *Z*-**4.6** and **4.5** is  $76 \text{ kJ mol}^{-1}$  and  $105 \text{ kJ mol}^{-1}$  between *E*-**4.6** and **4.7**. In comparison, the Gibbs free energy difference between the 2-phenyl-substituted DHA/VHF couple is only  $27.7 \text{ kJ mol}^{-1}$ .<sup>24</sup> The huge increase obtained by benzannulation makes it an interesting way of increasing the energy storage capacities of light-harvesting photochromes for solar energy storage,<sup>25</sup> despite the undesired switching properties at present for this purpose.

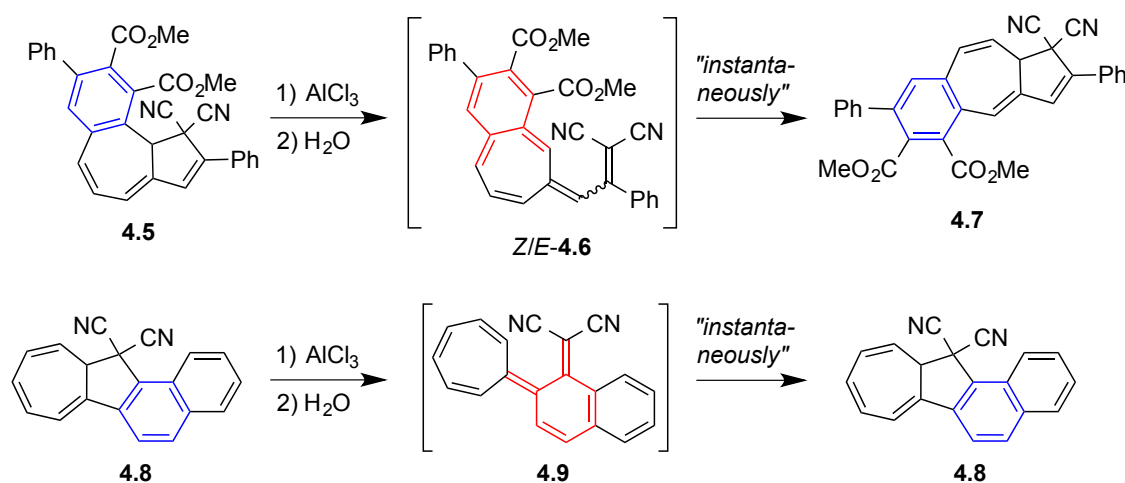


**Figure 4.7.** Benzannulation of DHA has significant influence on the switching properties.

On the other hand, when fusing a benzene ring to the VHF as in **4.12** (Figure 4.9), ring-closure to form the quinoid structure in DHA **4.13** is prevented – no conversion occurs even at elevated temperature.<sup>22</sup> The aromatic character of the fused aromatic



rings of **4.7**, **4.8**, and **4.12** were confirmed by X-ray crystallographic analyses; the structures are shown in Figure 4.10. The bond lengths of the fused benzene ring in **4.12** are in the range 1.36-1.42 Å, which are close to the value of 1.39 Å in benzene. The bond lengths of the planar naphthalene moiety of **4.8** (highlighted in Figure 4.11) are listed in Table 4.1 in comparison to those of naphthalene itself. It transpires that very similar lengths are obtained.

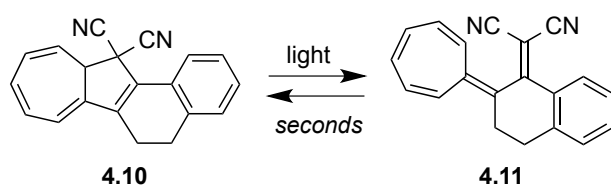


**Figure 4.8.** Locking the VHF in the reactive *s-cis* conformation results in ultrafast ring-closure of the VHF. Cover picture reproduced from Ref. 23 with permission from John Wiley and Sons.

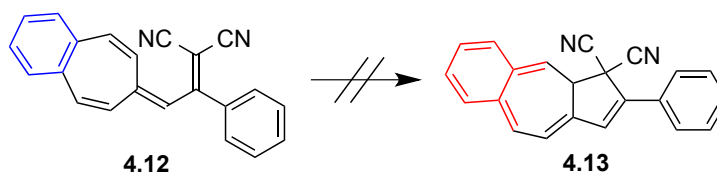


**Figure 4.9.** Benzannulation of VHF prevents ring-closure.

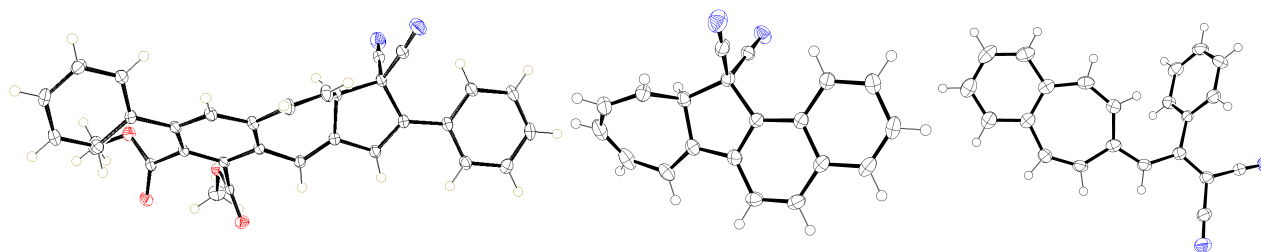


**Figure 4.10.** Molecular structures of benzannulated DHAs **4.7** (left) and **4.8** (middle) and benzannulated VHF **4.12** (right) according to X-ray crystallographic analyses. Left structure reproduced from Ref. 21 with permission from John Wiley and Sons. Middle and right structures reproduced from Ref. 22 with permission from John Wiley and Sons.

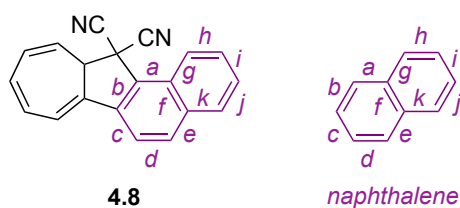


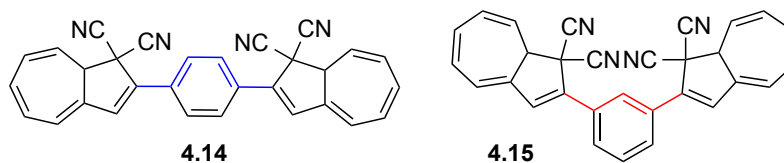
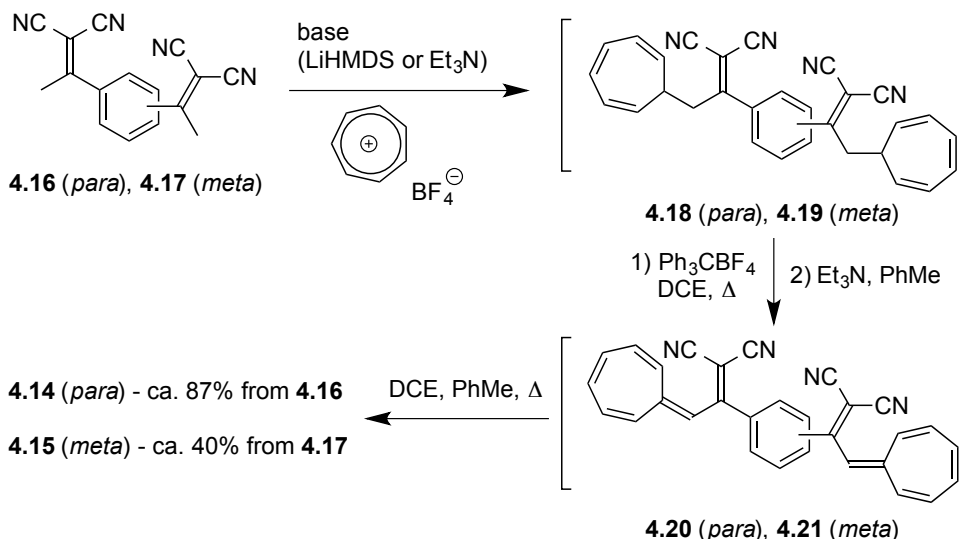
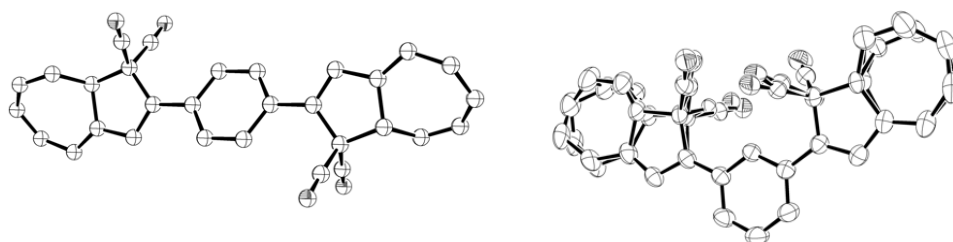
**Figure 4.11.** Designation of bonds – bond lengths are listed in Table 4.1.

**Table 4.1.** Comparison of bond lengths (in Å) in DHA **4.8** (Ref. 22) and naphthalene; see Figure 4.11 for labeling of bonds.

Bond	DHA <b>4.8</b>	<i>Naphthalene</i>	Difference
<i>a</i>	1.416	1.417	-0.001
<i>b</i>	1.372	1.364	0.008
<i>c</i>	1.416	1.416	0.000
<i>d</i>	1.364	1.350	0.014
<i>e</i>	1.419	1.423	-0.004
<i>f</i>	1.429	1.405	0.024
<i>g</i>	1.415	1.423	-0.008
<i>h</i>	1.371	1.350	0.021
<i>i</i>	1.402	1.416	-0.014
<i>j</i>	1.364	1.364	0.000
<i>k</i>	1.415	1.417	-0.002

## 4.6 Dimeric DHA Structures

Another objective of our research has been to elucidate how two DHA/VHF units interact when linked by either a linearly conjugated *p*-phenylene spacer (**4.14**; Figure 4.12) or a cross-conjugated *m*-phenylene spacer (**4.15**).<sup>26</sup> The syntheses of **4.14** and **4.15** resemble each other and are shown in Figure 4.13. Compounds **4.16** and **4.17** (prepared by Knoevenagel condensations from ketone precursors and malononitrile) were treated with a base (lithium hexamethyldisilazide in the case of **4.16** and triethylamine in the case of **4.17**) and tropylium tetrafluoroborate to provide compounds **4.18** and **4.19**, respectively. Hydride abstraction followed by deprotonation then gave the VHF dimers **4.20** and **4.21**, which upon heating gave the DHA dimers **4.14** and **4.15** (as mixtures of diastereoisomers). The intermediates were not isolated pure in this sequence as these isolations turned out to be somewhat challenging. The structures of **4.14** and **4.15** were confirmed by X-ray crystallographic analyses (Figure 4.14).

**Figure 4.12.** DHA dimers.**Figure 4.13.** Synthesis of DHA dimers. LiHMDS = lithium hexamethylsilazide; DCE = 1,2-dichloroethane.**Figure 4.14.** Molecular structures of DHA dimers **4.14** (left) and **4.15** (right) according to X-ray crystallographic analyses. Reproduced from Ref. 26 with permission from John Wiley and Sons.

The two DHA dimers were subjected to irradiation in MeCN, and the conversions of the two DHA units into VHF units were followed in time in collaboration with Prof. Henrik G. Kjaergaard at University of Copenhagen. As Figure 4.15 shows, the two compounds behave very differently. It takes significantly longer time to convert both DHA units of **4.14** into VHF units than it does for **4.15**. The reluctance of **4.14** to undergo photoisomerizations can be explained by a change of the chromophore part (less DHA character) by the linearly conjugated *p*-phenylene bridge. This interpretation is in accordance to a significantly redshifted longest-wavelength absorption maximum of 408 nm in MeCN, while the characteristic DHA absorption is usually at 355 nm. Indeed, a computational study by Prof. Kurt V. Mikkelsen and co-workers revealed that

both the HOMO and LUMO of **4.14** are significantly delocalized along the entire molecule with significant density on the central benzene ring.<sup>26</sup>

For compound **4.15** it turned out that the two DHA units were opened in a stepwise manner: DHA-DHA  $\rightarrow$  DHA-VHF  $\rightarrow$  VHF-VHF.<sup>26</sup> The first ring-opening reaction seemed to occur with a quantum yield similar to that of the parent 2-phenyl-substituted DHA. The second ring-opening reaction (DHA-VHF  $\rightarrow$  VHF-VHF) occurred much more reluctantly. By fitting the VHF absorption against time of irradiation with a double-exponential fit, the ratio between time constants was determined to 29 in MeCN. In consequence, it is possible to almost selectively open one DHA unit without affecting the second. The sequential ring-openings were also observed in CH<sub>2</sub>Cl<sub>2</sub>, toluene, and cyclohexane. Yet, they are more evident in polar solvents than in non-polar solvents. Thus, the ratio between time constants is significantly reduced from 29 in acetonitrile to 14 in cyclohexane. We interpreted this observation (in line with calculations) by a quenching of the DHA photoactivity in DHA-VHF by a charge-transfer mechanism (facilitated in a polar solvent) as the neighboring VHF unit is an electron acceptor unit. This is schematically illustrated in Figure 4.16.

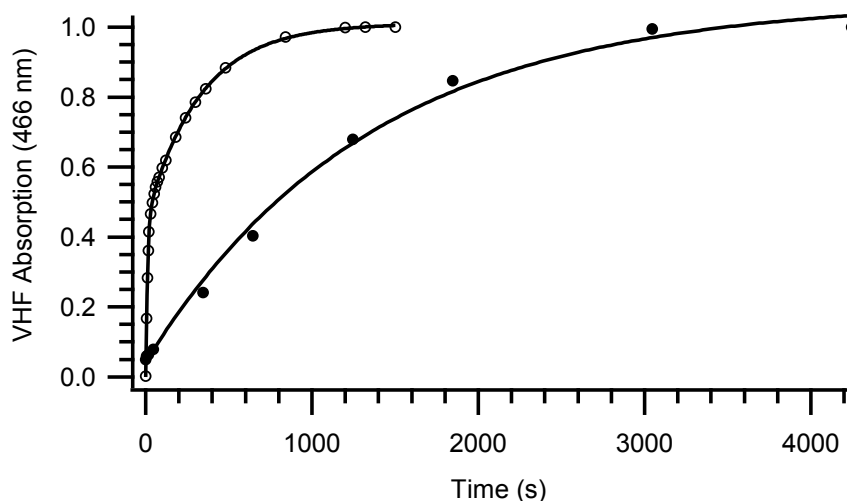


**Figure 4.15.** The VHF absorbance at the absorption maximum (normalized to unity for the final species) is plotted as a function of time of light irradiation; DHA-DHA  $\rightarrow$  DHA-VHF  $\rightarrow$  VHF-VHF for **4.14** (filled circles) and **4.15** (open circles). Irradiation of **4.14** was performed using a light source (4 lamps) with a broad radiation around 368 nm, while irradiation of **4.15** was done using a less intense 150-W Xenon arc lamp equipped with monochromator set at a wavelength of 365 nm. The time scales for DHA to VHF conversions for the two compounds can therefore not be directly compared in this figure. As the light source is less intense for **4.15**, it is clear, however, that both DHA ring-openings of this compound occur faster than those of **4.14**.

Reproduced from Ref. 26 with permission from John Wiley and Sons.

We have observed a quenching effect of the DHA photoactivity in other systems incorporating an electron acceptor unit. Thus, we have found that in DHA-C<sub>60</sub> conjugates, the quantum yield is reduced the closer the C<sub>60</sub> unit is to the DHA unit.<sup>17</sup> In

addition, we have found that the DHA photoactivity was reduced in a DHA-TTF dyad upon oxidizing the TTF unit to its radical cation.<sup>27</sup> It should be noted that both donor and acceptor units reduce the photoactivity, in both cases presumably via photoinduced electron transfer mechanisms. Thus, the photoactivity is already very low in the presence of the TTF unit as it also is for a derivative containing a dithiafulvene unit.<sup>28</sup>

The half-lives of the thermally induced VHF-to-DHA back-reactions of the VHF-VHF of **4.15** were only slightly different (the electron-withdrawing character of the VHF is not transmitted efficiently via the cross-conjugated *meta* bridge). This behavior is, however, different when the two VHF units are incorporated in a macrocyclic structure (based on **4.15** as the core structure), but this difference is now most likely due to conformational constraints.<sup>29</sup>



**Figure 4.16.** The DHA dimer **4.15** undergoes stepwise photoisomerizations, which seem to be a result of quenching of the DHA photoactivity in DHA-VHF by the VHF electron acceptor unit (transfer of electron from photoexcited DHA to VHF). Reproduced from Ref. 26 with permission from John Wiley and Sons.

### 4.7 DHA-Ruthenium Conjugates

Figure 4.17 shows a selection of DHA-ruthenium conjugates that we have prepared and studied.<sup>30</sup> Here we found that for compounds **4.22-4.24** with a bridging unit conveying a linear conjugation between the DHA and Ru center, the DHA photoactivity was quenched, while it was maintained in compound **4.25** that incorporates a cross-conjugated *meta*-phenylene unit.

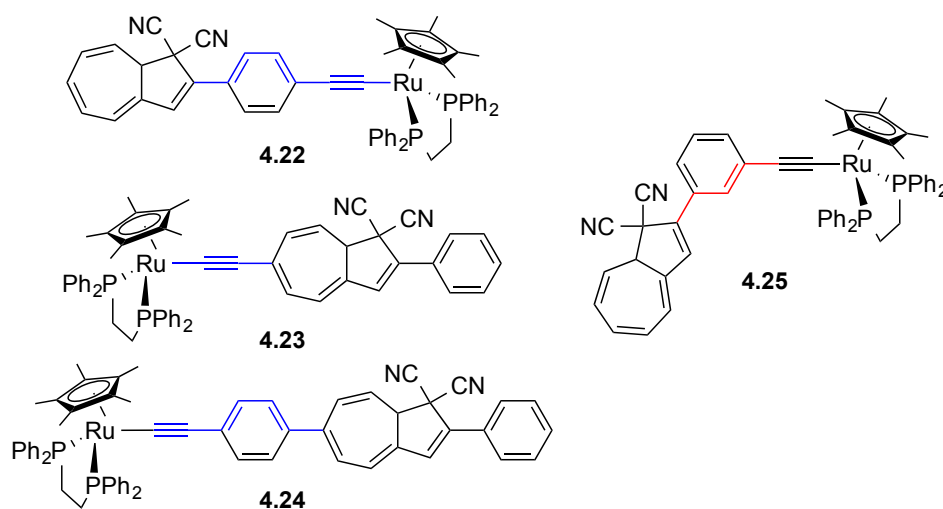


**Figure 4.17.** DHA-Ru conjugates.

### 4.8 Conclusions

This chapter on chemical reactivity has focused on how the VHF-to-DHA ring-closure reaction is influenced in different ways. Our studies have shown that it is promoted in polar solvents, by electron-donating groups at positions C-3 and C-7 of DHA, and by electron-withdrawing substituents at position C-2. Altogether, these results indicate that a polarized transition state structure is involved in the reaction. The reduced influence of donor/acceptor groups on the ring-closure reaction when placed in cross-conjugation to the VHF is also clearly evident from our studies. From the ring-closure kinetics of suitably functionalized DHA/VHF derivatives and the Hammett correlations, we are able to estimate Hammett  $\sigma$ -constants for substituent groups not yet determined. For example, it allowed us to quantify the electron-withdrawing character of 1,2,3-triazole groups.

Benzannulation of the DHA-VHF system has severe consequences for the switching properties since the aromaticity is lost upon generation of a cross-conjugated quinoid structure. When this quinoid unit is present in VHF, it returns instantaneously to DHA, while if instead the VHF incorporates an aromatic ring, it is too stable to undergo a ring-closure reaction.

Furthermore, we have found that linking two DHA units via a benzene ring in either *para* or *meta* configurations has strong implications for the switching properties. The DHA-to-VHF photoactivity of the linearly conjugated *para* compound is thus significantly reduced, while the cross-conjugated *meta* compound undergoes stepwise light-induced ring-opening reactions. For DHA-ruthenium conjugates, we found that the DHA photoactivity was quenched when the two units were connected via a *para*-phenylene unit, while retained via a *meta*-phenylene unit.

---

**References**

1. a) M. N. Paddon-Row, M. S. Sherburn, *Chem. Commun.* **2012**, 48, 832-834; b) C. G. Newton, M. S. Sherburn, "Cross-Conjugation in Synthesis," in *Cross-Conjugation: Modern Dendralene, Radialene and Fulvene Chemistry* (Eds. H. Hopf, M. S. Sherburn), Wiley-VCH, **2016**, pp. 337-363.
2. a) K. Hafner, *Pure Appl. Chem.* **1971**, 28, 153-180; b) K. Hafner, *Pure Appl. Chem.* **1982**, 54, 939-956.
3. a) K. S. Halskov, T. K. Johansen, R. L. Davis, M. Steurer, F. Jensen, K. A. Jørgensen, *J. Am. Chem. Soc.* **2012**, 134, 12943-12946; b) L. Klier, F. Tur, P. H. Poulsen, K. A. Jørgensen, *Chem. Soc. Rev.* **2017**, 46, 1080-1102.
4. a) J. Daub, T. Knöchel, A. Mannschreck, *Angew. Chem. Int. Ed. Engl.* **1984**, 23, 960-961; b) H. Görner, C. Fischer, S. Gierisch, J. Daub, *J. Phys. Chem.* **1993**, 97, 4110-4117; c) T. Mrozek, A. Ajayaghosh, J. Daub, in *Molecular Switches* (Ed. B. L. Feringa), Wiley-VCH, Weinheim, Germany, **2001**, pp. 63-106; and references cited therein.
5. S. L. Broman, M. B. Nielsen, *Phys. Chem. Chem. Phys.* **2014**, 16, 21172-21182.
6. S. L. Broman, S. L. Brand, C. R. Parker, M. Å. Petersen, C. G. Tortzen, A. Kadziola, K. Kilså, M. B. Nielsen, *Arkivoc* **2011**, ix, 51-67.
7. a) M. Å. Petersen, S. L. Broman, K. Kilså, A. Kadziola, M. B. Nielsen, *Eur. J. Org. Chem.* **2011**, 1033-1039; b) S. L. Broman, M. Jevric, A. D. Bond, M. B. Nielsen, *J. Org. Chem.* **2014**, 79, 41-64.
8. N. Miyaura, A. Suzuki, *J. Chem. Soc., Chem. Commun.* **1979**, 866-867
9. S. L. Broman, M. Jevric, M. B. Nielsen, *Chem. Eur. J.* **2013**, 19, 9542-9548.
10. a) L. P. Hammett, *J. Am. Chem. Soc.* **1937**, 59, 96-103; b) H. H. Jaffé, *Chem. Rev.* **1953**, 53, 191-261; c) C. Hansch, A. Leo, R. W. Taft, *Chem. Rev.* **1991**, 91, 165-195.
11. S. L. Broman, M. Å. Petersen, C. Tortzen, A. Kadziola, K. Kilså, M. B. Nielsen, *J. Am. Chem. Soc.* **2010**, 132, 9165-9174.
12. a) C. W. Tornøe, C. Christensen, M. Meldal, *J. Org. Chem.* **2002**, 67, 3057-3064; b) V. V. Rostovtsev, L. G. Green, V. V. Fokin, K. B. Sharpless, *Angew. Chem. Int. Ed.* **2002**, 41, 2596-2599; c) L. Zhang, X. Chen, P. Xue, H. H. Y. Sun, I. D. Williams, K. B. Sharpless, V. V. Fokin, G. Jia, *J. Am. Chem. Soc.* **2005**, 127, 15998-15999; d) L. K. Rasmussen, B. C. Boren, V. V. Fokin, *Org. Lett.* **2007**, 9, 5337-5339; e) M. Meldal, C. W. Tornøe, *Chem. Rev.* **2008**, 108, 2952-3015.
13. H. Lissau, S. L. Broman, M. Jevric, A. Ø. Madsen, M. B. Nielsen, *Aust. J. Chem.* **2014**, 67, 531-534.
14. V. E. Matulis, Y. S. Halauko, O. A. Ivashkevich, P. N. Gaponik, *J. Mol. Struct.: THEOCHEM* **2009**, 909, 19-24.
15. a) Y. Li, A. H. Flood, *Angew. Chem. Int. Ed.* **2008**, 47, 2649-2652; b) Y. Hua, A. H. Flood, *Chem. Soc. Rev.* **2010**, 39, 1262-1271.
16. K. Fjelbye, T. N. Christensen, M. Jevric, S. L. Broman, A. U. Petersen, A. Kadziola, M. B. Nielsen, *Eur. J. Org. Chem.* **2014**, 7859-7864.
17. M. Santella, V. Mazzanti, M. Jevric, C. R. Parker, S. L. Broman, A. D. Bond, M. B. Nielsen, *J. Org. Chem.* **2012**, 77, 8922-8932.



- 
18. a) V. Mazzanti, M. Cacciarini, S. L. Broman, C. R. Parker, M. Schau-Magnussen, A. D. Bond, M. B. Nielsen, *Beilstein J. Org. Chem.* **2012**, *8*, 958-966; b) M. D. Kilde, M. H. Hansen, S. L. Broman, K. V. Mikkelsen, M. B. Nielsen, *Eur. J. Org. Chem.* **2017**, 1052-1062.
  19. R. H. Mitchell, *Eur. J. Org. Chem.* **1999**, 2695-2703.
  20. Y. Yang, Y. Xie, Q. Zhang, K. Nakatani, H. Tian, W. Zhu, *Chem. Eur. J.* **2012**, *18*, 11685-11694.
  21. A. B. Skov, J. F. Petersen, J. F. Petersen, J. Elm, B. N. Frandsen, M. Santella, M. D. Kilde, H. G. Kjaergaard, K. V. Mikkelsen, M. B. Nielsen, *ChemPhotoChem* **2017**, In press.
  22. A. B. Skov, S. L. Broman, A. S. Gertsen, J. Elm, M. Jevric, M. Cacciarini, A. Kadziola, K. V. Mikkelsen, M. B. Nielsen, *Chem. Eur. J.* **2016**, *22*, 14567-14575.
  23. S. L. Broman, O. Kushnir, M. Rosenberg, A. Kadziola, J. Daub, M. B. Nielsen, *Eur. J. Org. Chem.* **2015**, 4119-4130.
  24. S. T. Olsen, J. Elm, F. E. Storm, A. N. Gejl, A. S. Hansen, M. H. Hansen, J. R. Nikolajsen, M. B. Nielsen, H. G. Kjaergaard, K. V. Mikkelsen, *J. Phys. Chem. A* **2015**, *119*, 896-904.
  25. For some recent reviews on photochromic molecules potentially suitable for storage of solar energy, see: a) T. J. Kucharski, Y. Tian, S. Akbulatov, R. Boulatov, *Energy Environ. Sci.* **2011**, *4*, 4449-4472; b) K. Moth-Poulsen, in *Organic Synthesis and Molecular Engineering* (Ed. M. B. Nielsen), Wiley, Hoboken, USA, **2014**, pp. 179-196; c) A. Lennartson, A. Roffey, K. Moth-Poulsen, *Tetrahedron Lett.* **2015**, *56*, 1457-1465.
  26. A. U. Petersen, S. L. Broman, S. T. Olsen, A. S. Hansen, L. Du, A. Kadziola, T. Hansen, H. G. Kjaergaard, K. V. Mikkelsen, M. B. Nielsen, *Chem. Eur. J.* **2015**, *21*, 3968-3977.
  27. M. Å. Petersen, A. S. Andersson, K. Kilså, M. B. Nielsen, *Eur. J. Org. Chem.* **2009**, 1855-1858.
  28. M. Å. Petersen, L. Zhu, S. H. Jensen, A. S. Andersson, A. Kadziola, K. Kilså, M. B. Nielsen, *Adv. Funct. Mater.* **2007**, *17*, 797-804.
  29. A. Vlasceanu, S. L. Broman, A. S. Hansen, A. B. Skov, M. Cacciarini, A. Kadziola, H. G. Kjaergaard, K. V. Mikkelsen, M. B. Nielsen, *Chem. Eur. J.* **2016**, *22*, 10796-101800.
  30. A. Vlasceanu, C. L. Andersen, C. R. Parker, O. Hammerich, T. J. Morsing, M. Jevric, S. L. Broman, A. Kadziola, M. B. Nielsen, *Chem. Eur. J.* **2016**, *22*, 7514-7523.

# SINGLE-MOLECULE CONDUCTANCE STUDIES

## 5.1 Introduction

The nature of the conjugation has strong influence on the single-molecule conductance as was illustrated by a few examples in the first chapter. In collaboration with Prof. Herre van der Zant (Delft University of Technology) and Prof. Wenjing Hong (Xiamen University, China), the single molecule conductance properties of a large selection of our molecules have been studied. In this chapter, I shall discuss mainly those results that directly relate to cross-conjugation. These include studies on cruciform-like molecules based on an oligo(phenyleneethynylene) (OPE) molecular wire with an extended tetrathiafulvalene (TTF) situated orthogonally to the OPE, studies on indenofluorene-extended TTFs, studies on donor-acceptor substituted OPEs, and studies on the dihydroazulene-vinylheptafulvene (DHA-VHF) photo-/thermoswitch. Since sulfur binds strongly to gold,<sup>1</sup> acetyl-protected thiolates were employed as electrode anchoring groups (with *in-situ* deprotection). The conductance properties were measured in various kinds of junctions. In the mechanically controlled break-junction, a gap is formed between two gold electrodes (source and drain) by mechanically bending a gold wire. By controlling the width of the gap, a molecule can be bridged between the two electrodes, and the conductance is measured at a certain bias voltage during many opening/closure cycles. Another way of creating a nanogap is by electromigration where a gold wire is broken by a high current. A third gold electrode covered with atomic layer deposited aluminium oxide can be used as gate to control the charge state of the molecule, providing a three-terminal device. A more detailed description of the physical methods for measuring single-molecule conductances is outside the scope of this dissertation, and the reader is instead referred to a recent review.<sup>2</sup>

## 5.2 OPE-TTF Cruciform Molecules

In a transistor the current between source and drain electrodes is controlled by a third electrode, the gate electrode. We reasoned that TTF could be used as the “third leg” in a molecular transistor for which the conductance is controlled by the TTF redox state.<sup>3, 4</sup> TTF has played a prominent role in the field of molecular electronics since Aviram and Ratner<sup>5</sup> in 1974 proposed molecular rectification in a TTF-TCNQ dyad with an aliphatic bridging unit. With instead the transistor picture in mind, we designed the motif shown

in Figure 5.1.<sup>6</sup> It contains an OPE molecular wire with an extended TTF in the orthogonal direction. In the neutral state, the conjugation along the molecular wire is linearly conjugated, but upon oxidation of the extended TTF unit, either a quinoid and cross-conjugated structure or a diradical structure is generated, which should alter the conductance. On account of the almost orthogonal arrangement of the OPE and extended TTF moieties, we have used the term cruciform for such molecules. Cruciform motifs based on two orthogonal  $\pi$ -systems have in general received interest for their electronic and optical properties.<sup>7</sup>

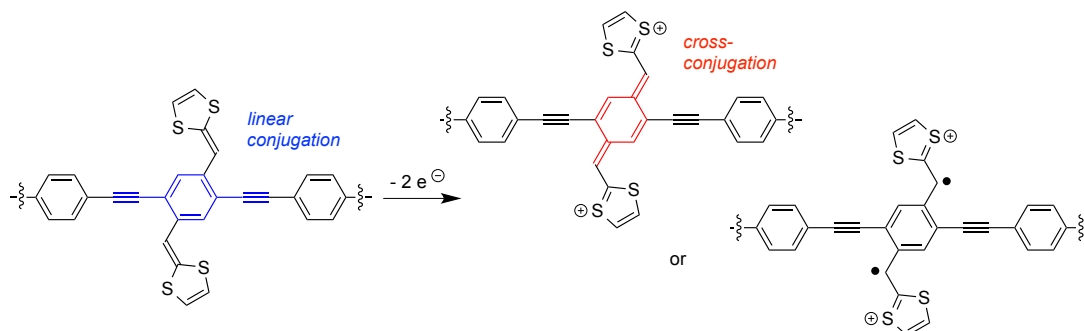


**Figure 5.1.** Cruciform motif based on OPE molecular wire with an “orthogonal” extended TTF.

Our synthesis of an OPE5-TTF cruciform is shown in Figure 5.2.<sup>8,9</sup> It starts by a Wittig reaction between the dialdehyde **5.1** (for which we developed a synthesis <sup>6a</sup>) and

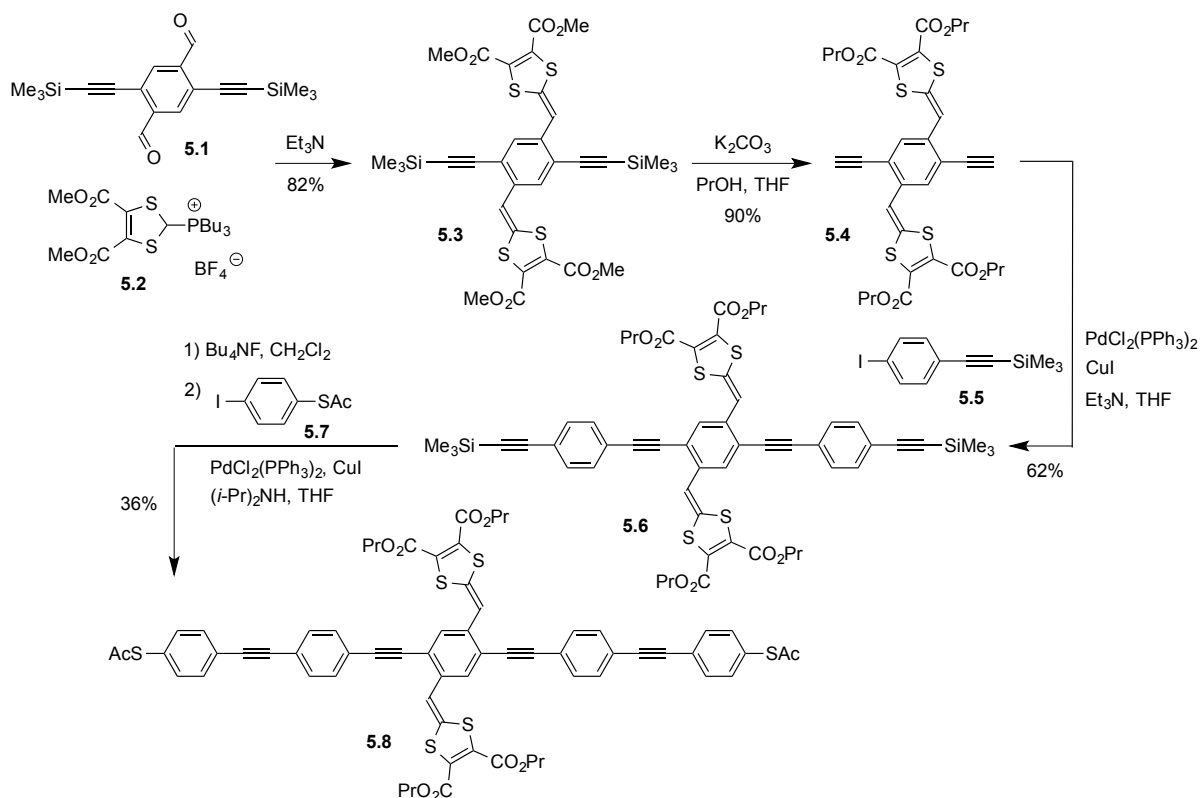


**Figure 5.2.** Synthesis of OPE5-TTF cruciform.

the phosphonium salt **5.2**<sup>10</sup>. Treating the product **5.3** with potassium carbonate and 1-propanol resulted in both desilylations and transesterifications of the peripheral ester groups, providing compound **5.4**. This compound was treated with the aryl iodide **5.5** under Sonogashira conditions to provide the OPE3-TTF cruciform **5.6**. Finally, a desilylation followed by Sonogashira coupling with the aryl iodide **5.7** gave the target OPE5-TTF **5.8** with thioacetate electrode anchoring groups. In a similar manner, the OPE3-TTF cruciform **5.9** was prepared<sup>11</sup> (as well as derivatives containing thioacetate end-groups<sup>6a,8</sup>), and X-ray crystallographic analysis revealed an almost planar  $\pi$ -system (Figure 5.3).

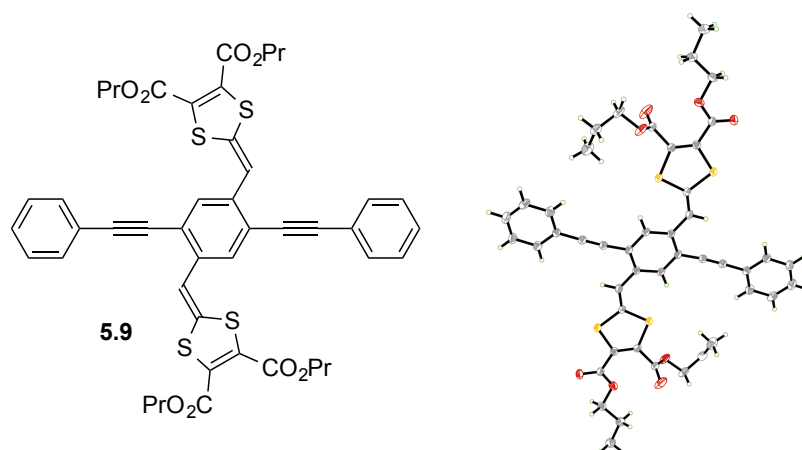


**Figure 5.3.** Molecular structure of OPE3-TTF **5.9** according to X-ray crystallographic analysis. Reproduced from Ref. 11 with permission from John Wiley and Sons.

A three-terminal device (using the electromigration method) was prepared by Herre van der Zant and co-workers from the OPE5-TTF **5.8** in which the molecule is anchored to two gold electrodes (source and drain), and a third electrode (gate) was then employed to control the redox state of the molecule;<sup>12</sup> a schematic drawing of how we imagine the molecule could be anchored in the junction is shown in Figure 5.4. The acetyl protecting groups are removed *in situ* under the experimental conditions. A plot of the single molecule conductance as a function of bias and gate potentials is shown in Figure 5.5 where blue color represents low or no current (*off* states) and orange to red color represents high current (*on* states). The figure also shows an assignment of the various regions (so-called Coulomb blockade diamonds) to charge and spin states of the molecule. This analysis required detailed theoretical modeling and was performed by physicists Prof. Per Hedegård, Prof. Jens Paaske, and Dr. Martin Leijnse in Copenhagen.

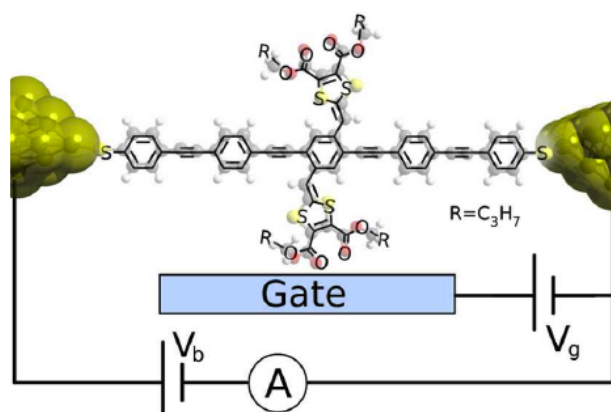


**Figure 5.4.** Schematic drawing of OPE5-TTF **5.8** in three-terminal device. The molecule is spanned between source and drain electrodes (gold), presumably via the sulfur atoms. Reproduced from Ref. 12 with permission from the American Physical Society.

The horizontal lines showing conductance at zero bias were sort of molecular “fingerprint regions” used for assigning the charge states. These zero bias conductances are called Kondo resonances and are a consequence of unpaired spins. Electron transport is here accompanied by a spin flip of the molecule. A very strong Kondo effect is observed in the region furthest to the right (signaling one spin  $1/2$ ), and this region was assigned to the radical anion state where an electron has been added to one of the rings along the wire (and with a mirror image charge in the electrode). The Kondo resonance splits into two lines in the presence of a magnetic field (8 T), which corresponds to the Zeeman effect where the spin up and down states are no longer degenerate. When removing an electron from this molecule (proceeding to the left in the plot), the neutral species is generated, but a Kondo resonance is still observed, albeit weaker. The weaker Kondo resonance can be explained by a flipping of two spins instead of just one. Therefore, we assign this region to a state with two unpaired electrons (triplet ground state), and where the electron has been removed from one of the DTF units. This is a structure of the neutral molecule that is promoted in the junction, but of course not in solution. Further oxidation removes an electron from the second DTF unit, providing three interacting spins (region furthest to the left). Thus, now we have most likely a diradical structure on the central extended TTF unit. In all, the molecule is switched between polyradical states via the gate potential. Importantly, the diradical depiction of the extended TTF moiety keeps the central aromatic benzene core intact instead of turning it into a quinoid structure. In other words, cross-conjugation is avoided. The experiments show how the molecule behaves as a molecular transistor, but in a quite complicated fashion.

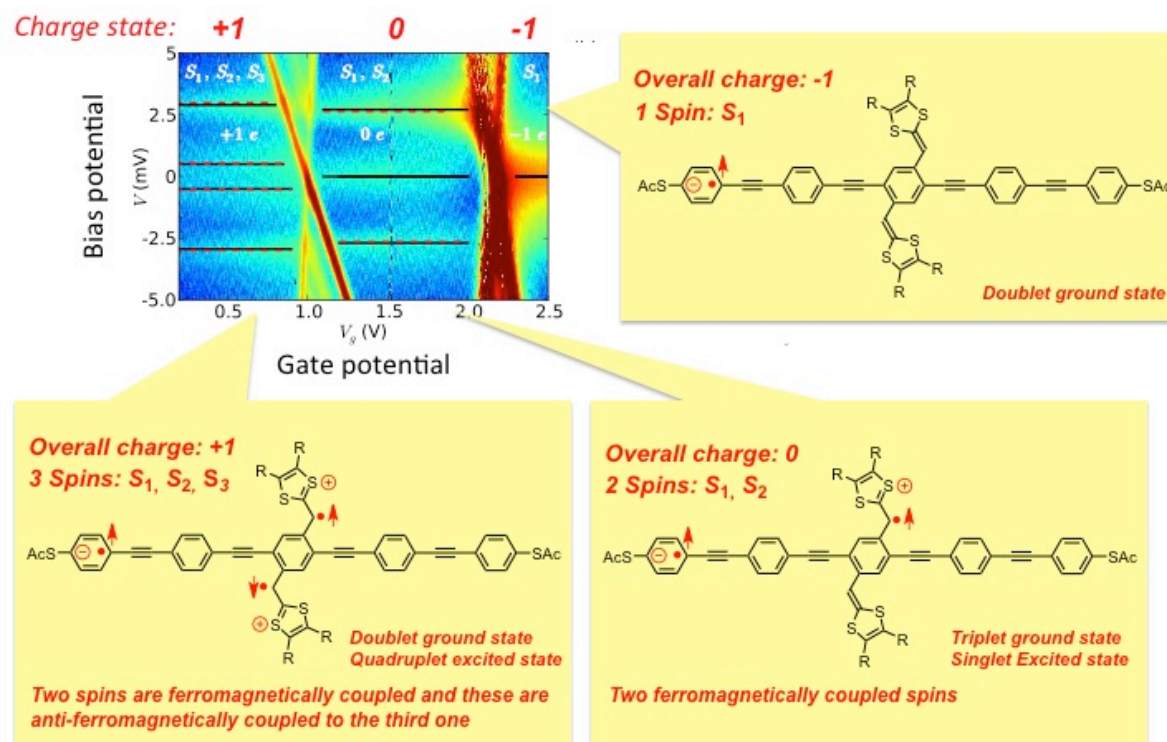


**Figure 5.5.** Conductance plot of OPE5-TTF **5.8** ( $R = \text{CO}_2\text{Pr}$ ) in three-terminal device (measurements performed at temperature of 2 K). Blue color represents low current and orange to red color represents high current as a function of bias and gate voltages. An assignment of the various regions to charge and spin states of the molecule is shown. Conductance plot reproduced from Ref. 12 with permission from the American Physical Society.

More recently, we prepared the indenofluorene-extended TTF **5.10** shown in Figure 5.6, being a significantly stronger electron donor than **5.8**, and it was subjected to three-terminal conductance measurements in Delft.<sup>13</sup> This molecule showed a strong Kondo resonance that was assigned to a spin 1/2 state (reproduced in several devices), but we cannot say unambiguously whether it is due to generation of a spin within the molecular wire by oxidation of the DTF unit since only a part of one charge state region (diamond) could be measured within the potential window.

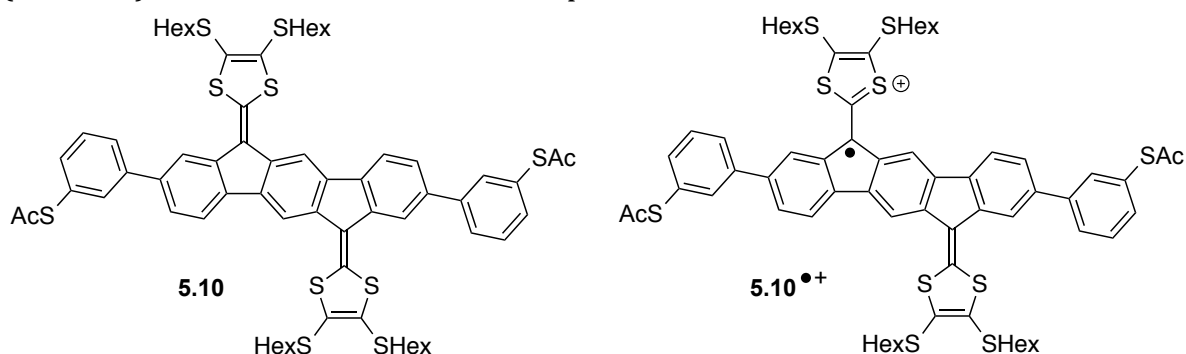


**Figure 5.6.** Indenofluorene-extended TTF (left) prepared by us and studied in Delft in three-terminal device. Oxidation of the DTF unit would in this case generate an unpaired spin within the molecular wire itself (right), but we cannot say unambiguously whether the measured Kondo resonance is due to this spin.

### 5.3 Donor-Acceptor Cruciforms

By changing one of the two DTF units into an acceptor group, we reasoned that some degree of quinoid and hence cross-conjugated character of the central benzene ring in an OPE cruciform could possibly be promoted (Figure 5.7). First, we prepared the key building block **5.11** (Figure 5.8) by treating the dialdehyde **5.1** with only one equivalent of the ylide generated from the phosphonium salt **5.2** (providing the product in a yield of 64%).<sup>14</sup> Desilylation and transesterification of **5.11** followed by Sonogashira couplings with the aryl iodide **5.7** gave the OPE3 donor-acceptor cruciform **5.12** with thioacetate end-caps. This compound can be further transformed into the donor-acceptor cruciform **5.13** in a Knoevenagel condensation with indan-1,3-dione.

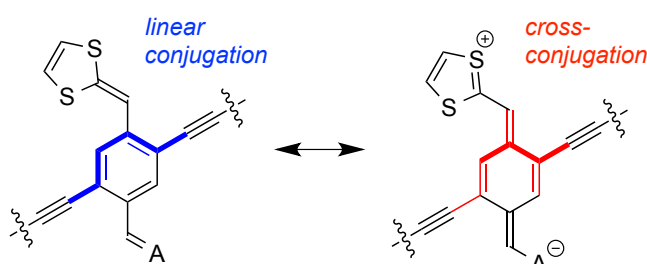


**Figure 5.7.** Two resonance forms of donor-acceptor cruciform motif. A = acceptor.

From X-ray crystallographic analysis of **5.11** (Figure 5.9), we estimate a quinoid character of 0.03 and 0.02 Å for the two asymmetric parts (calculated as  $[a + b - 2c] / 2$ , where  $a$ ,  $b$ , and  $c$  are the lengths of the three C-C bonds in the ring between the DTF and CHO units). This is about 15% of the quinoid character of *p*-benzoquinone (0.16 Å).<sup>15</sup> Some degree of quinoid character was also supported by electrochemistry. Thus, **5.11** underwent an irreversible oxidation at +0.88 V vs. Fc/Fc<sup>+</sup> in CH<sub>2</sub>Cl<sub>2</sub> (0.1 M Bu<sub>4</sub>NPF<sub>6</sub>), while a related compound with one DTF unit and no aldehyde group underwent irreversible oxidation at +0.75 V vs. Fc/Fc<sup>+</sup>.<sup>16</sup> It is thus significantly more difficult to oxidize **5.11**.

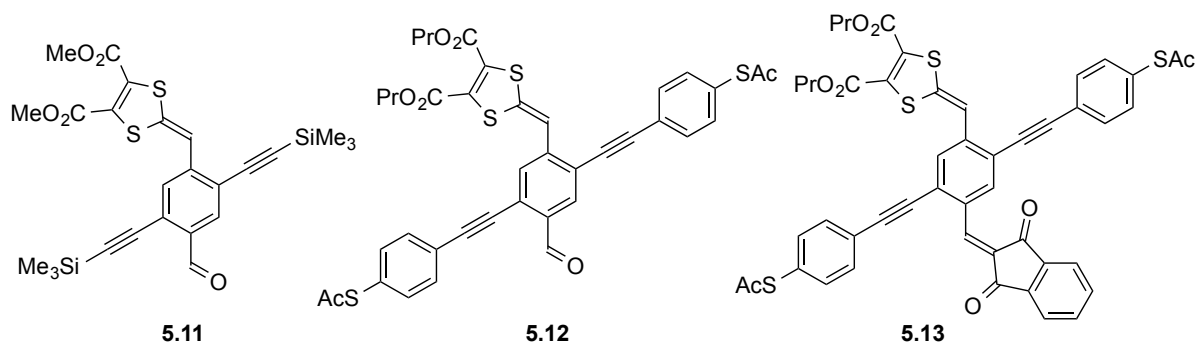


**Figure 5.8.** Donor-acceptor OPE3 cruciform molecules.

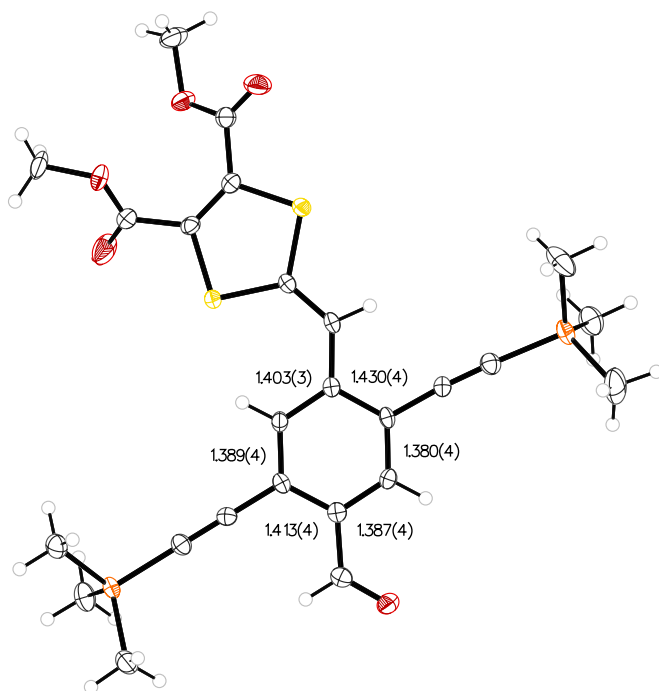


**Figure 5.9.** Molecular structure of **5.11** from X-ray crystallographic analysis. Bond lengths (Å) of the central benzene ring are indicated (used for calculating the quinoid character): 1.430(4), 1.380(4), 1.387(4), 1.413(4), 1.389(4), 1.403(3) Å. Reproduced from Ref. 14 (*Nature Communications*).

The single-molecule conductances of the donor-acceptor OPE3 molecular wires and the unsubstituted **OPE3** were studied in a mechanically controlled break-junction by the Delft group. Figure 5.10 shows the conductance histograms for the three compounds at a finite bias voltage of 0.1 V.<sup>14</sup> Interestingly, the two donor-acceptor compounds exhibit a very broad distribution of conductances, which could be fitted by the sum of two Gaussian curves. The highest conductance peak is close to that of the simple **OPE3** (and also to that of an OPE3 with only one DTF group, but no acceptor group<sup>16</sup>). The second peak is about one order of magnitude lower in conductance than the first. These broad conductance histograms are in contrast to the sharp peak measured for the simple **OPE3**. The environment of a molecule in a break-junction at a certain bias may change from one opening-closure experiment to the other and from one electrodes position to the other along the same opening experiment. Therefore, we explain the broad conductance histograms of **5.12** and **5.13** by small variations in the environment for each measurement, and these small variations may enhance either the linearly conjugated resonance form shown in Figure 5.7 or the cross-conjugated one (or any structure in-between). The linearly conjugated resonance form should thus correspond to the upper limit of the conductance (resembling **OPE3**), while the cross-conjugated form should correspond to the lower limit. Transport calculations by Prof. Kurt V. Mikkelsen and co-workers at University of Copenhagen on **5.12•H<sup>+</sup>** and **5.14** (Figure 5.11) added further support for this interpretation. Protonation of **5.12** enhances the quinoid resonance form and it had a transmission that was ca. one-fourth of that calculated for the linearly conjugated **OPE3** in a junction. The inherently cross-conjugated molecule **5.14** had a transmission close to that of **5.12•H<sup>+</sup>**.



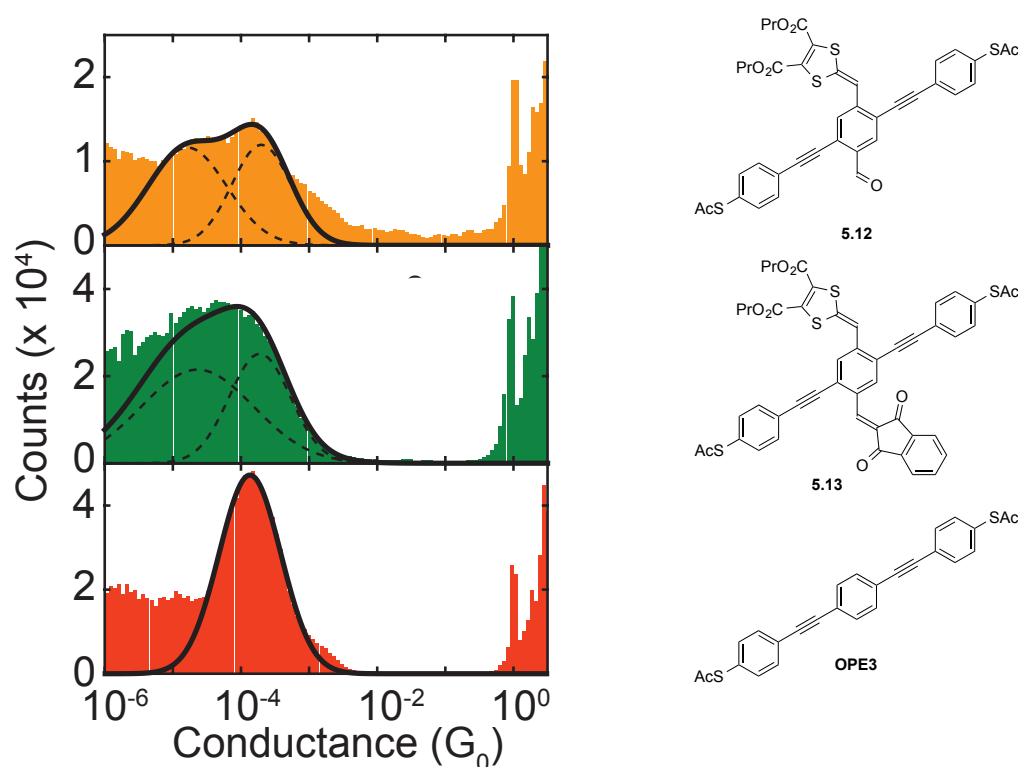


**Figure 5.10.** Conductance histograms of **5.12** (top), **5.13** (middle), and **OPE3** (bottom), which were built from more than 1000 traces each. The thick black lines represent the fit of the molecular peak to a sum of two Gaussian curves and the dashed lines represent the individual Gaussian peaks. The conductances  $G$  are reported in units of the conductance quantum  $G_0$ . Reproduced from Ref. 14 (*Nature Communications*).

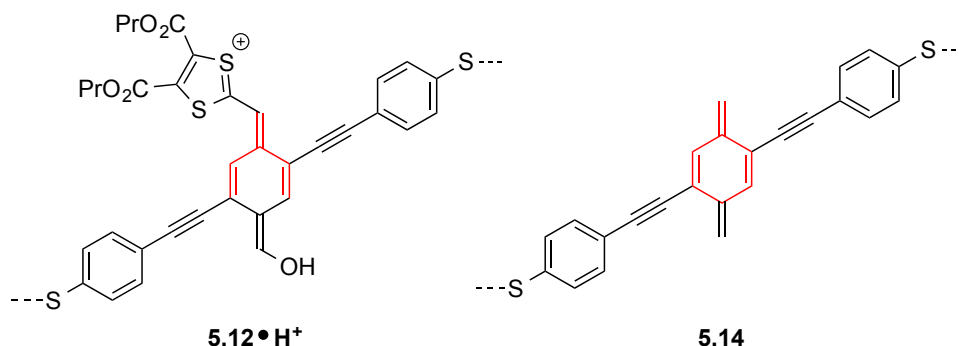


**Figure 5.11.** Cross-conjugated structures studied theoretically between two gold clusters each of 9 gold atoms.

#### 5.4 Dihydroazulene-Vinylheptafulvene Molecular Wires

The conductance properties of the two DHA isomers **5.15** and **5.16** (Figure 5.12), which we prepared by our bromination – elimination – cross-coupling protocol,<sup>17</sup> and the VHF **5.17** (*E/Z*) obtained by irradiation were studied by Prof. Wenjing Hong and co-workers by break-junction experiments.<sup>17b</sup> A significant difference in the single-molecule conductances of the three isomers was observed (Figure 5.13). DHA **5.15** for which a linearly conjugated pathway can be drawn between the ends of the molecule was found to exhibit the highest conductance. The VHF **5.17**, which is cross-conjugated

at the vinyl part, had the second-highest conductance. DHA **5.16** had the lowest conductance, which is explained not only by the cross-conjugation between the aryl substituent and the 7-seven-membered ring, but also by the strong deviation from coplanarity between the aryl substituent and the DHA unit as evident from the X-ray crystal structure shown in Figure 5.14. The less efficient  $\pi$ -electron delocalization in DHA **5.16** relative to that in **5.15** is also reflected by their longest-wavelength absorption maxima: 372 nm (**5.16**) and 393 nm (**5.15**) in acetonitrile. The above interpretation and assigned sequence of conductances were supported by a calculational study by Prof. Gemma Solomon and co-workers in Copenhagen. Interestingly, it was possible to switch between DHA **5.15** and VHF **5.17** in the junction by time and thermal stimuli; the system thus behaved as a light-controlled molecular *on/off* switch.

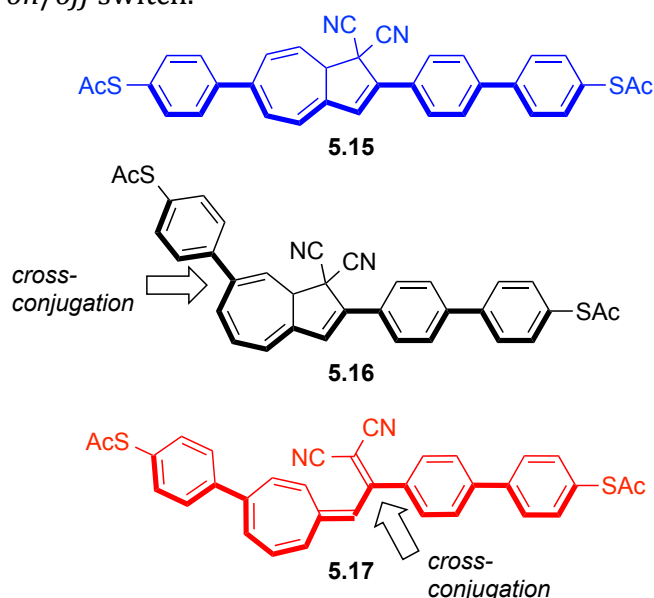


**Figure 5.12.** DHA/VHF molecular wires studied in break-junctions. One conjugation pathway between the two sulfur end-groups is highlighted by solid bonds for each structure.

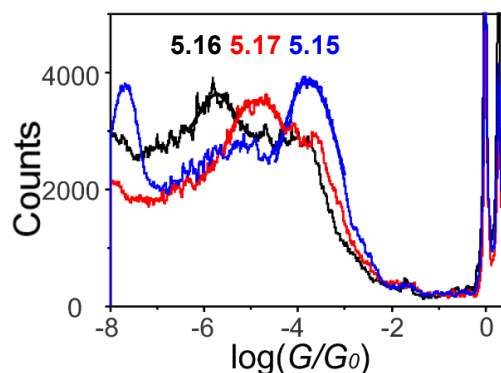


**Figure 5.13.** Conductance histograms for molecules **5.15** (blue), **5.16** (black), and **5.17** (red). The conductances  $G$  are reported in units of the conductance quantum  $G_0$ . Reproduced from Ref. 17b (*Nature Communications* – In revision).

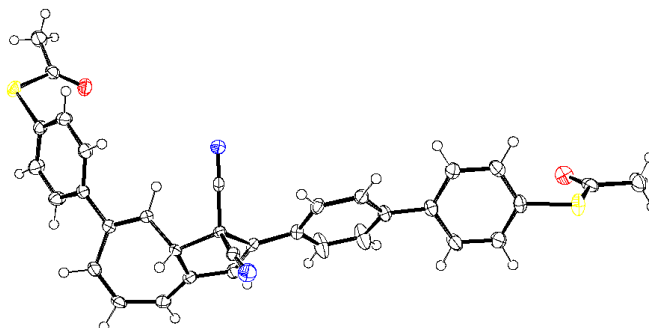


**Figure 5.14.** Molecular structure of DHA **5.16** according to X-ray crystallographic analysis. Reproduced from Ref. 17b (*Nature Communications* – In revision).

Light/heat controlled conductance switching was also achieved for one of our other DHA/VHF molecules (**5.18/5.19**) when organized in a self-assembled monolayer between gold electrodes (source and drain) and a reduced graphene oxide transparent top contact, functioning as the interfacial layer to top metal electrodes.<sup>18</sup> The experimental conductance studies were performed by my colleagues Prof.s Bo Wegge Laursen and Kasper Nørgaard (and co-workers) at University of Copenhagen. A schematic illustration of the molecular test bed is shown in Figure 5.15. For this system, anchoring to the gold source and drain substrates was achieved via a thioacetate group sitting on the *meta* position of a phenyl substituent located at C-2 of the DHA. Conductance switching for the system was achieved by alternating UV irradiation and heating (Figure 5.16), and the studies revealed the DHA isomer (**5.18**) to be of higher conductance than the VHF isomer (**5.19**). As the break-junction experiments described above clearly showed, the position of anchoring plays an important role in regard to whether DHA or VHF is most conducting. For the set-up in Figure 5.15 it is therefore more difficult to make conclusions rooted in cross-conjugation as the contact between the physisorbed top electrode and the molecules is not well defined (only anchoring to the gold surface is controlled by the SAc group); that is, we cannot say how the reduced graphene oxide electrode couples to the molecules (to either an atom of the seven-membered ring or possibly to one of the cyano groups for some conformations). Nevertheless, this work presents another example on how the DHA/VHF system can conveniently be used for conductance switching. In addition, it deserves mention that conductance switching has been observed for a DHA/VHF system integrated in a gated single-molecule device operating in the Coulomb blockade regime (work in collaboration with Prof.s Sergey Kubatkin and Andrey Danilov at Chalmers University of Technology in Gothenburg).<sup>19</sup>

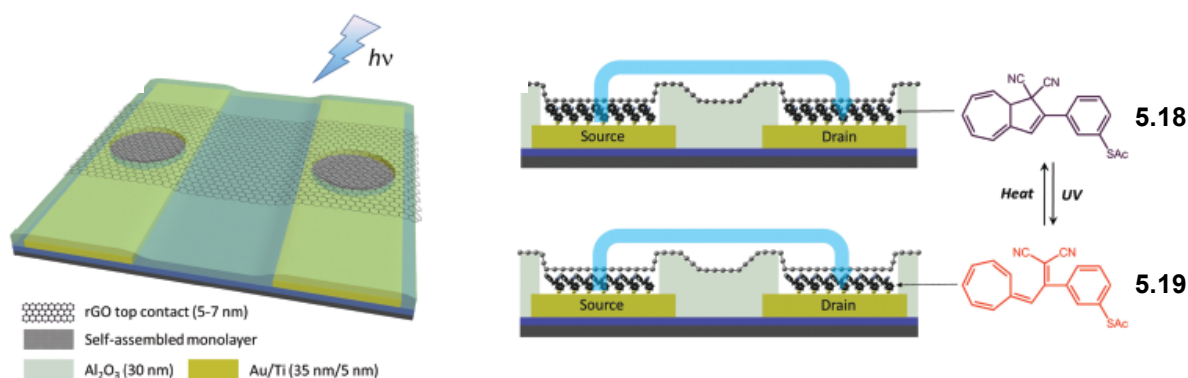


**Figure 5.15.** Left: Illustration of junction based on a reduced graphene oxide thin film as top contact between two self-assembled molecular monolayers on source and drain gold substrates. Right: Illustration of cross-section of the molecular junction containing DHA/VHF molecules **5.18** and **5.19**. Reproduced from Ref. 18 with permission from John Wiley and Sons.

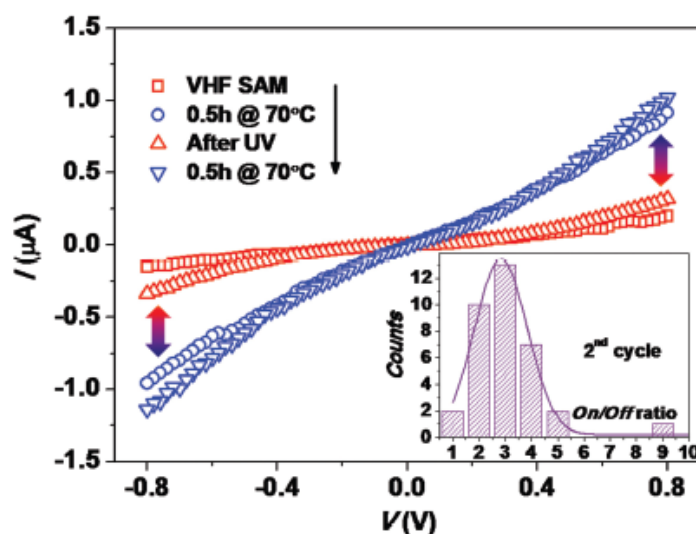


**Figure 5.16.** Current-voltage ( $I$ - $V$ ) characteristics of the junction illustrated in Figure 5.15. Conductance switching was promoted by heating (VHF to DHA conversion) and UV irradiation (DHA to VHF conversion); the DHA (blue color) exhibited higher conductance than the VHF (red color). Reproduced from Ref. 18 with permission from John Wiley and Sons.

## 5.5 Conclusions

The presence or absence of cross-conjugation has been tracked in various ways from single-molecule conductance studies on DTF-functionalized molecular wires. Studies showed that for an OPE5-TTF cruciform structure, the cross-conjugated and quinoid structure was avoided for the oxidized species as clear signatures (Kondo resonances) were observed that could be attributed to unpaired electrons. Quinoid structures could, however, be tracked for donor-acceptor cruciforms studied in break-junctions at a finite bias voltage. These molecules showed remarkably broad conductance histograms, which we ascribe to the promotion of either the linearly conjugated (high conductance) or cross-conjugated (low conductance) resonance form as the main contributor to the overall resonance hybrid. Small changes in the environment and orientation of the donor-acceptor molecule in the junction for each conductance measurement are likely responsible for this effect. This resembles in some way the solvatochromism of molecules exhibiting charge-transfer absorptions where solvent polarity perturbs the ground and excited states.

The influence of cross-conjugation was also seen in studies of DHA and VHF isomers in a break-junction. The one DHA isomer for which a linear conjugation pathway can be drawn between the two electrode anchoring groups exhibited a higher conductance than the two other isomers, which both have one cross-conjugated unit. Deviations from planarity should of course also be taken into account in these rather complicated structures, but altogether our results combined with those of others do

support the conclusion that electron transport is less efficient along cross-conjugated molecular wires than along linearly conjugated ones. Several other devices have shown conductance switching of the DHA/VHF system, but we cannot from these studies directly extract information on the influence of cross-conjugation.

---

## References

1. a) J. C. Love, L. A. Estroff, J. K. Kriebel, R. G. Nuzzo, G. M. Whitesides, *Chem. Rev.* **2005**, *105*, 1103-1169; b) K. Nørgaard, M. B. Nielsen, T. Bjørnholm, "Thiol End-Capped Molecules for Molecular Electronics: Synthetic Methods, Molecular Junctions, and Structure-Property Relationships," in *Functional Organic Materials* (Eds. T. J. J. Müller, U. H. F. Bunz), Wiley-VCH, Weinheim, **2007**, pp. 353-392.
2. D. Xiang, X. Wang, C. Jia, T. Lee, X. Guo, *Chem. Rev.* **2016**, *116*, 4318-4440.
3. For other examples that employ switching between TTF redox states in molecular electronics, see: a) J. Liao, J. S. Agustsson, S. Wu, C. Schönenberger, M. Calame, Y. Leroux, M. Mayor, O. Jeannin, Y.-F. Ran, S.-X. Liu, S. Decurtins, *Nano Lett.* **2010**, *10*, 759-764; b) Y. Luo, C. P. Collier, J. O. Jeppesen, K. A. Nielsen, E. Delonno, G. Ho, J. Perkins, H.-R. Tseng, T. Yamamoto, J. F. Stoddart, J. R. Heath, *ChemPhysChem* **2002**, *3*, 519-525.
4. For an account on redox- and light-controlled molecular switches for molecular electronics, see: M. B. Nielsen, "Molecular Switches," in *Handbook of Single Molecule Electronics* (Ed. K. Moth-Poulsen), Pan Stanford Publishing, **2015**, pp. 233-261.
5. A. Aviram, M. A. Ratner, *Chem. Phys. Lett.* **1974**, *29*, 277-283.
6. a) J. K. Sørensen, M. Vestergaard, A. Kadziola, K. Kilså, M. B. Nielsen, *Org. Lett.* **2006**, *8*, 1173-1176; b) M. Vestergaard, K. S. Jennum, J. K. Sørensen, K. Kilså, M. B. Nielsen, *J. Org. Chem.* **2008**, *73*, 3175-3183.
7. A. J. Zuccherro, P. L. McGrier, U. H. F. Bunz, *Acc. Chem. Res.* **2010**, *43*, 397-408.
8. K. Jennum, M. Vestergaard, A. H. Pedersen, J. Fock, J. Jensen, M. Santella, J. J. Led, K. Kilså, T. Bjørnholm, M. B. Nielsen, *Synthesis* **2011**, 539-548.
9. For reviews on our synthetic protocols for preparing OPE-TTF cruciforms and related structures, see: a) M. B. Nielsen, *Phosphorus, Sulfur, and Silicon and the Related Elements* **2011**, *186*, 1055-1073; b) K. Jennum, M. B. Nielsen, *Chem. Lett.* **2011**, *40*, 662-667.
10. M. Sato, N. C. Gonnella, M. P. Cava, *J. Org. Chem.* **1979**, *44*, 930-933.
11. C. R. Parker, Z. Wei, C. A. Rodríguez, K. Jennum, T. Li, M. Santella, N. Bovet, G. Yhao, W. Hu, H. S. J. van der Zant, M. Vanin, G. C. Solomon, B. W. Laursen, K. Nørgaard, M. B. Nielsen, *Adv. Mater.* **2013**, *25*, 405-409.
12. J. Fock, M. Leijnse, K. Jennum, A. S. Zyazin, J. Paaske, P. Hedegård, M. B. Nielsen, H. S. J. van der Zant, *Phys. Rev. B* **2012**, *86*, 235403.
13. M. Mansø, M. Koole, M. Mulder, I. J. Olavarria-Contreras, C. L. Andersen, M. Jevric, S. L. Broman, A. Kadziola, O. Hammerich, H. S. J. van der Zant, M. B. Nielsen, *J. Org. Chem.* **2016**, *81*, 8406-8414.
14. H. Lissau, R. Frisenda, S. T. Olsen, M. Jevric, C. R. Parker, A. Kadziola, T. Hansen, H. S. J. van der Zant, M. B. Nielsen, K. V. Mikkelsen, *Nat. Commun.* **2015**, *6*:10233.
15. J. A. Trotter, *Acta Cryst.* **1960**, *13*, 86-95.
16. C. R. Parker, E. Leary, R. Frisenda, Z. Wei, K. S. Jennum, E. Glibstrup, P. B. Abrahamsen, M. Santella, M. A. Christensen, E. A. Della Pia, T. Li, M. T. Gonzalez, B. W. Laursen, K. Nørgaard, H. van der Zant, N. Agraït, M. B. Nielsen, *J. Am. Chem. Soc.* **2014**, *136*, 16497-16507.
17. a) M. Jevric, S. L. Broman, M. B. Nielsen, *J. Org. Chem.* **2013**, *78*, 4348-4356; b) C. Huang, M. Jevric, A. Borges, S. T. Olsen, J. Hamill, A. Rudnev, M. Baghernejad, P. Broekman, T.

- Wandlowski, K. V. Mikkelsen, G. C. Solomon, M. B. Nielsen, W. Hong, *Nat. Commun.*, In revision.
18. T. Li, M. Jevric, J. R. Hauptmann, R. Hviid, Z. Wei, R. Wang, N. E. A. Reeler, E. Thyrhaug, S. V. Petersen, J. A. S. Meyer, N. E. Bovet, T. A. J. Vosch, J. Nygård, X. Qiu, W. Hu, Y. Liu, G. C. Solomon, H. G. Kjaergaard, T. Bjørnholm, M. B. Nielsen, B. W. Laursen, K. Nørgaard, *Adv. Mater.* **2013**, *25*, 4164-4170.
19. S. L. Broman, S. Lara-Avila, C. L. Thisted, A. D. Bond, S. Kubatkin, A. Danilov, M. B. Nielsen, *Adv. Funct. Mater.* **2012**, *22*, 4249-4258.

# SYNTHETIC METHODS

## 6.1 Introduction

I have in the previous chapters shown several examples on how we have developed synthetic protocols for cross-conjugated molecules. In general, the methods rely on combinations of acetylenic coupling reactions and methods for preparing and functionalizing dithiafulvenes/tetrathiafulvalenes, heptafulvenes, dihydroazulenes, and azulenes. I have together with co-authors reviewed some of our methods in the field of acetylenic scaffolding<sup>1</sup> as well as functionalization methods of dihydroazulenes<sup>2</sup>. In addition, procedures for preparing cruciform-like extended tetrathiafulvalenes have been reviewed.<sup>3</sup> This chapter will provide a more detailed overview of synthetic methods, with an emphasis on how each method has been important for the ultimate synthesis of cross-conjugated molecules or for their functionalization. The properties of the target molecules have in some cases contributed to fundamental understanding of cross-conjugation as described in previous chapters, but in others the cross-conjugation is just a segment of the molecule, and other properties were focused upon in the work that was published. This chapter will only focus on synthesis.

## 6.2 Acetylenic Scaffolding

### 6.2.1 The Oxidative Hay Homo-coupling of Alkynes

Homo-coupling of two terminal alkynes to form a buta-1,3-diyne using the oxidative Hay coupling<sup>4</sup> plays a key role in the synthesis of several of our scaffolds, such as the macrocycle **6.1**<sup>5</sup> (Figure 6.1). The terminal alkyne is stirred in a solvent like acetone or dichloromethane using the CuCl-TMEDA catalyst system under open air as the reaction requires oxygen as oxidizing agent (TMEDA = *N,N,N',N'*-tetramethylethylenediamine).

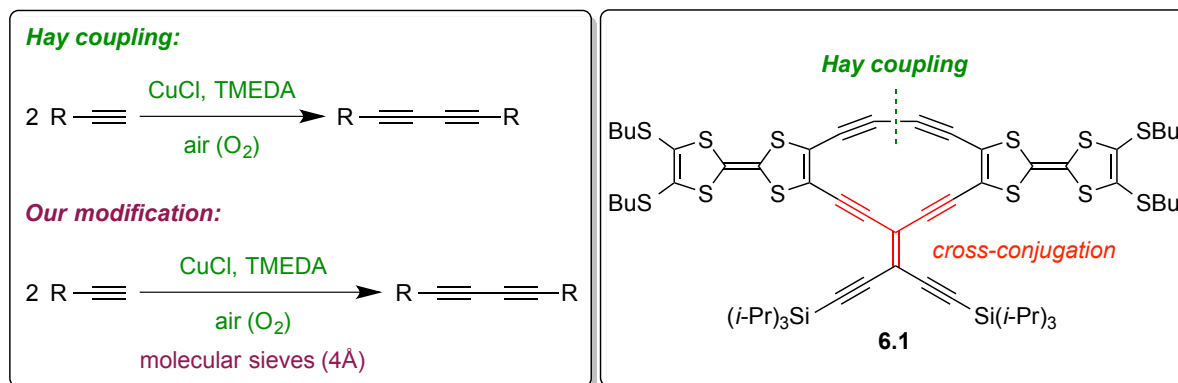


**Figure 6.1.** Homo-coupling of two terminal alkynes via the oxidative Hay coupling – the modified conditions were employed in the synthesis of the macrocycle **6.1**. TMEDA = *N,N,N',N'*-tetramethylethylenediamine.



We found that the reaction time can be reduced significantly by adding molecular sieves to the reaction mixture.<sup>6</sup> This finding was based on detailed kinetics studies using the simple substrate *p*-methylphenylacetylene. We found that the reaction is zero-order in the alkyne, but in time it changes to a slower zero-order kinetics. Thus, using 3.0 mmol of substrate in 25 mL CH<sub>2</sub>Cl<sub>2</sub> and ca. 5 mol% CuCl and 10 mol% TMEDA, a shift to slower zero-order kinetics was observed after ca. 56%-conversion (Figure 2, left). The shift could be postponed to a higher conversion percentage by increasing the catalyst loading. Yet, it could be avoided simply by adding 4Å-molecular sieves to the mixture. Coupling of two alkynes consumes O<sub>2</sub>, and water should be generated. It seems that this water has a retarding influence on the coupling (confirmed by addition of water), and it is therefore beneficial to remove it by molecular sieves. Interestingly, we found a linear correlation between the percentage of remaining acetylene after 30-min reaction time and the stirring rate; this reflects the importance of the efficiency by which oxygen is entering the reaction mixture.

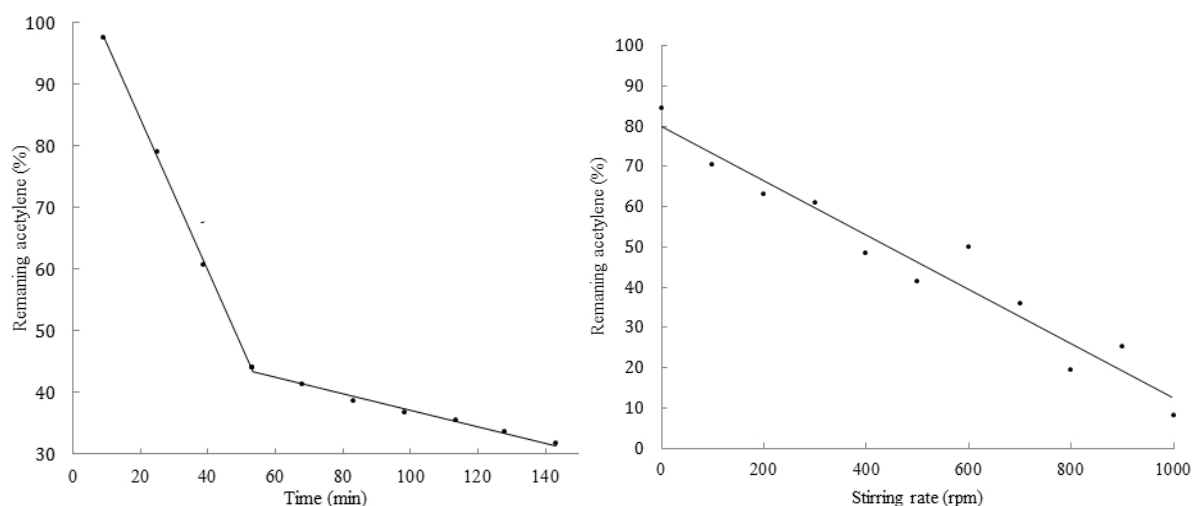


**Figure 6.2.** Left: Conversion of *p*-methylphenylacetylene over time under Hay conditions (3.0 mmol acetylene, 5.5 mol% CuCl and 11 mol% TMEDA in CH<sub>2</sub>Cl<sub>2</sub> (25 mL)). A shift between a fast to slow zero-order kinetics is observed after ca. 53 min. The data points are based on <sup>13</sup>C-NMR spectroscopic investigations using a highly sensitive cryoprobe NMR instrument; this is a rather unconventional method, but applicable as the aryl carbon resonances of reactants and products have similar NOE and relaxation times. Right: Conversion of *p*-methylphenylacetylene after 30 min as a function of stirring rate (3.0 mmol acetylene, 10 mol% CuCl and 30 mol% TMEDA in CH<sub>2</sub>Cl<sub>2</sub> (25 mL)) in the presence of molecular sieves (4 Å). Reproduced from Ref. 6 with permission from John Wiley and Sons.

### 6.2.2 Synthesis and Unsymmetrical Coupling Reactions of 1-Chloroalkynes

Synthesis of unsymmetrical buta-1,3-diynes can be accomplished by the Cadiot-Chodkiewicz coupling<sup>7</sup> and in particular by Pd-catalyzed versions thereof.<sup>8</sup> A terminal alkyne and a 1-haloalkyne, usually 1-bromo- or 1-iodoalkyne, are used as substrates. The bromo- and iodoalkynes are not always stable, and we therefore decided to

investigate the use of 1-chloroalkynes, often being more stable. We found that 1-chloroalkynes can be conveniently prepared by treating the trimethylsilyl-protected alkyne with trichloroisocyanuric acid (TCCA) and  $\text{AgNO}_3$ .<sup>9</sup> This method works well for arylated alkynes with electron-withdrawing substituents as shown in Figure 6.3. For unsubstituted or donor-substituted arylalkynes, chlorinated ketones become instead the dominant products. Conversion of the differentially protected penta-1,4-diyn-3-one **6.2** provided the product **6.3** (Figure 6.4). This product is a potentially interesting cross-conjugated building block for further scaffolding, but we have not yet subjected it to further reactions.

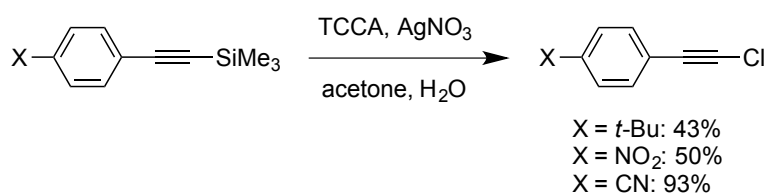


**Figure 6.3.** Synthesis of 1-chloroalkynes. TCCA = trichloroisocyanuric acid.

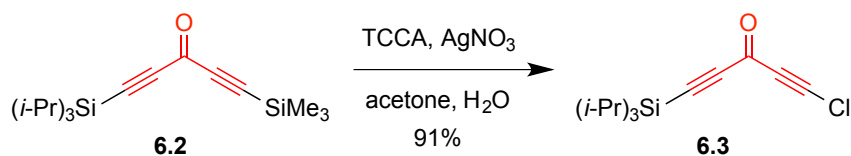


**Figure 6.4.** Chlorination of differentially protected penta-1,4-diyn-3-one derivative.

Gratifyingly, 1-chloroalkynes undergo readily cross-coupling reactions with terminal alkynes under standard Sonogashira conditions.<sup>10</sup> From competition experiments, we found that the reactivity of (chloroethynyl)benzene resembles that of iodobenzene, and it is hence much more reactive than bromobenzene (Figure 6.5).

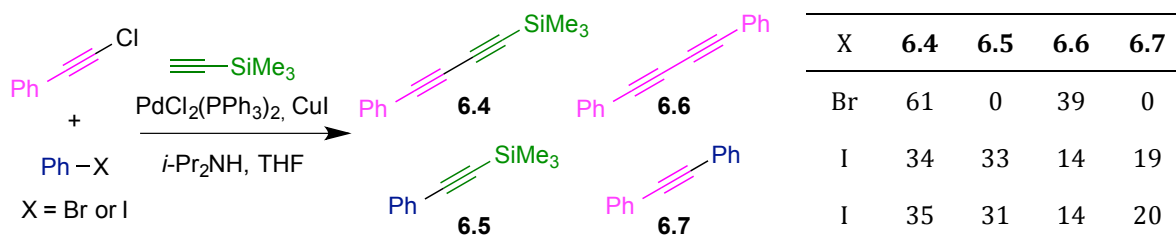


**Figure 6.5.** Cross-coupling outcomes of competition experiments; product distributions (in relative percentage) based on gas chromatography – mass spectrometric (GC-MS) analysis.

### 6.2.3 Ultrasound-Promoted Sonogashira Couplings – Acetylenic Scaffolding with TTF derivatives

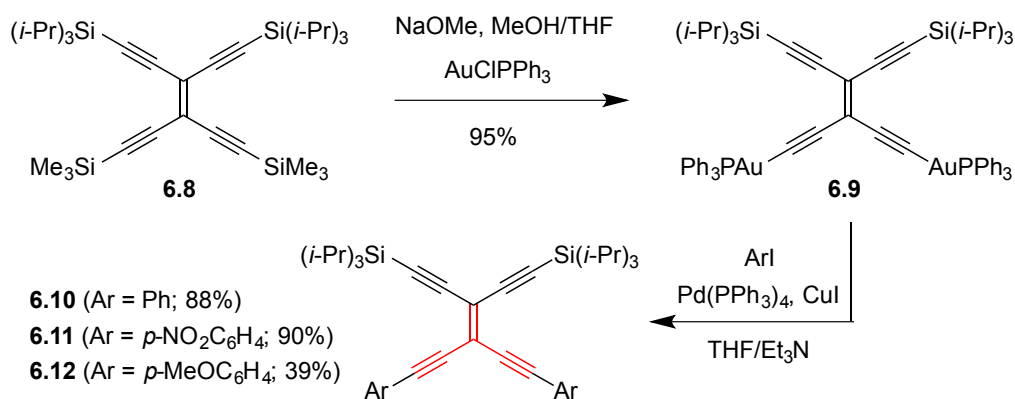
Our beneficial use of ultrasound to promote the Sonogashira coupling has been described in Chapters 2 and 3. In general, the method is useful whenever the substrates

exhibit limited reactivity and at the same time they or the products are sensitive to elevated temperature (often the case for acetylenic DTFs/TTFs) as a means of promoting the reaction.<sup>11</sup>

#### 6.2.4 Phosphine-Gold(I) Oligoynyl Complexes

Terminal alkynes of oligo(en)ynes such as tetraethynylethene (TEE; having four terminal alkynes) are often unstable compounds, and for this reason cross-coupling reactions are sometimes challenging. Usually, the alkynes are protected with trialkylsilyl groups. Bruce and co-workers<sup>12</sup> have shown that trimethylsilyl groups can be easily substituted with triphenylphosphine-gold(I) fragments. These compounds are stable and can be isolated, and, in addition, they can like the terminal alkynes undergo Pd-catalyzed Cadiot-Chodkiewicz and Sonogashira-like coupling reactions with iodoalkynes and aryl iodides.<sup>13</sup>

We have investigated the wider scope of Sonogashira-like couplings with gold(I) functionalized TEEs as outlined in Figure 6.6.<sup>14</sup> The silyl-protected TEE **6.8** was converted into the bis(gold(I) ethynyl) complex **6.9** upon treatment with NaOMe and AuClPPh<sub>3</sub>. Only the trimethylsilyl groups were removed under these conditions, leaving the triisopropylsilyl groups unreacted. The stable complex **6.9** was treated with different aryl iodides under Sonogashira conditions, which gave the arylated TEEs **6.10-6.12**. We obtained excellent yields with iodobenzene and 1-iodo-4-nitrobenzene as substrates, while a moderate yield was obtained with 1-iodo-4-methoxybenzene. We also successfully subjected compound **6.13** to coupling reactions with iodobenzene via the intermediate gold(I) complex **6.14** (Figure 6.7).<sup>14</sup> The product **6.15** could not be achieved from **6.13** by a protodesilylation (using K<sub>2</sub>CO<sub>3</sub> in MeOH) followed by coupling protocol (at least not in our hands) as the intermediate, desilylated penta-1,4-diyn-3-one is very unstable.<sup>15</sup>



**Figure 6.6.** Preparation of phosphine-gold(I) end-capped TEE and its use in Sonogashira-like coupling reactions with aryl iodides.

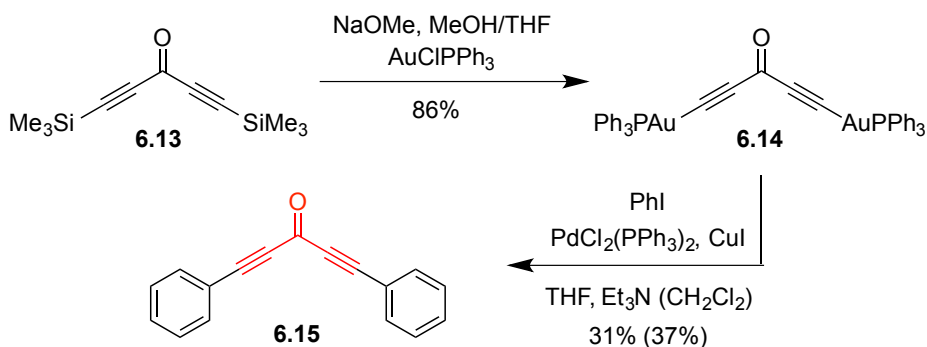


**Figure 6.7.** Functionalization of penta-1,4-diyne-3-one, which is not stable in the absence of end-capping groups (either trialkylsilyl or gold(I) complexes).

In Chapter 3, I presented the synthesis of a TTF-radiaannulene (compound **3.11**; yield of 10%) in a step involving four Sonogashira couplings. We have found that the yield of such reactions can be doubled by employing **6.9** as substrate. Thus, Pd-catalyzed cyclization of **6.9** and the TTF-diiodide **6.16** gave the TTF-radiaannulene **6.17** in a yield of 22% (Figure 6.8).<sup>14</sup>

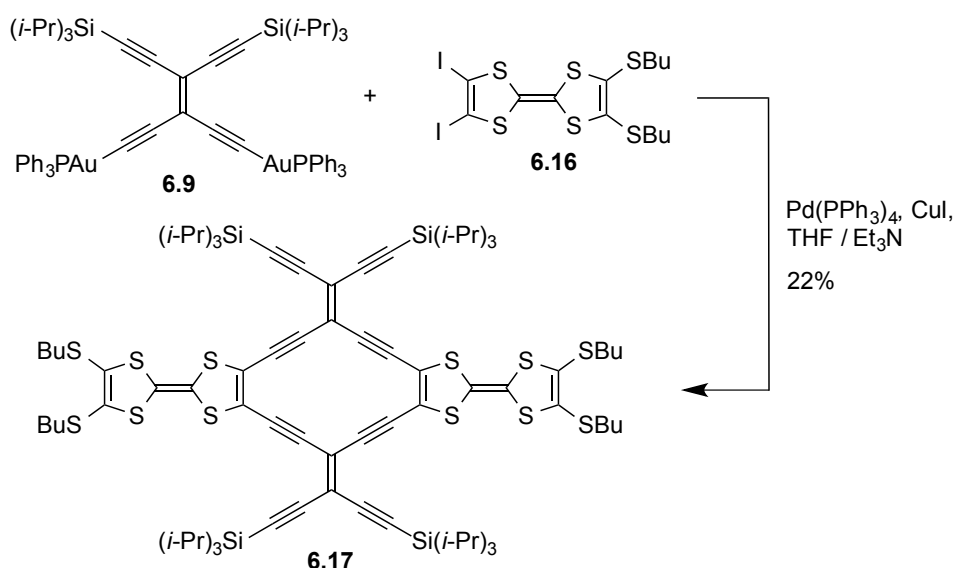


**Figure 6.8.** Synthesis of TTF-radiaannulene.

Most likely the oxidative addition step of the Pd/Cu catalyzed coupling between an aryl halide and the gold(I) alkynyl complex involves the Pd(0) catalyst, but there are different transmetallation routes that can be imagined for the alkynyl species: 1) direct transmetallation from gold to palladium, 2) stepwise transmetallations, that is, from gold to copper and then to palladium involving the Cu(I) acetylide as an intermediate, or 3) Cu(I)-aided direct transmetallation from gold to palladium. According to a computational study by us,<sup>16</sup> the most likely mechanism seems to be route 2. An intermediate Cu(I) acetylide is further supported by work of Bruce, Low, and co-workers<sup>17</sup> showing that transmetallation from gold to copper proceeds in near-quantitative yield.

TEE-based complexes **6.18** and **6.19** (Figure 6.9) were prepared in similar high yields as that of **6.9**.<sup>14</sup> The structures of both **6.9** and **6.18** were confirmed by X-ray crystallographic analysis as shown in Figure 6.10. Compound **6.19** (showing limited stability) was prepared from the diol **6.20** (Figure 6.9) for which we also devised a synthesis.<sup>18</sup> The alcohol groups are convenient sites for further functionalization. Thus, we have shown that they allow for linking of TEE and perylene diimide (PDI) chromophores via esterification reactions. Diol **6.20** and the carboxylic acid **6.21** were coupled together using dicyclohexyl carbodiimide (DCC) promoted esterification reactions to furnish the PDI-TEE-PDI scaffold **6.22** according to Figure 6.11.<sup>18</sup>

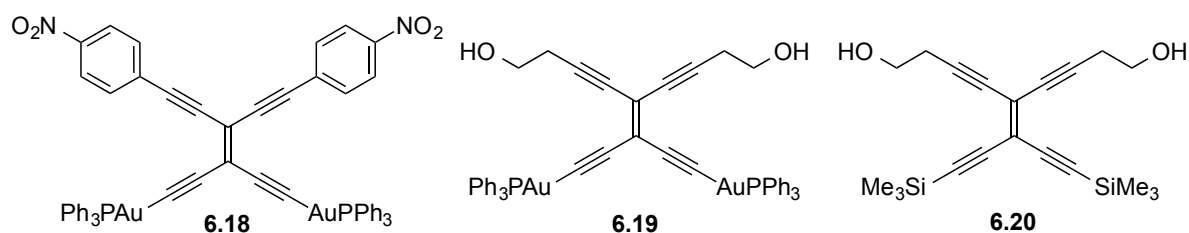


**Figure 6.9.** Various TEE building blocks.

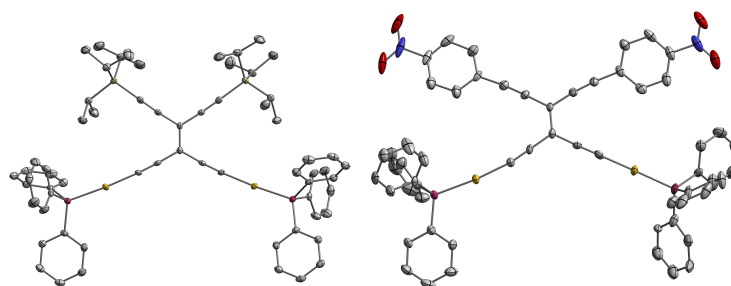


**Figure 6.10.** Molecular structures of TEE-based gold complexes **6.9** (left) and **6.18** (right) according to X-ray crystallographic analyses. Reproduced from Ref. 14.

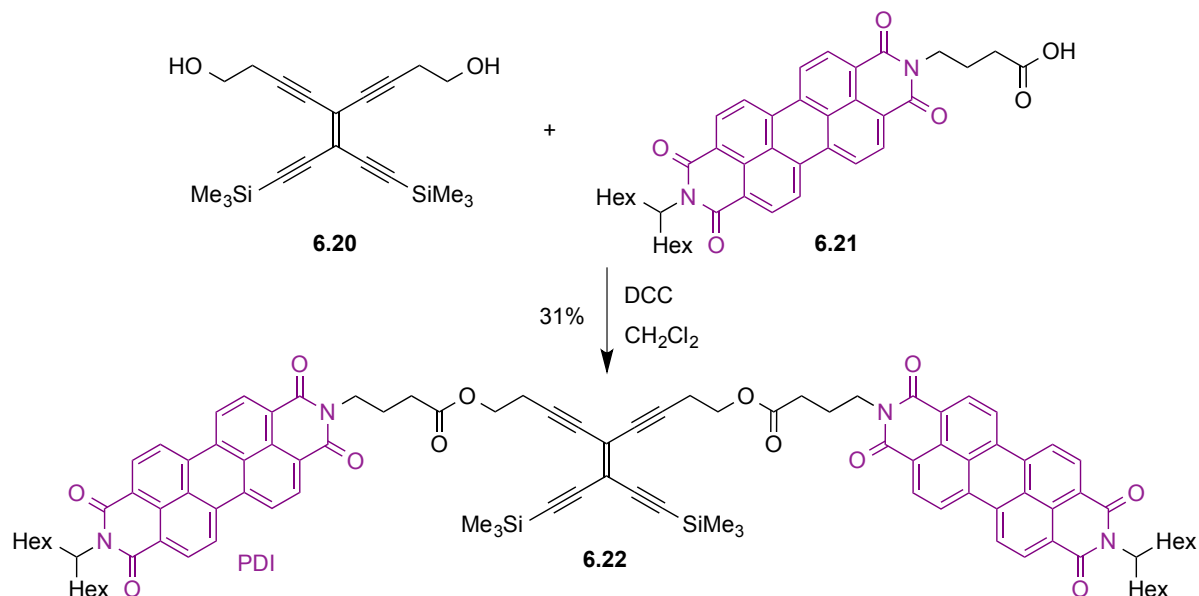


**Figure 6.11.** Synthesis of PDI-TEE-PDI scaffold. PDI = perylene diimide; DCC = dicyclohexyl carbodiimide.

### 6.2.5 Acetylenic Scaffolding with Boron Subphthalocyanines

Boron subphthalocyanines (SubPc's) are  $\pi$ -conjugated macrocycles, which are of interest as light-harvesting systems for artificial photosynthesis, organic photovoltaics, and other optical applications on account of their strong chromophoric properties.<sup>19</sup> We have developed synthetic protocols for the SubPc building blocks **6.23**<sup>20</sup> and **6.24**<sup>21</sup> with alkyne units at the axial position (Figures 6.12). The concave structure of the SubPc is shown in Figure 6.13. The synthesis of **6.23** starts from the readily available SubPc boron chloride **6.25**,<sup>22</sup> which according to a procedure by Torres and co-workers<sup>23</sup> was treated with silver(I) triflate to form a boron triflate intermediate. Treating this compound with but-3-yn-1-ol then furnished **6.23**. This building block allowed the incorporation of the SubPc chromophore onto a cross-conjugated TEE scaffold as shown in Figure 6.14. Thus, a Sonogashira reaction between **6.23** and **6.26** gave the SubPc-TEE-SubPc scaffold **6.27** in high yield.<sup>20</sup> Initial attempts of using triphenylphosphine as the ligand for the palladium catalyst failed to give any product, but using instead triphenylarsine turned out successfully. As mentioned in Chapter 2, separating chromophores and donor/acceptor units by a cross-conjugated bridge has consequences for light-induced electron transfer processes,<sup>24</sup> and synthesis of such compounds is subject of current work on SubPc in my group.

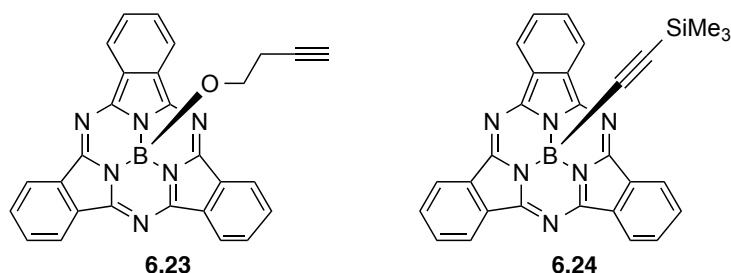


**Figure 6.12.** Subphthalocyanine (SubPc) building blocks with alkyne units at the axial boron positions.

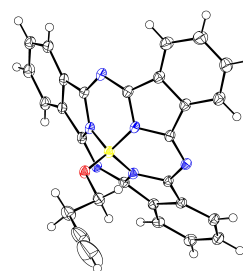


**Figure 6.13.** Molecular structure of compound **6.23** according to X-ray crystallographic analysis. Reproduced from Ref. 20 with permission from John Wiley and Sons.

It has been shown by several groups that it is also possible to attach directly an acetylide to the boron of SubPc by treating the boron triflate intermediate with Grignard reagents, generating a SubPc-C $\equiv$ C-R compound.<sup>25</sup> It was also shown by Morse and Bender<sup>26</sup> that **6.25** can be functionalized at the axial position with oxygen, sulfur, and nitrogen based nucleophiles in the presence of AlCl<sub>3</sub>, and it can be functionalized with trimethylsilyl-capped nucleophiles with the release of trimethylsilylchloride according to Torres and co-workers.<sup>27</sup> The latter reaction involved refluxing the reaction mixture in toluene or nitrobenzene, and it did not allow

trimethylsilylacetylenes as substrates. We found that treating **6.25** with bis(trimethylsilyl)acetylene in the presence of  $\text{AlCl}_3$  at room temperature provided a very gentle way of preparing the acetylenic building block **6.24** shown in Figure 6.12.<sup>21</sup> In fact, the method worked well for a large selection of trimethylsilyl-protected alkynes.

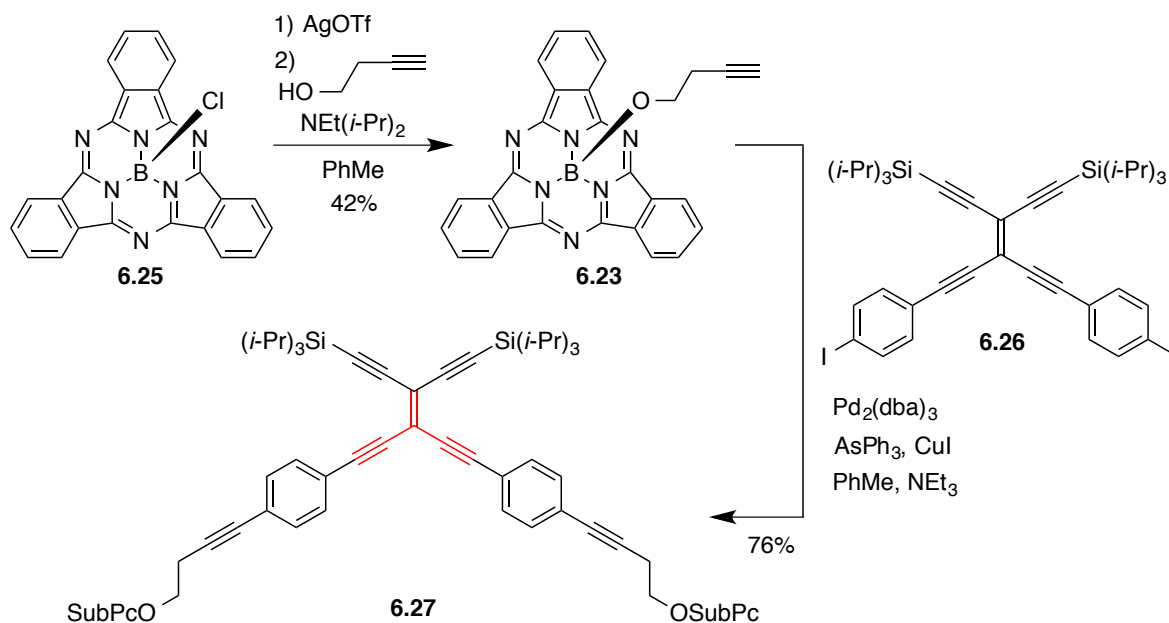


**Figure 6.14.** Synthesis of the acetylenic building block **6.23** and its further use in the preparation of a SubPc-TEE-SubPc scaffold. SubPc = subphthalocyanine; Tf = triflic; dba = dibenzylideneacetone.

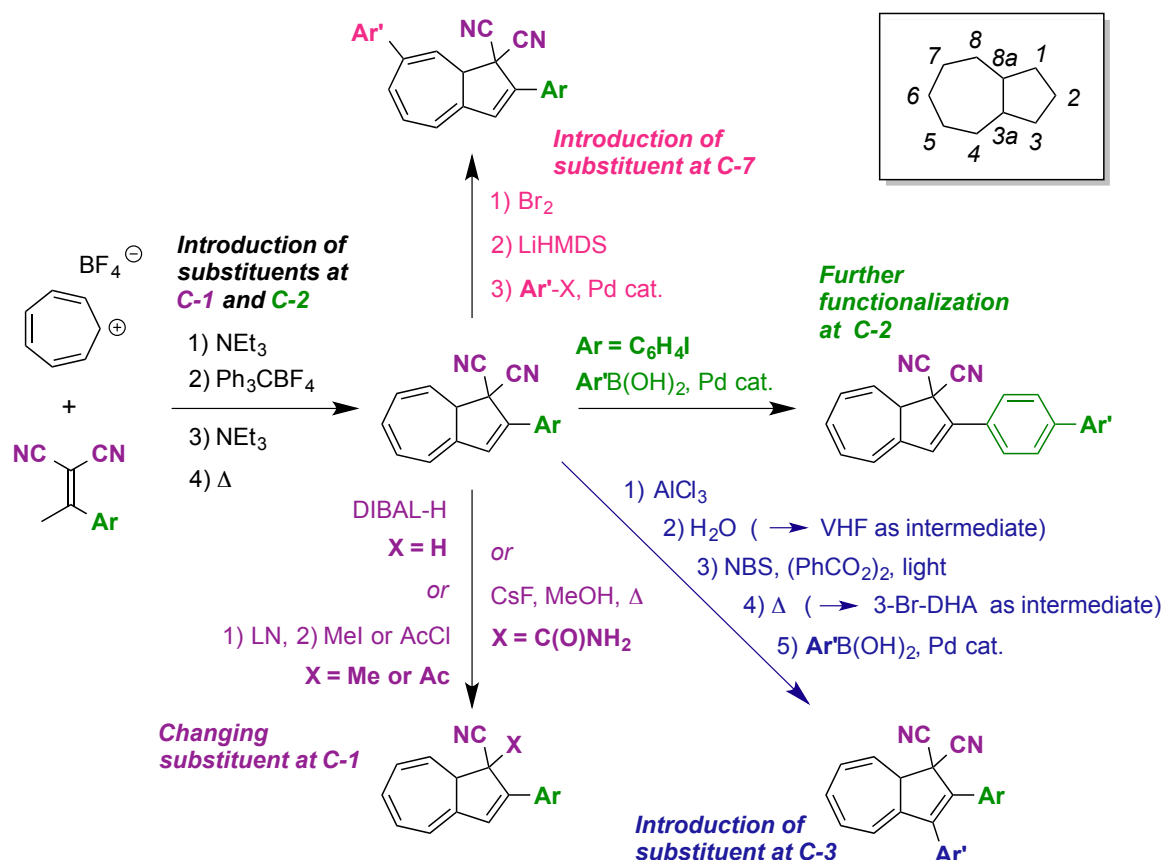
## 6.3 Functionalization of Dihydroazulenes

### 6.3.1 Regioselective Methods

The 1,8a-dihydroazulene (DHA) photoswitch has several positions available for functionalization and hence for tuning of its properties (Figure 6.15). For example, I have described in Chapter 2 how an aryl substituent at position 6 is in linear conjugation to the  $\pi$ -system comprised of carbons C-2 to C-6, and this functionalization results in a redshifted absorption maximum relative to the compound where the aryl substituent is placed at position C-7, where it is cross-conjugated to the  $\pi$ -system comprised of C-2 to C-6 and significantly out of co-planarity with this part.

Figure 6.15 summarizes the various functionalization methods where we have contributed with work. Substituents at positions C-1 (electron-withdrawing cyano groups originating from the malononitrile substrate) and C-2 are conveniently introduced in the actual synthesis of the DHA structure. Thus, various aryl groups can be introduced at C-2 via the acetophenone derivative used as substrate as first shown by Gierisch and Daub.<sup>28</sup> Diederich and co-workers<sup>29</sup> prepared a DHA with a 4-iodophenyl group at C-2 and employed this compound for further Sonogashira

reactions (providing access to TEE-DHA scaffolds). We have further optimized this protocol for preparing the 2-phenyl-substituted DHA on large scale and other aryl-substituted DHAs,<sup>30</sup> and we have subjected successfully 2-(4-iodo/4-bromo-phenyl)-substituted DHAs to Suzuki couplings.<sup>30b, 31</sup> It should be mentioned that the very first synthesis of DHAs by Daub and co-workers<sup>32</sup> employed an [8+2] cycloaddition reaction between 8-methoxyheptafulvene and a 2-aryl-substituted 1,1-dicyanoethylene followed by elimination of MeOH from the tetrahydroazulene cycloadduct using P<sub>2</sub>O<sub>5</sub>.



We have shown that the DHA structure can be employed as a precursor for regioselective functionalization at several positions. Subjecting it to AlCl<sub>3</sub> followed by water generates the VHF,<sup>33</sup> which is a more convenient protocol for generating VHF on large scale than photoisomerization. Bromination using *N*-bromosuccinimide (NBS) followed by ring-closure generates the 3-bromo-substituted DHA.<sup>34</sup> Such compounds are not so reactive in metal-catalyzed cross-coupling reactions, but we did manage to prepare Suzuki cross-coupling products (containing an aryl group at C-3), albeit in poor yields.<sup>34b</sup> An alternative strategy (not shown in Figure 6.15) is to introduce the C-3 aryl



substituent in the precursor from which the DHA core structure is prepared, a method first reported by Daub and co-workers<sup>35</sup> and further expanded by us.<sup>34b</sup>

Bromination of the DHA using Br<sub>2</sub> followed by treatment with base generates the 7-bromo-substituted DHA,<sup>36</sup> which in contrast to the 3-bromo-substituted derivative is very reactive in cross-coupling reactions, and this allowed us to introduce a large variety of aryl groups at position C-7.<sup>30b</sup> The 7-bromo-substituted DHA can also be successfully subjected to Sonogashira reactions with terminal alkynes.<sup>36b,c</sup> Gratifyingly, the regioselective bromination – elimination – cross-coupling protocol also works for dimeric structures containing two DHA units linked by a *m*-phenylene unit (compound **4.15** of Chapter 4), which allowed us to prepare macrocycles with two DHA units.<sup>37</sup>

At position C-1, one of the cyano groups of the DHA can be converted to another group as shown in Figure 6.15. Thus, we found that a reductive DIBAL-H reduction substitutes one cyano group for a hydrogen atom,<sup>38</sup> while methyl or acetyl groups can be introduced by treatment with lithium naphthalenide followed by either methyl iodide or acetyl chloride as electrophile.<sup>38, 39</sup> Treatment with CsF in a solvent mixture of THF and methanol under reflux conditions resulted in formation of an amide.<sup>39</sup> It is also possible to convert one of the cyano groups to a 4,5-dihydro-1,3-thiazole or a benzothiazole (not shown in Figure 6.15) by treatment with either cysteine or 2-aminothiophenol.<sup>39, 40</sup>

In Chapter 4, I covered the switching properties of benzannulated derivatives. I shall here add details on how these compounds were regioselectively prepared. We developed a protocol for doing benzannulation in the seven-membered ring according to Figure 6.16.<sup>41</sup> The synthesis starts with our bromination – elimination – cross-coupling protocol by which DHA **6.28** via the bromide **6.29** was converted to the styryl-functionalized DHA **6.30**. The styrene double bond together with the C-7 – C8 double bond on DHA acts as a diene, which successfully underwent a diastereoselective Diels-Alder cycloaddition with dimethyl acetylenedicarboxylate to furnish the product **6.31** as a racemic mixture (*N.B.* the substrate **6.28** is a racemate). A final oxidation using DDQ gave the benzannulated derivative **6.32**. Unfortunately, this compound has lost the ability to undergo DHA-VHF photoisomerization. Nevertheless, it could be converted to the corresponding VHF **6.33** by chemical means, by treatment with AlCl<sub>3</sub> followed by water. The resulting VHF returned, however, instantaneously to a DHA, but now to the isomerized one, DHA **6.34**, where the benzannulation is instead at the C-5 – C-6 bond. Calculations reveal that this DHA isomer is significantly more stable than the original isomer (by 23.4 kJ mol<sup>-1</sup>).

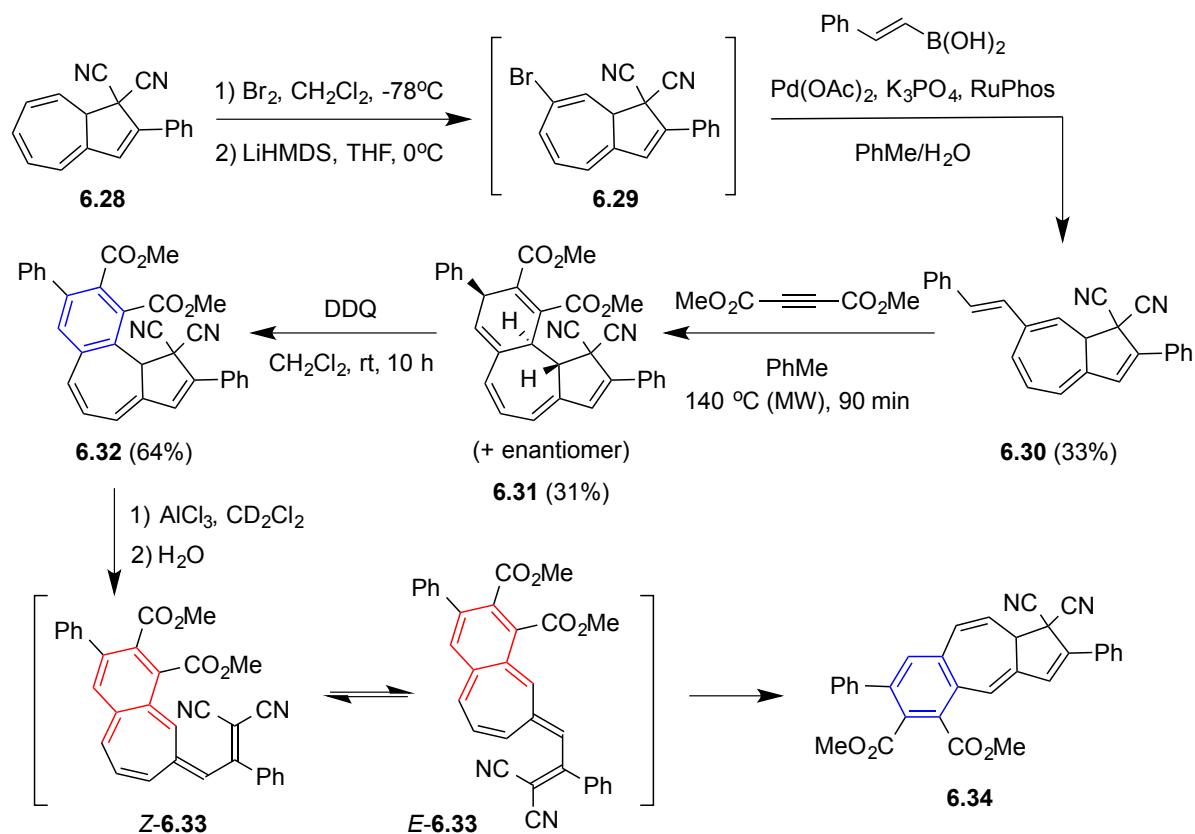


**Figure 6.16.** Benzannulation at positions C-7 – C-8 followed by isomerization. RuPhos = 2-dicyclohexylphosphino-2',6'-diisopropoxybiphenyl; DDQ = 4,5-dichloro-3,6-dioxo-1,4-cyclohexadiene-1,2-dicarbonitrile; MW = microwave heating.

Benzannulation at the C-2 – C3 bond was accomplished according to Figure 6.17.<sup>42</sup> First, a Knoevenagel condensation converted the starting material **6.35** to the product **6.36** that was then deprotonated and treated with tropylium tetrafluoroborate. The resulting product **6.37** was oxidized to form the corresponding VHF, which underwent ring-closure to form DHA **6.38**. The *tert*-butyldimethylsilyl protecting group was removed by treatment with acetic acid and tetrabutylammonium fluoride, and the resulting alcohol **6.39** was treated with *p*-toluenesulfonic acid to ultimately provide the aromatic DHA **6.40** in an elimination reaction. Alternatively, compound **6.38** could be converted directly to **6.40** upon treatment with *p*-toluenesulfonic acid and water. This DHA underwent undesired tautomerization upon irradiation, like **6.32**, but could be opened to the VHF by  $\text{AlCl}_3$  followed by water treatment. Yet, the VHF underwent immediate ring-closure, regenerating **6.40**.

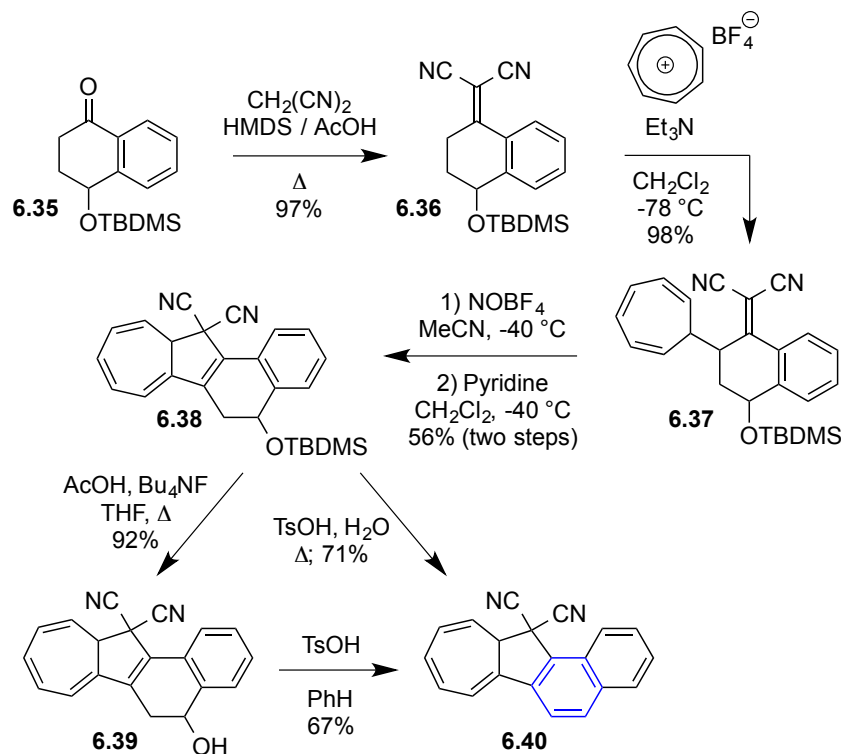


**Figure 6.17.** Synthetic protocol for benzannulated DHA. HMDS = hexamethyldisilazane; TBDMS = *tert*-butyldimethylsilyl; Ts = *p*-toluenesulfonyl.

Benzannulation in the seven-membered ring of VHF was accomplished by us according to Figure 6.18.<sup>42</sup> The 7*H*-benzo[7]annulene **6.41**<sup>43</sup> was converted to the benzotropylium salt **6.42**, which was then treated with **6.43**, deprotonated by triethylamine, furnishing the two isomers **6.44** and **6.45**. Oxidation of the mixture allowed us to isolate the VHF product **6.46**. This VHF was so stable due to the benzannulation that it could not be converted to a DHA, not even after prolonged heating.

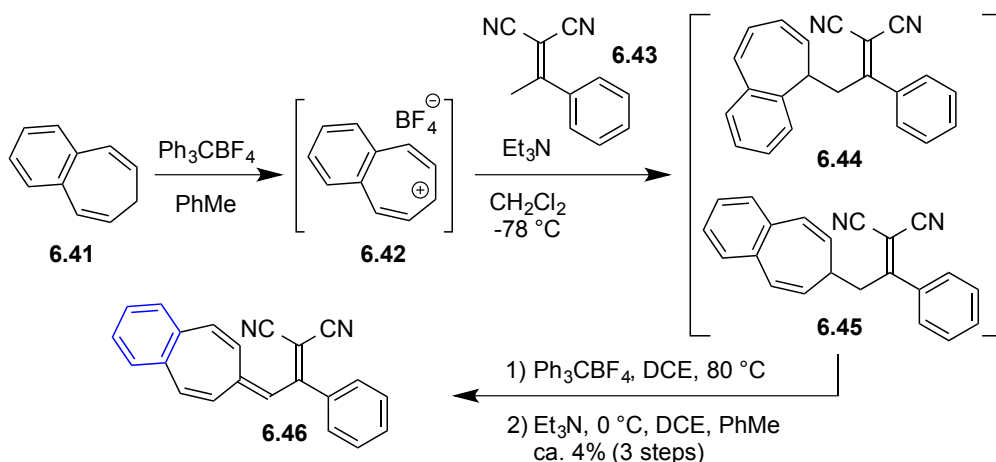


**Figure 6.18.** Synthetic protocol for benzannulated VHF. DCE = 1,2-dichloroethane.

### 6.3.2 Non-regioselective Methods

By introducing a phenyl substituent on the tropylium starting material for the DHA synthesis, we isolated after the four standard steps (outlined in Figure 6.15, left) the mixture of phenyl-substituted DHA isomers **6.47-6.50** (Figure 6.19).<sup>44</sup> Only by repeated chromatography we managed to isolate one isomer pure, the 2,5-diphenyl-substituted DHA **6.48**. Isomer **6.51** is likely also formed in the reaction, but was not isolated in the crude mixture. The conditions involved heating, and we found that under such conditions this isomer is able to undergo ring-opening/closure to form instead **6.48**. This was evidenced as some **6.51** is formed when subjecting **6.48** to a light/heat ring-opening/closure cycle according to <sup>1</sup>H-NMR spectroscopic analysis, but in time this isomer was observed to thermally return in the dark to **6.48** (*i.e.*, not promoted by a light-induced ring-opening).

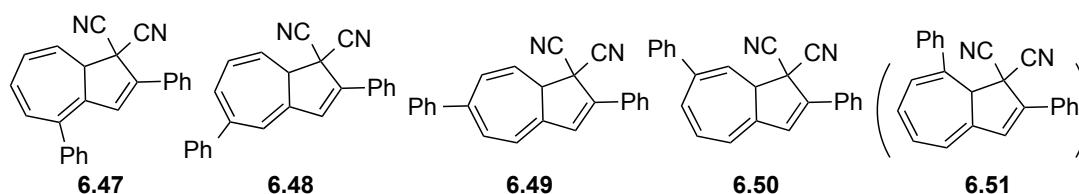
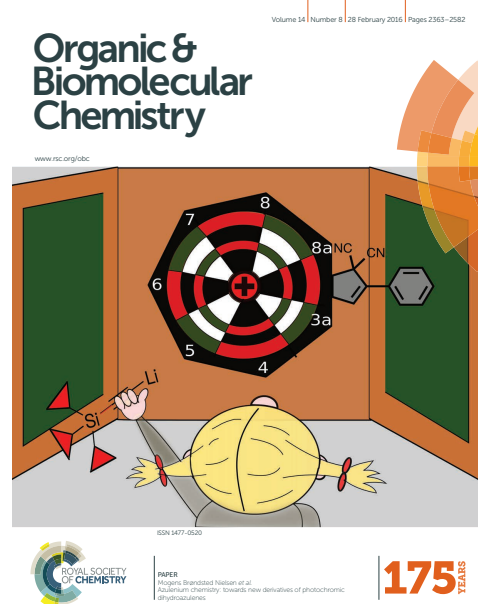
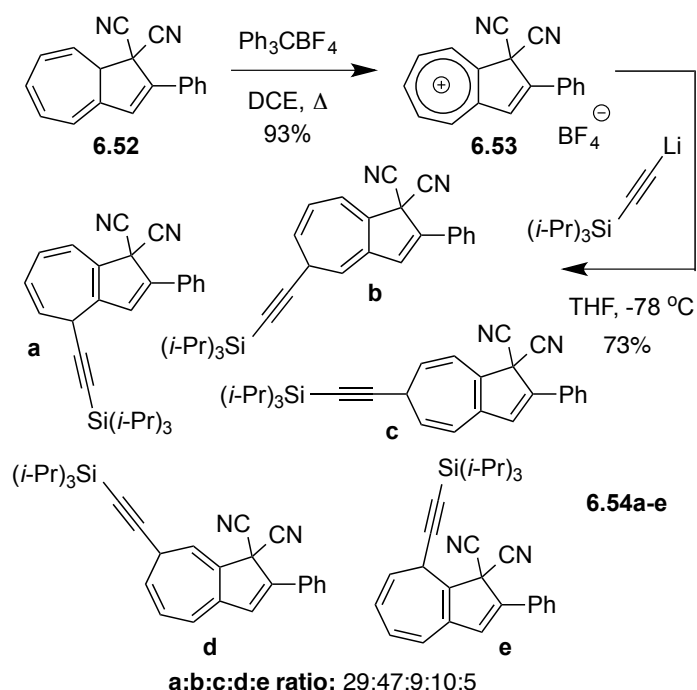


Figure 6.19. Regioisomeric DHAs.

In another approach (Figure 6.20), DHA **6.52** was subjected to hydride abstraction to generate the tropylium salt **6.53**,<sup>45</sup> which was next treated with lithium triisopropylsilylacetylide to provide the mixture of dihydroazulenes **6.54a-e** in a good overall yield of 73%.<sup>45b</sup> Positions C-4 and in particular C-5 of the tropylium salt were found to be the preferred sites of nucleophilic attack. For comparison, a calculational study by Okazaki and Laali<sup>46</sup> on the parent 1*H*-azulenium cation (without cyano substituent groups) showed it to have a clear vinyltropylium ion character and with the charge predominantly located on C-3a, C-5, C-7, and C-8a in the seven-membered ring and on C-2 and C-3 in the five-membered ring.

None of the dihydroazulenes **6.54a-e** are photochromic as they do not have the sp<sup>3</sup>-hybridized carbon at C-8a. It was possible to isolate **6.54a** pure and upon heating it in DMF, some of it tautomerized to the desired photochromic 1,8a-dihydroazulene (together with other products) that could subsequently be isolated pure.<sup>45b</sup> Yet, overall, the method is not an efficient way of functionalizing DHA, but the work has revealed the reactivity of the tropylium salt derived from DHA towards a nucleophile.

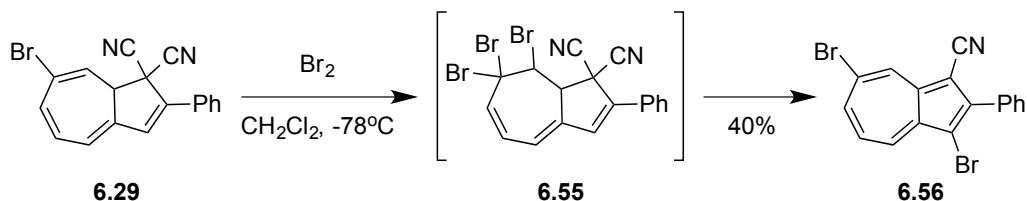


**Figure 6.20.** Left: Synthesis of mixture of non-photochromic dihydroazulenes. DCE = 1,2-dichloroethane. Right: Illustration of the different positions on the seven-membered ring that the acetylide “arrow” can attack. Positions C-4 and C-5 were found to be the preferred ones.

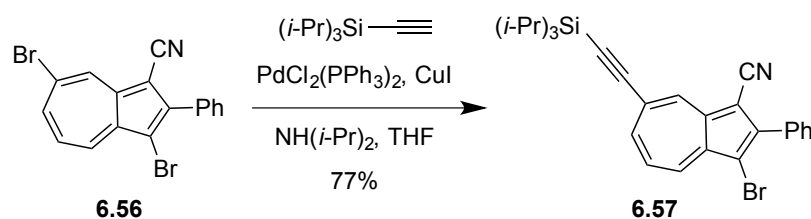
Reproduced from Ref. 45b [A. U. Petersen, M. Jevric, J. Elm, S. T. Olsen, C. G. Tortzen, A. Kadziola, K. V. Mikkelsen, M. B. Nielsen, *Org. Biomol. Chem.* **2016**, *14*, 2403-2412] - Published by The Royal Society of Chemistry.

## 6.4 Synthesis of Functionalized Azulenes

DHA **6.28** and the 7-bromo-substituted DHA **6.29** (Figure 6.21) can be used as convenient precursors to functionalized azulenes by elimination of HCN.<sup>34a,36a</sup> When first treated with bromine at  $-78^\circ\text{C}$ , **6.29** was transformed to a very unstable intermediate, presumably **6.55**, which underwent ready conversion, without the need of adding a base, to the azulene **6.56** (and other unidentified azulene products) containing a bromo substituent at both C-3 and C-7.<sup>34a</sup> Compound **6.56** was found to be significantly more reactive at C-7 than at C-3 for metal-catalyzed coupling reactions. Thus, from a Sonogashira coupling of **6.56** with triisopropylsilylacetylene, we isolated the product **6.57** resulting from reaction at C-7 only (Figure 6.22). On the other hand, azulenes are reactive at positions C-1 and C-3 for electrophilic aromatic substitution reactions (and potentially at C-5 if C-1 and C-3 are blocked).<sup>47</sup> For functionalization at positions C-2 and C-6 by cross-coupling reactions, the reader is referred to the examples provided in Ref. 48 (based on the work of other groups).

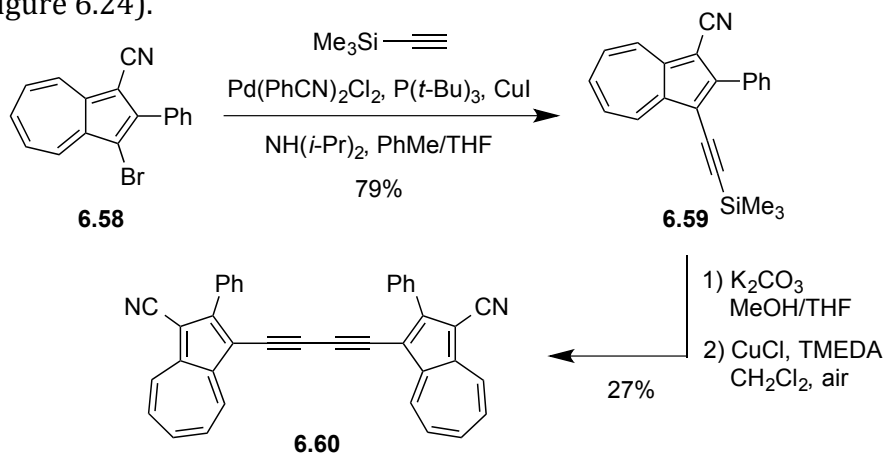


**Figure 6.21.** Synthesis of 3,7-dibromo-2-phenylazulene-1-carbonitrile.

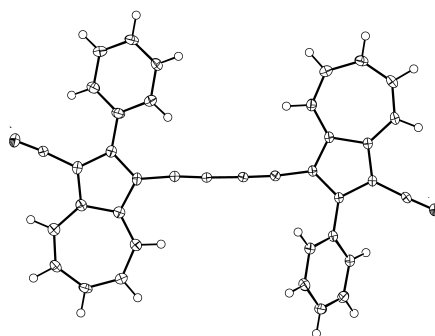


**Figure 6.22.** Selective Sonogashira coupling at position C-7.

It is, however, possible to perform Sonogashira reactions at C-3 if enhancing the reactivity of the Pd catalyst, using bulky and electron-rich tris(*tert*-butyl)phosphine ligands, as illustrated in the conversion of **6.58** into **6.59** (Figure 6.23).<sup>36a</sup> We found that this product could be desilylated and subjected to an oxidative Glaser-Hay coupling to provide the azulene dimer **6.60**, confirmed by X-ray crystallographic analysis (Figure 6.24).



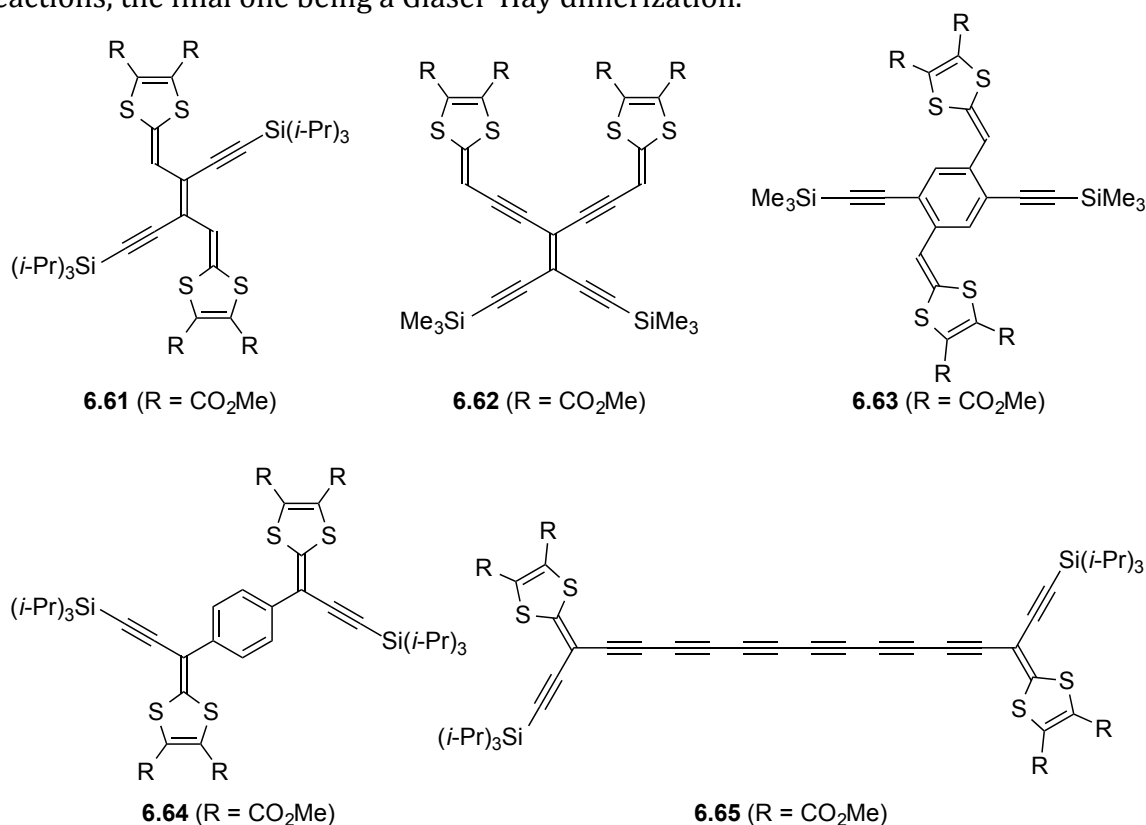
**Figure 6.23.** Sonogashira coupling at position C-3 of 3-bromo-substituted azulene, enforced by using more reactive Pd catalyst (having  $\text{P}(t\text{-Bu})_3$  ligands instead of  $\text{PPh}_3$ ).



**Figure 6.24.** Molecular structure of **6.60** according to X-ray crystallographic analysis. Reproduced from Ref. 36a with permission from John Wiley and Sons.

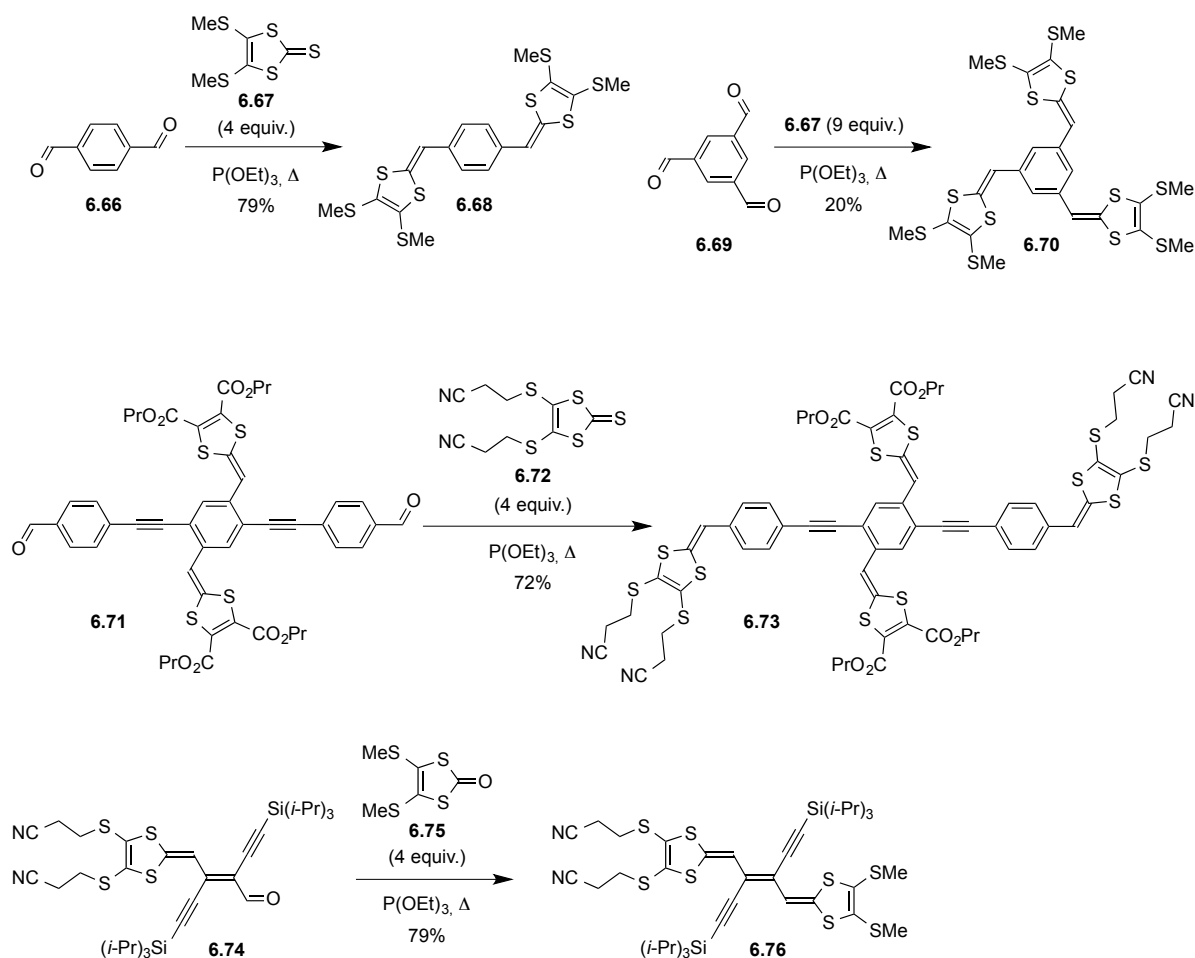
### 6.5 Cruciform-Like Extended Tetrathiafulvalenes

Figure 6.25 summarizes some of the cruciform-like motifs that we have developed incorporating an extended TTF using either a Wittig, Sonogashira or Glaser-Hay reaction as the key step. The syntheses of **6.61-6.63** were covered in chapters 3 and 5. The synthesis of **6.64** was accomplished by a Wittig reaction from the corresponding dione precursor.<sup>49</sup> The oligyne **6.65** was achieved by stepwise alkyne coupling reactions, the final one being a Glaser-Hay dimerization.<sup>50</sup>



**Figure 6.25.** Cruciform-like extended TTFs.

Phosphite-mediated coupling of 1,3-dithiol-2-chalcogenones is an important reaction to form derivatives of TTF.<sup>51</sup> We have also employed it for synthesis of various extended TTFs using an aldehyde as the one substrate. Several examples are shown in Figure 6.26. These include the phenylene-extended TTFs **6.68** and **6.70** (whose optical properties were compared in Chapter 2),<sup>52, 53</sup> the cruciform-shaped compound **6.73** that can be considered as two extended TTFs placed orthogonally to each other (and with either linear or cross-conjugated pathways between two DTF units),<sup>54</sup> and the diethynylethene-extended TTF **6.76**.<sup>11b, 55</sup>



**Figure 6.26.** Synthesis of extended TTFs by phosphite-mediated couplings.

By serendipity we found that more advanced cruciform motifs, with “H-cruciform” shape, were obtained in a phosphite coupling between the trimethylsilyl-protected diethynyl terephthalaldehyde **6.77** and either of the 1,3-dithiol-2-thiones **6.78** and **6.79** (Figure 6.27; *Method A*).<sup>52</sup> The products **6.80** and **6.81** result from the formation of two DTF units and a central stilbene unit. The structure of the H-cruciform **6.80** was confirmed by X-ray crystallographic analysis, revealing an almost planar  $\pi$ -system (Figure 6.28).



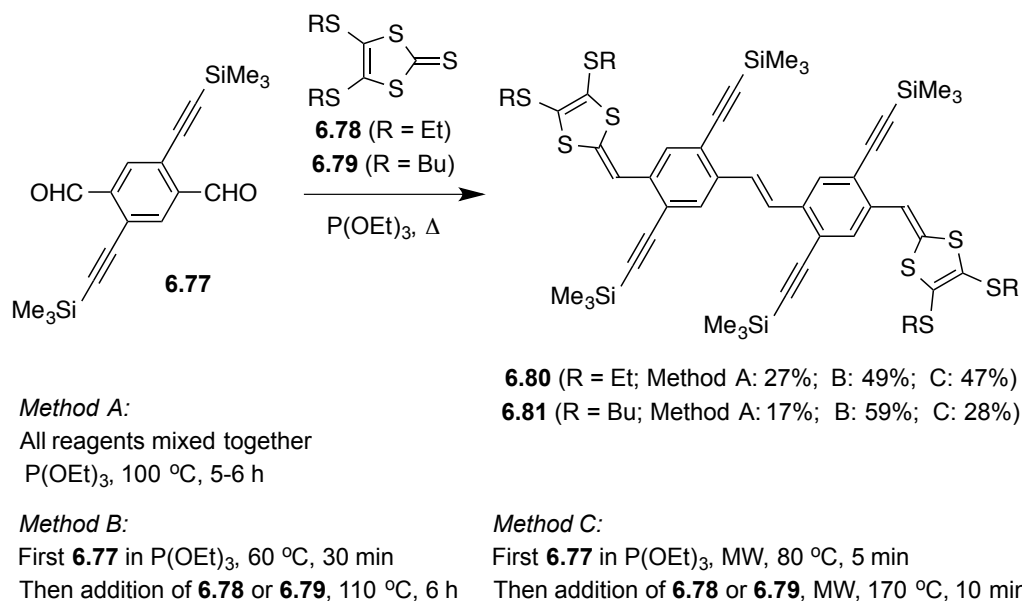


**Figure 6.27.** Phosphite-mediated synthesis of H-cruciform shaped extended TTFs containing a central stilbene unit. MW = microwave heating.

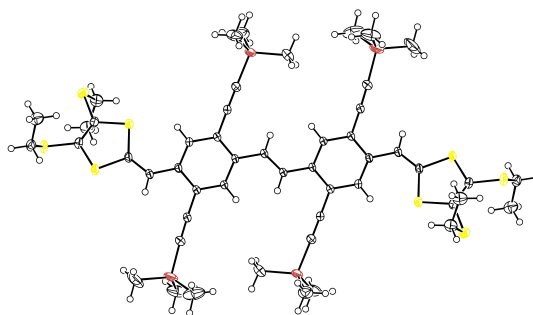


**Figure 6.28.** Molecular structure of **6.80** according to X-ray crystallographic analysis. Reproduced from Ref. 52 with permission from Georg Thieme Verlag KH (© Georg Thieme Verlag KG).

We found from NMR spectroscopic studies that the dioxaphospholane **I** shown in Figure 6.29 was an intermediate in the reaction, and its formation relied on electron-withdrawing substituents (various substrates were investigated in a systematic study).<sup>56</sup> In contrast, the ultimate conversion of this dioxaphospholane to a stilbene, presumably via an epoxide, relied on the conversion of the two remaining aldehyde groups into electron-donating DTF units (intermediate **II**). Thus, a sort of “umpolung” is important for the stilbene formation. Indeed, we found that the yields could be improved by performing the reaction in a stepwise manner, forming the dioxaphospholane intermediate first before adding the 1,3-dithiol-2-thione (Figure 6.27; *Methods B and C*).<sup>56, 57</sup> By protodesilylations followed by Sonogashira reactions, we expanded the H-cruciforms to larger scaffolds incorporating two parallel OPE3 or OPE5 molecular wires with thioester end-caps as shown in Figure 6.30.<sup>57, 58</sup> The central stilbene unit is here employed to align two molecular wires, and such molecules are

potentially interesting for molecular electronics applications (with the sulfur end-caps acting as electrode anchoring groups).

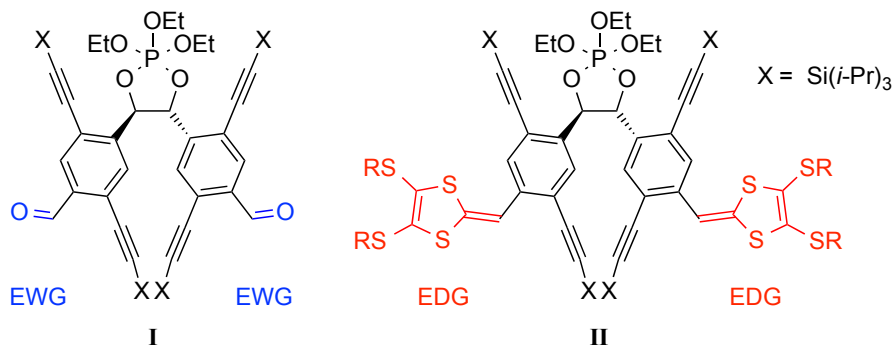


**Figure 6.29.** The formation of the stilbene unit of the H-cruciforms seems to involve intermediates **I** and **II**. The “umpolung” from electron-withdrawing groups (EWG) to electron-donating groups (EDG) in the *para* positions to the central dioxaphospholane unit plays a key role for this reaction.



**Figure 6.30.** OPE3 and OPE5 based H-cruciforms with a stilbene-extended TTF as central part and with thioacetate groups as potential electrode anchoring groups. Reproduced from Ref. 57 with permission from John Wiley and sons.

## 6.6 Dibenzodithiapentalene

Thieno[3,4-*c*]thiophene (**6.82**, Figure 6.31) is a very unstable compound,<sup>59</sup> but the stability can be enhanced by substitution, and Furukawa and co-workers<sup>60</sup> reported the first synthesis of the stable dibenzo-fused analog, dibenzo[*bc,fg*][1,4]dithiapentalene

(**6.83**), by photolysis of the precursor **6.84**. According to X-ray crystallography, **6.83** was found to have a completely planar structure.

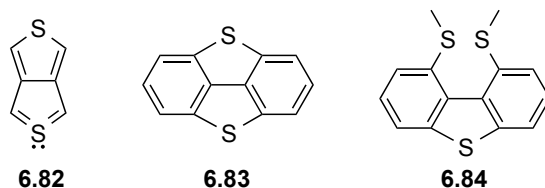


**Figure 6.31.** Dithiapentalenes **6.82** and **6.83** and the precursor (**6.84**) for obtaining **6.83** used by Furukawa and co-workers.<sup>60</sup>

In a MSc project by Tue H. Jepsen conducted at Lundbeck *a/s*, with Dr. Mogens Larsen and Dr. Morten Jørgensen as daily supervisors and me as the university supervisor, an alternative synthesis of **6.83** was developed as outlined in Figure 6.32.<sup>61, 62</sup>

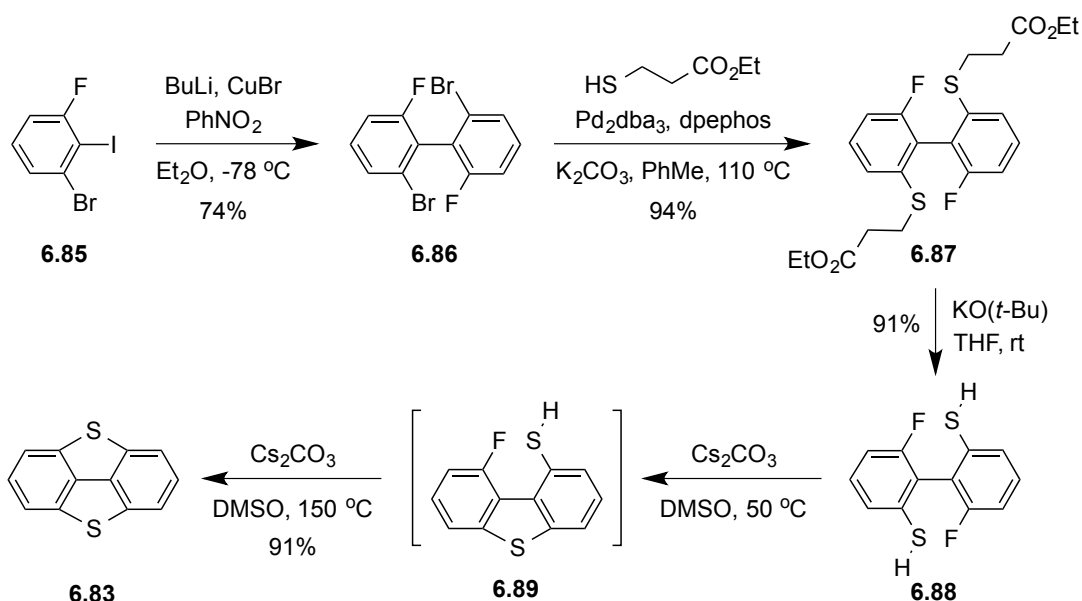


**Figure 6.32.** Synthesis of dibenzodithiapentalene. dba = dibenzylideneacetone; dpephos = bis[(2-diphenylphosphino)phenyl] ether.

The synthesis consists of the following steps: *i*) an Ullmann-type coupling of the tri-halobenzene **6.85** at low temperature forming the 2,2',6,6'-tetrahalobiphenyl **6.86** (following gentle conditions reported by Leroux *et al.*<sup>63</sup>), *ii*) a Pd-catalyzed C-S coupling of the arylbromides with ethyl-3-mercaptopropionate (inspired by conditions of Itoh and Mase<sup>64</sup>) to furnish compound **6.87**, *iii*) a base-promoted deprotection of **6.87** to form the dithiol **6.88**, and finally *iv*) a tandem cyclization *via* intramolecular S<sub>N</sub>Ar-reactions to obtain the desired product **6.83** in high yield *via* **6.89** as an intermediate. We had previously used similar conditions of steps *iii* and *iv* for synthesizing a large selection of dibenzothiophene derivatives.<sup>65</sup> Yet, in that work we could do the two

steps of deprotection and subsequent ring-closure in a one-pot reaction, which did not work for the synthesis of the dibenzodithiapentalene.

## 6.7 Conclusions

Acetylenic coupling reactions play a major role for the synthesis of the cross-conjugated molecules targeted in our research. The coupling reactions often need to be modified to take into account poor reactivity or instability of substrates or products. In particular, we have had success with adding molecular sieves to enhance oxidative Glaser-Hay dimerizations, using ultrasound for promoting Sonogashira reactions, using chloroalkynes as coupling partners for preparing unsymmetrical 1,3-butadiynes, and using gold(I) alkynyl complexes as stable substrates in Sonogashira-like coupling reactions. We have employed these methods for the synthesis of a large selection of acetylenic TTF and SubPc scaffolds.

Functionalized DHAs are conveniently functionalized using the “parent” system incorporating a substituent at position C-2 as a precursor. Protocols for regioselective functionalizations at positions C-1, C-3, and C-7 have been developed in addition to protocols for fusing a benzene ring to either the C-2 – C-3 or the C-7 – C-8 bonds. By treatment with Lewis acids, these DHAs can be opened to VHF; this conversion is accompanied by a transformation of the fused aromatic ring into an unfavourable cross-conjugated, quinoid structure. In consequence, the VHF were found to return quickly to DHAs.

Hydride abstraction from DHAs can readily be achieved using tritylium tetrafluoroborate. This reaction allowed us to prepare in high yield a 1,1-dicyano-2-phenyl-1*H*-azulenium salt, which was subsequently found to exhibit the highest electrophilicity towards the lithium acetylide nucleophile at positions C-4 and C-5 (in particular at C-5).

The DHAs can also be employed as precursors for fully unsaturated, substituted azulenes. Of particular importance, preparation of bromo-substituted azulenes can easily be achieved. A clear reactivity difference between 3-bromo- and 7-bromo-substituted azulenes for palladium-catalyzed coupling reactions was observed (as well as for the related DHAs); the former being less reactive. Oxidative addition at the vinylic bromide at C-3 is thus less favorable than at C-7 despite the presence of an electron-withdrawing cyano group at C-1.

A variety of cruciform-like motifs with an extended TTF unit has been prepared by Wittig reactions from simple carbonyl precursors. In addition, phosphite-mediated couplings present a convenient way of introducing DTF units to  $\pi$ -conjugated systems, and we have prepared a large selection of extended TTFs and cruciform-like motifs by this method (more examples from our work than shown in this chapter can be found in

Ref. 54b) where the DTF units are either placed in linear or cross-conjugated pathways relative to each other. We found that stilbenes could also be formed from phosphite mediated coupling of benzaldehyde derivatives when the electronic character of a *para* substituent on the benzaldehyde was changed from electron-withdrawing to electron-donating during the conditions. This can be considered as a sort of “umpolung”. Further acetylenic scaffolding has allowed the synthesis of various H-cruciform shaped molecules incorporating OPE units, which are potentially interesting wires for molecular electronics applications.

As first shown by Furukawa and co-workers,<sup>60</sup> the cross-conjugated dibenzo[*bc,fg*][1,4]dithiapentalene is a stable compound (in contrast to the unsubstituted dithiapentalene core). We have developed a convenient synthesis of this compound employing S<sub>N</sub>Ar reactions.

---

## References

1. a) M. Jevric, M. B. Nielsen, *Asian J. Org. Chem.* **2015**, 4, 286-295; b) M. B. Nielsen, *Synthesis* **2016**, 48, 2732-2738.
2. a) M. B. Nielsen, S. L. Broman, M. Å. Petersen, A. S. Andersson, T. S. Jensen, K. Kilså, A. Kadziola, *Pure Appl. Chem.* **2010**, 82, 843-852; b) M. Cacciarini, S. L. Broman, M. B. Nielsen, *Arkivoc* **2014**, i, 249-263.
3. a) K. Jennum, M. B. Nielsen, *Chem. Lett.* **2011**, 40, 662-667; b) M. B. Nielsen, *Phosphorus, Sulfur, and Silicon and the Related Elements* **2011**, 186, 1055-1073.
4. a) A. S. Hay, *J. Org. Chem.*, **1960**, 25, 1275-1276; b) A. S. Hay, *J. Org. Chem.* **1962**, 27, 3320-3321.
5. H. Jiang, V. Mazzanti, C. R. Parker, S. L. Broman, J. H. Wallberg, K. Lušpai, A. Brincko, H. G. Kjaergaard, A. Kadziola, P. Rapta, O. Hammerich, M. B. Nielsen, *Beilstein J. Org. Chem.* **2015**, 11, 930-948.
6. M. H. Vilhelmsen, J. Jensen, C. G. Tortzen, M. B. Nielsen, *Eur. J. Org. Chem.* **2013**, 701-711.
7. P. Cadiot, W. Chodkiewicz, *C. R. Hebd. Seance Acad. Sci.* **1955**, 241, 1055-1057.
8. a) J. Wityak, J. B. Chan, *Synth. Commun.* **1991**, 21, 977-979; b) D. Elbaum, T. B. Nguyen, W. L. Jorgensen, S. L. Schreiber, *Tetrahedron* **1994**, 50, 1503-1518; c) J. Alzeer, A. Vasella, *Helv. Chim. Acta* **1995**, 78, 177-193; d) C. Cai, A. Vasella, *Helv. Chim. Acta* **1995**, 78, 2053-2064; e) M. Alami, F. Ferri, *Tetrahedron Lett.* **1996**, 37, 2763-2766.
9. M. H. Vilhelmsen, A. S. Andersson, M. B. Nielsen, *Synthesis* **2009**, 1469-1472; *Synthesis* **2011**, 158.
10. M. A. Christensen, M. Rimmen, M. B. Nielsen, *Synlett* **2013**, 24, 2715-2719.
11. a) K. Qvortrup, A. S. Andersson, J.-P. Mayer, A. S. Jepsen, M. B. Nielsen, *Synlett* **2004**, 2818-2820; b) A. S. Andersson, K. Qvortrup, E. R. Torbensen, J.-P. Mayer, J.-P. Gisselbrecht, C. Boudon, M. Gross, A. Kadziola, K. Kilså, M. B. Nielsen, *Eur. J. Org. Chem.* **2005**, 3660-3671; c) A. S. Andersson, L. Kerndrup, A. Ø. Madsen, K. Kilså, M. B. Nielsen, P. R. La Porta, I. Biaggio, *J. Org. Chem.* **2009**, 74, 375-382.
12. a) M. I. Bruce, D. N. Duffy, *Aust. J. Chem.* **1986**, 39, 1697-1701; b) R. J. Cross, M. F. Davidson, *J. Chem. Soc., Dalton Trans* **1986**, 411-414; c) J. Vicente, M.-T. Chicote, M.-D. Abrisqueta, *J. Chem. Soc., Dalton Trans* **1995**, 497-498; d) M. I. Bruce, M. Jevric, B. W. Skelton, M. E. Smith, A. H. White, N. N. Zaitseva, *J. Organomet. Chem.* **2006**, 691, 361-370; e) W. M. Khairul, D. Albasa-Jove, D. S. Yufit, M. R. Al-Haddad, J. C. Collings, F. Hartl, J. A. K. Howard, T. B. Marder, P. J. Low, *Inorg. Chim. Acta* **2008**, 361, 1646-1658; f) M. I. Bruce, M. J., B. W. Skelton, A. H. White, N. N. Zaitseva, *J. Organomet. Chem.* **2010**, 695, 1906-1910; g) D. J. Armit, M. I. Bruce, J. C. Morris, B. K. Nicholson, C. R. Parker, B. W. Skelton, N. N. Zaitseva, *Organometallics* **2011**, 30, 5452-5456.
13. a) A. B. Antonova, M. I. Bruce, B. G. Ellis, M. Gaudio, P. A. Humphrey, M. Jevric, G. Melino, B. K. Nicholson, G. J. Perkins, B. W. Skelton, B. Stapleton, A. H. White, N. N. Zaitseva, *Chem. Commun.* **2004**, 960-961; b) M. I. Bruce, N. N. Zaitseva, B. K. Nicholson, B. W. Skelton, A. H. White, *J. Organomet. Chem.* **2008**, 693, 2887-2897; c) M. I. Bruce, B. K. Nicholson, N. N. Zaitseva, *C. C. Chimie* **2009**, 12, 1280-1286; d) W. Y. Man, S. Bock, N. N. Zaitseva, M. I. Bruce, P. J. Low, *J. Organomet. Chem.* **2011**, 696, 2172-2176.

14. V. Mazzanti, J. Huixin, H. Gotfredsen, T. J. Morsing, C. R. Parker, M. B. Nielsen, *Org. Lett.* **2014**, *16*, 3736-3739.
15. It should be mentioned that there is an alternative method for unstable alkyne substrates based on cross-coupling after *in-situ* desilylation; see for example: a) D. A. Shultz, K. P. Gwaltney, H. Lee, *J. Org. Chem.* **1998**, *63*, 4034-4038; b) K. Osowska, T. Lis, S. Szafert, *Eur. J. Org. Chem.* **2008**, 4598-4606; c) A. Nakhi, B. Prasad, U. Reddy, R. M. Rao, S. Sandra, R. Kapavarapu, D. Rambabu, G. R. Krishna, C. M. Reddy, K. Ravada, P. Misra, J. Iqbal, M. Pal, *Med. Chem. Comm.* **2011**, *2*, 1006-1010.
16. M. H. Larsen, M. B. Nielsen, *Organometallics* **2015**, *34*, 3678-3685.
17. W. M. Khairul, M. A. Fox, N. N. Zaitseva, M. Gaudio, D. S. Yufit, B. W. Skelton, A. H. White, J. A. K. Howard, M. I. Bruce, P. J. Low, *J. Chem. Soc., Dalton Trans.* **2009**, 610-620.
18. D. Shanks, S. Preus, K. Qvortrup, T. Hassenkam, M. B. Nielsen, K. Kilså, *New J. Chem.* **2009**, *33*, 507-516.
19. a) G. E. Morse, T. P. Bender, *ACS Appl. Mater. Interfaces* **2012**, *4*, 5055-5068; b) C. G. Claessens, D. González-Rodríguez, M. S. Rodríguez-Morgade, A. Medina, T. Torres, *Chem. Rev.* **2014**, *114*, 2192-2277.
20. H. Gotfredsen, M. Jevric, A. Kadziola, M. B. Nielsen, *Eur. J. Org. Chem.* **2016**, 17-21.
21. H. Gotfredsen, M. Jevric, S. L. Broman, A. U. Petersen, M. B. Nielsen, *J. Org. Chem.* **2016**, *81*, 1-5.
22. A. Meller, A. Ossko, *Monatsh. Chem.* **1972**, *103*, 150-155.
23. J. Guilleme, D. González-Rodríguez, T. Torres, *Angew. Chem. Int.* **2011**, *50*, 3506-3509.
24. A. B. Ricks, G. C. Solomon, M. T. Colvin, A. M. Scott, K. Chen, M. A. Ratner, M. R. Wasielewski, *J. Am. Chem. Soc.* **2010**, *132*, 15427-15434.
25. a) F. Camerel, G. Ulrich, P. Retailleau, R. Ziessel, *Angew. Chem. Int. Ed.* **2008**, *47*, 8876-8880; b) C. E. Mauldin, C. Piliago, D. Poulsen, D. A. Unruh, C. Woo, B. Ma, J. L. Mynar, J. M. Fréchet, *ACS Appl. Mater. Interfaces* **2010**, *2*, 2833-2838; c) H.-P. Jacquot de Rouville, R. Garbage, F. Ample, A. Nickel, J. Meyer, F. Moresco, C. Joachim, G. Rapenne, *Chem. Eur. J.* **2012**, *18*, 8925-8928. d) E. Maligaspe, M. R. Hauwiller, Y. V. Zatsikha, J. A. Hinke, P. V. Solntsev, D. A. Blank, V. N. Nemykin, *Inorg. Chem.* **2014**, *53*, 9336-9347.
26. G. E. Morse, T. P. Bender, *Inorg. Chem.* **2012**, *51*, 6460-6467.
27. J. Guilleme, L. Martínez-Fernández, I. Corral, M. Yáñez, D. González-Rodríguez, T. Torres, *Org. Lett.* **2015**, *17*, 4722-4725.
28. S. Gierisch, J. Daub, *Chem. Ber.* **1989**, *122*, 69-75.
29. L. Gobbi, P. Seiler, F. Diederich, *Helv. Chim. Acta.* **2001**, *84*, 743-776.
30. a) S. L. Broman, S. L. Brand, C. R. Parker, M. Å. Petersen, C. G. Tortzen, A. Kadziola, K. Kilså, M. B. Nielsen, *Arkivoc* **2011**, *ix*, 51-67; b) S. L. Broman, M. Jevric, A.D. Bond, M. B. Nielsen, *J. Org. Chem.* **2014**, *79*, 41-64.
31. S. L. Broman, S. Lara-Avila, C. L. Thisted, A. D. Bond, S. Kubatkin, A. Danilov, M. B. Nielsen, *Adv. Funct. Mater.* **2012**, *22*, 4249-4258.
32. a) J. Daub, T. Knöchel, A. Mannschreck, *Angew. Chem. Int. Ed. Engl.* **1984**, *23*, 960-961; b) J. Daub, S. Gierisch, U. Klement, T. Knöchel, G. Maas, U. Seitz, *Chem. Ber.* **1986**, *119*, 2631-2646.

- 
33. C. R. Parker, C. G. Tortzen, S. L. Broman, M. Schau-Magnussen, K. Kilså, M. B. Nielsen, *Chem. Commun.* **2011**, 47, 6102-6104.
34. a) V. Mazzanti, M. Cacciarini, S. L. Broman, C. R. Parker, M. Schau-Magnussen, A. D. Bond, M. B. Nielsen, *Beilstein J. Org. Chem.* **2012**, 8, 958-966; b) M. D. Kilde, M. H. Hansen, S. L. Broman, K. V. Mikkelsen, M. B. Nielsen, *Eur. J. Org. Chem.* **2017**, 1052-1062.
35. T. Mrozek, H. Görner, J. Daub, *Chem. Eur. J.* **2001**, 7, 1028-1040.
36. a) M. Å. Petersen, K. Kilså, A. Kadziola, M. B. Nielsen, *Eur. J. Org. Chem.* **2007**, 1415-1418; b) M. Å. Petersen, S. L. Broman, A. Kadziola, K. Kilså, M. B. Nielsen, *Eur. J. Org. Chem.* **2009**, 2733-2736; c) S. L. Broman, M. Å. Petersen, C. Tortzen, A. Kadziola, K. Kilså, M. B. Nielsen, *J. Am. Chem. Soc.* **2010**, 132, 9165-9174; d) M. D. Kilde, S. L. Broman, A. Kadziola, M. B. Nielsen, *Synlett* **2016**, 27, 450-454.
37. A. Vlasceanu, S. L. Broman, A. S. Hansen, A. B. Skov, M. Cacciarini, A. Kadziola, H. G. Kjaergaard, K. V. Mikkelsen, M. B. Nielsen, *Chem. Eur. J.* **2016**, 22, 10796-101800.
38. M. Cacciarini, A. B. Skov, M. Jevric, A. S. Hansen, J. Elm, H. G. Kjaergaard, K. V. Mikkelsen, M. B. Nielsen, *Chem. Eur. J.* **2015**, 21, 7454-7461.
39. M. Cacciarini, M. Jevric, J. Elm, A. U. Petersen, K. V. Mikkelsen, M. B. Nielsen, *RSC Adv.* **2016**, 6, 49003-49010.
40. M. Cacciarini, E. A. Della Pia, M. B. Nielsen, *Eur. J. Org. Chem.* **2012**, 6064-6069.
41. A. B. Skov, J. F. Petersen, J. F. Petersen, J. Elm, B. N. Frandsen, M. Santella, M. D. Kilde, H. G. Kjaergaard, K. V. Mikkelsen, M. B. Nielsen, *ChemPhotoChem* **2017**, In press. DOI: 10.1002/cptc.201600046
42. A. B. Skov, S. L. Broman, A. S. Gertsen, J. Elm, M. Jevric, M. Cacciarini, A. Kadziola, K. V. Mikkelsen, M. B. Nielsen, *Chem. Eur. J.* **2016**, 22, 14567-14575.
43. A. M. Khan, G. R. Proctor, L. Rees, *J. Chem. Soc. (C)* **1996**, 990-994.
44. L. Skov, M. Å. Petersen, S. L. Broman, A. D. Bond, M. B. Nielsen, *Org. Biomol. Chem.* **2011**, 9, 6498-6501.
45. a) S. L. Broman, A. U. Petersen, C. G. Tortzen, J. Vibenholt, A. D. Bond, M. B. Nielsen, *Org. Lett.* **2012**, 14, 318-321; b) A. U. Petersen, M. Jevric, J. Elm, S. T. Olsen, C. G. Tortzen, A. Kadziola, K. V. Mikkelsen, M. B. Nielsen, *Org. Biomol. Chem.* **2016**, 14, 2403-2412.
46. T. Okazaki, K. K. Laali, *Org. Biomol. Chem.* **2003**, 1, 3078-3093.
47. V. B. Mochalin, Y. N. Porshnev, *Russ. Chem. Rev.* **1977**, 46, 530-547.
48. a) T. Okujima, S. Ito, N. Morita, *Tetrahedron Lett.* **2002**, 43, 1261-1264; b) S. Ito, T. Okujima and N. Morita, *J. Chem. Soc., Perkin Trans. 1* **2002**, 1896-1905; c) T. Ito, T. Terazono, T. Kubo, T. Okujima, N. Morita, T. Murafuji, Y. Sugihara, K. Fujimori, J. Kawakami, A. Tajiri, *Tetrahedron* **2004**, 60, 5357-5366; d) T. Shoji, A. Maruyama, T. Araki, S. Ito, T. Okujima, *Org. Biomol. Chem.* **2015**, 13, 10191-10197.
49. M. B. Nielsen, *Synlett* **2003**, 1423-1426.
50. K. Qvortrup, M. T. Jakobsen, J.-P. Gisselbrecht, C. Boudon, F. Jensen, S. B. Nielsen, M. B. Nielsen, *J. Mater. Chem.* **2004**, 14, 1768-1773.
51. J. M. Fabre, *Chem. Rev.* **2004**, 104, 5133-5150; and references cited therein.
52. S. S. Schou, C. R. Parker, K. Lincke, K. Jennum, J. Vibenholt, A. Kadziola, M. B. Nielsen, *Synlett* **2013**, 24, 231-235.



- 
53. Sallé and co-workers prepared related phenylene-extended TTFs using Horner-Wadsworth-Emmons reactions: M. Sallé, A. Belyasmine, A. Gorgues, M. Jubault, N. Soyer, *Tetrahedron Lett.* **1991**, 32, 2897-2900.
54. a) C. R. Parker, Z. Wei, C. A. Rodríguez, K. Jennum, T. Li, M. Santella, N. Bovet, G. Yhao, W. Hu, H. S. J. van der Zant, M. Vanin, G. C. Solomon, B. W. Laursen, K. Nørgaard, M. B. Nielsen, *Adv. Mater.* **2013**, 25, 405-409; b) C. R. Parker, E. Leary, R. Frisenda, Z. Wei, K. S. Jennum, E. Glibstrup, P. B. Abrahamsen, M. Santella, M. A. Christensen, E. A. Della Pia, T. Li, M. T. Gonzalez, B. W. Laursen, K. Nørgaard, H. van der Zant, N. Agraït, M. B. Nielsen, *J. Am. Chem. Soc.* **2014**, 136, 16497-16507.
55. M. B. Nielsen, J.-P. Gisselbrecht, N. Thorup, S. P. Piotto, C. Boudon, M. Gross, *Tetrahedron Lett.* **2003**, 44, 6721-6723.
56. J. F. Petersen, C. G. Tortzen, F. P. Jørgensen, C. R. Parker, M. B. Nielsen, *Tetrahedron Lett.* **2015**, 56, 1894-1897.
57. F. P. Jørgensen, J. F. Petersen, C. L. Andersen, A. B. Skov, M. Jevric, O. Hammerich, M. B. Nielsen, *Eur. J. Org. Chem.*, In press. DOI: 10.1002/ejoc.201601367
58. For examples of H-cruciform shaped molecules not containing DTF units, see: a) N. Zhou, L. Wang, D. W. Thompson, Y. Zhao, *Org. Lett.* **2008**, 10, 3001-3004; b) F. He, Y. Zhou, S. Liu, L. Tian, H. Xu, H. Zhang, B. Yang, Q. Dong, W. Tian, Y. Ma, J. Shen, *Chem. Commun.* **2008**, 3912-3914; c) W. Cui, Y. Fu, Y. Qu, H. Tian, J. Zhang, Z. Xie, Y. Geng, F. Wang, *Chem. Asian J.* **2010**, 5, 932-940; d) N. Zhou, L. Wang, D. W. Thompson, Y. Zhao, *Tetrahedron* **2011**, 67, 125-143; e) Y. Li, Z. Jia, S. Xiao, H. Liu, Y. Li, *Nat. Commun.* **2016**, 7:11637.
59. a) M. P. Cava, G. E. M. Husbands, *J. Am. Chem. Soc.* **1969**, 91, 3952-3953; b) M. P. Cava, M. V. Lakshmikantham, *Acc. Chem. Res.* **1975**, 8, 139-144; c) V. P. Litvinov, *Russ. Chem. Rev.* **2005**, 74, 217-248.
60. a) T. Kimura, Y. Ishikawa, S. Ogawa, T. Nishio, I. Iida, N. Furukawa, *Tetrahedron Lett.* **1992**, 33, 6355-6358; b) T. Kimura, Y. Ishikawa, Y. Minoshima, N. Furukawa, *Heterocycles* **1994**, 37, 541-552.
61. T. H. Jepsen, M. Larsen, M. Jørgensen, M. B. Nielsen, *Tetrahedron Lett.* **2011**, 52, 4045-4047.
62. A route to substituted dibenzo[bcfg][1,4]dithiapentalene derivatives has also been described: M. Cariou, T. Douadi, J. Simonet, *New. J. Chem.* **1996**, 20, 1031-1039.
63. F. R. Leroux, R. Simon, N. Nicod, *Lett. Org. Chem.* **2006**, 3, 948-954.
64. T. Itoh, T. Mase, *Org. Lett.* **2004**, 6, 4587-4590.
65. T. H. Jepsen, M. Larsen, M. Jørgensen, K. A. Solanko, A. D. Bond, A. Kadziola, M. B. Nielsen, *Eur. J. Org. Chem.* **2011**, 53-57.

## CONCLUDING REMARKS

This dissertation work has shown how cross-conjugation strongly influences optical, redox, chemical reactivity (exemplified by electrocyclic reactions), and single-molecule conductance properties. The findings are summarized schematically in Figure 7.1.

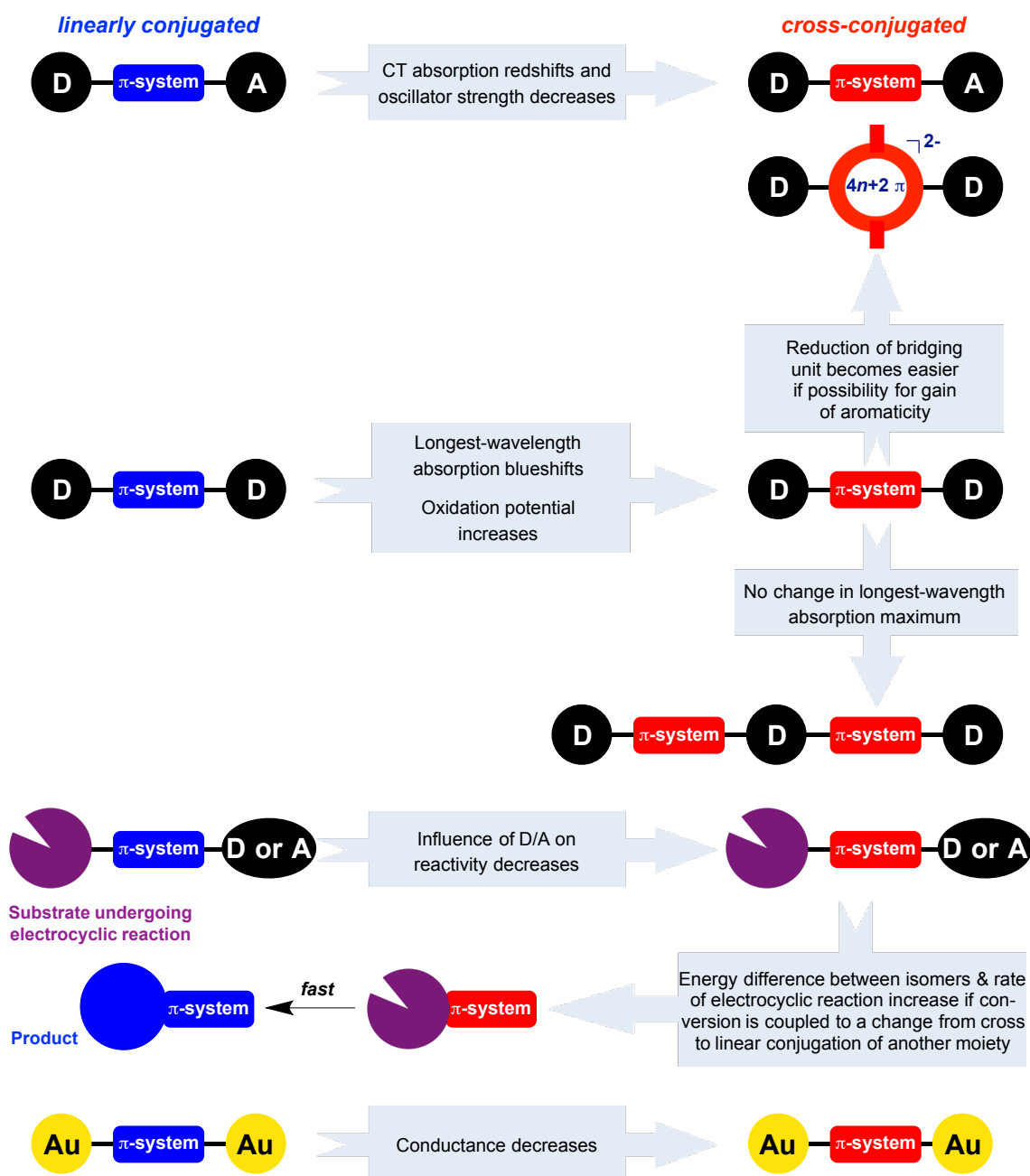


**Figure 7.1.** Summary of the consequences of cross-conjugation. Absorption redshifts and blueshifts refer to intrinsic molecular properties, ignoring solvation effects.

D = donor; A = acceptor; Au = gold electrode.

The molecules that we have prepared and studied are in general structurally complicated, and it should be emphasized that other contributions to the electronic properties than cross-conjugation, such as non-planarity of the  $\pi$ -system, may also play important roles. No matter what, altogether our results (together with those of others) do support the key conclusion:

***$\pi$ -Electron delocalization is significantly less efficient via cross-conjugation than via linear conjugation, and cross-conjugation can therefore be employed as a structural tool to decouple two functional units.***

The obtained results are important in the further design of advanced organic materials with low HOMO-LUMO gaps based on donor-acceptor chromophores, in the design of photochromic molecules and materials with high energy storage capacities, controllable rates of interconversions and optimum absorption maxima (with potential applications for storage of solar energy based on closed energy cycles of harvesting, storage, and release), in the design of multiple redox systems as “electron or hole reservoirs” (with potential applications for photovoltaics), in the design of molecular switches for molecular electronics applications that upon an external stimulus can undergo conductance switching, and in the design of organic polyradical spin systems for spintronics applications.

